

**Expression, Function and Regulation of the Heat Shock  
Protein 70 (*hsp70*) Gene during Normal Zebrafish  
(*Danio rerio*) Embryogenesis**

A Thesis Submitted to the College of Graduate Studies and Research in Partial  
Fulfillment of the Requirements for the Degree of Doctor of Philosophy  
in the Department of Anatomy and Cell Biology

University of Saskatchewan

Saskatoon

By

Tyler G Evans



Library and  
Archives Canada

Bibliothèque et  
Archives Canada

Published Heritage  
Branch

Direction du  
Patrimoine de l'édition

395 Wellington Street  
Ottawa ON K1A 0N4  
Canada

395, rue Wellington  
Ottawa ON K1A 0N4  
Canada

*Your file* *Votre référence*  
*ISBN: 978-0-494-18180-5*  
*Our file* *Notre référence*  
*ISBN: 978-0-494-18180-5*

#### NOTICE:

The author has granted a non-exclusive license allowing Library and Archives Canada to reproduce, publish, archive, preserve, conserve, communicate to the public by telecommunication or on the Internet, loan, distribute and sell theses worldwide, for commercial or non-commercial purposes, in microform, paper, electronic and/or any other formats.

The author retains copyright ownership and moral rights in this thesis. Neither the thesis nor substantial extracts from it may be printed or otherwise reproduced without the author's permission.

#### AVIS:

L'auteur a accordé une licence non exclusive permettant à la Bibliothèque et Archives Canada de reproduire, publier, archiver, sauvegarder, conserver, transmettre au public par télécommunication ou par l'Internet, prêter, distribuer et vendre des thèses partout dans le monde, à des fins commerciales ou autres, sur support microforme, papier, électronique et/ou autres formats.

L'auteur conserve la propriété du droit d'auteur et des droits moraux qui protègent cette thèse. Ni la thèse ni des extraits substantiels de celle-ci ne doivent être imprimés ou autrement reproduits sans son autorisation.

---

In compliance with the Canadian Privacy Act some supporting forms may have been removed from this thesis.

Conformément à la loi canadienne sur la protection de la vie privée, quelques formulaires secondaires ont été enlevés de cette thèse.

While these forms may be included in the document page count, their removal does not represent any loss of content from the thesis.

Bien que ces formulaires aient inclus dans la pagination, il n'y aura aucun contenu manquant.

  
**Canada**

**UNIVERSITY OF SASKATCHEWAN**

College of Graduate Studies and Research

**SUMMARY OF DISSERTATION**

Submitted in partial fulfillment

of the requirements for the

**DEGREE OF DOCTOR OF PHILOSOPHY**

by

Tyler Evans

Department of Anatomy and Cell Biology

University of Saskatchewan

Spring 2006

Examining Committee:

Dr. C. Havele	Dean/Associate Dean, Dean's Designate, Chair College of Graduate Studies and Research
Dr. W. Kulyk	Chair of Advisory Committee Department of Anatomy and Cell Biology
Dr. P. Krone	Supervisory, Department of Anatomy and Cell Biology
Dr. R. Doucette	Department of Anatomy and Cell Biology
Dr. D. Schreyer	Department of Anatomy and Cell Biology
Dr. A. Nazarali	College of Pharmacy and Nutrition

External Examiner:

Dr. Gregory Kelly  
Department of Biology  
Molecular Genetics Unit  
University of Western Ontario  
London ON N6A 5B7

## **BIOGRAPHICAL**

June 30, 1979

Born in Saskatoon, SK, Canada

Spring 2001

B Sc. (Hon) Biology, University of Saskatchewan

## **HONOURS**

2005-2006 College of Medicine Arthur Smyth Memorial Scholarship

2002-2005 College of Medicine Graduate Scholarship

2001-2002 Department of Anatomy and Cell Biology Graduate Scholarship

2001 USTEP Summer Student Award

## PUBLICATIONS

Evans, TG., Yamamoto, Y., Jeffery, WR., Krone, PH. (2005) Zebrafish Hsp70 is required for normal lens formation. *Cell Stress Chaperones*. 10: 66-78.

Krone, PH., Blechinger, SR., Evans, TG., Ryan, JA., Noonan, EJ., Hightower, LE. (2005) Use of PLHC-1 cells and zebrafish embryos in cytotoxicity assays. *Methods*. (35): 176-187.

Blechinger, SR., Evans, TG., Tang, PT., Kuwada, JY., Warren, JT., Krone, PH. (2002) The heat inducible zebrafish *hsp70* gene is expressed during normal lens development under non-stress conditions. *Mech. Dev.* (112): 213-215.

Evans, TG., Krone, PH. (2005) Heat shock proteins: molecular chaperones as critical players in normal eukaryotic development. *Trends in Dev Biol*. In Press.

Krone, PH., Evans, TG., Belchinger, SR. (2003) Heat shock gene expression and function during zebrafish embryogenesis. *Sem. Cell Dev. Biol.* 14: 267-276.

Evans, TG., Krone, PH. (2005) HSF1 regulates endogenous expression of *hsp70* in developing zebrafish lens. Expected submission date: November 2005.

“The stress inducible *hsp70* is required for normal embryonic lens formation in zebrafish. Evans, TG., Yamamoto, Y., Jeffery, WR., Krone, PH. Presented at the 63<sup>rd</sup> Annual Meeting of the Society for Developmental Biology (July 2004) and Life Sciences Research Day (2004)

“Disruption of zebrafish lens formation by microinjection of Hsp70 morpholino modified antisense oligonucleotide.” Evans, TG., Blechinger, SR., Krone, PH. Presented at the 5<sup>th</sup> International Meeting on Zebrafish Development and Genetics (June 2002) and Life Sciences Research Day (Jan 2003).

*“This vain presumption of understanding everything can have no other basis than never understanding anything.”*

-Galileo, The Two Chief World Systems

## **Permission to Use**

In presenting this thesis in partial fulfillment of the requirements for a postgraduate degree from the University of Saskatchewan, I hereby grant to the University of Saskatchewan and/or its agents the non-exclusive license to archive and make accessible, under the conditions specified below, my thesis, dissertation, or project report in whole or in part in all forms of media, now or for the duration of my copyright ownership. I retain all other ownership rights to the copyright of the thesis, dissertation or project report. I also reserve the right to use in future works (such as articles or books) all or part of this thesis, dissertation, or project report.

I hereby certify that, if appropriate, I have obtained and attached hereto a written permission statement from the owner(s) of each third party copyrighted matter that is included in my thesis, dissertation, or project report, allowing distribution as specified below. I certify that the version I submitted is the same as that approved by my advisory committee.

## Abstract

Heat shock proteins (Hsps) and heat shock transcription factors (HSFs) are critical to the ability of cells to cope with disturbances in their environment, and the function of Hsps and HSFs during the stress response has been well characterized. However, both classes of molecules are known to be expressed constitutively under non-stress conditions, and only recently have studies begun to address the specific consequences of inhibiting Hsp or HSF expression. Interestingly, these studies have demonstrated that both Hsps and HSFs are important players in eukaryotic development. Accordingly, this thesis focused on the expression, function, and regulation of the normally stress-inducible *hsp70* gene during the normal development of the zebrafish (*Danio rerio*).

Whole mount *in situ* hybridization analysis was used to show that the heat-inducible zebrafish *hsp70* gene is expressed during a distinct temporal window of embryonic lens formation at the normal growth temperature of 28°C. In addition, a 1.5 kb fragment of the zebrafish *hsp70* gene promoter is sufficient to direct expression of a green fluorescent protein (GFP) reporter gene to the lens, suggesting that lens-specific expression of the *hsp70* gene is regulated by promoter sequences and is expressed as part of the normal lens development program. To elucidate a possible role for the lens specific expression of *hsp70* during normal embryonic development, morpholino modified antisense oligonucleotides (MO) directed against *hsp70* mRNA (*hsp70*-MO) were microinjected into early zebrafish embryos to reduce the levels of Hsp70 during zebrafish development. *hsp70*-MO injected embryos exhibited a small eye phenotype relative to wildtype and control injected animals, with the phenotype discernable during the second day of development. Histological and immunological analysis revealed a small, underdeveloped lens and a disorganized retinal structure. Numerous TUNEL-positive nuclei also appeared in the lens of small eye embryos beyond 2 days of development, whereas they were no



longer apparent in untreated embryos by 48 hours post-fertilization (hpf). Lenses transplanted from *hsp70*-MO injected embryos into wildtype hosts failed to recover and retained the immature morphology characteristic of the small eye phenotype, indicating that the phenotype is lens autonomous. These data suggest that the lens defect in *hsp70*-MO injected embryos is predominantly at the level of post-mitotic lens fibre differentiation, a result supported by the appearance of mature lens organization in these embryos at 5 days post fertilization (dpf), once MO degradation/dilution has occurred.

The role of HSFs in normal zebrafish development, and whether these molecules are involved in regulating the expression of *hsp70* in the zebrafish lens, has not been investigated prior to this thesis. Microinjecting MO targeted to the three zebrafish HSFs (HSF1, HSF2, and HSF3), demonstrated a requirement for HSF1 in normal zebrafish eye development. Specifically, *hsf1*-MO injected embryos phenocopy the lens and retinal defects observed with *hsp70*-MO injection. Furthermore, western blot analysis shows a marked decrease in Hsp70 in *hsf1*-MO injected embryos. Taken collectively, these data indicate that *hsp70* is expressed during a brief window of lens fibre development, and that this expression is required for the proper development of the zebrafish lens. In addition, lens-specific *hsp70* expression appears to be regulated by HSF1, as microinjection of *hsf1*-MO can phenocopy the defects observed in *hsp70*-MO injected embryos.

## **Acknowledgements**

A project of this magnitude could not be the sole work of one author. I am deeply indebted to a number of people whose assistance and advice made this thesis possible. I would foremost like to thank my supervisor Pat Krone for his patience, support, and guidance. Secondly, I would like to acknowledge the work of the collaborating scientists in this project, who not only made significant contributions to this thesis, but who became close friends and with whom I hope to work with again in the future. In particular, Scott Blechinger who helped immensely with the zebrafish expression data, and who is one of the most truly original people I have met. Also Yoshiyuki Yamamoto, Bill Jeffery and the rest of the cavefish lab at the University of Maryland for their contribution to the lens transplantations. Our paths are certain to cross again soon. Esmond Sanders and Ewa Parker for their contributions to the chicken expression data, and for their generous hospitality at the University of Alberta. I would also like to thank Bill Kulyk and Brent Bobick for their assistance with continuing the chicken work here in the department. I would like to thank Zack Belak for his contribution to the gel mobility shift assays. I would like to thank current and former lab members who were helpful most of time, and good people all of the time. Thank you Ali Taherian, Heather Salisbury, Amy MacKay, and Carlyn Matz, as well, all other members of the Department of Anatomy and Cell Biology. There few people in this department who have not had some hand in this work or my life during my time here. I would also like to acknowledge the guidance of my committee members Bill Kulyk, Ron Doucette, Adil Nazarali, and David Schreyer. Their advice greatly added to this thesis. Finally I would like to thank all of my friends and family whose support and kindness is always appreciated.

## Table of Contents

Permission to use	ii
Abstract	iii
Acknowledgements	v
Table of Contents	vi
List of Tables	xi
List of Figures	xii
List of Abbreviations	xv
1.0 Introduction	1
1.1 General introduction	1
1.2 Introduction to heat shock proteins	2
1.3 The heat shock response	3
1.4 Heat shock proteins and development	6
1.4.1 The small heat shock protein family and development	6
1.4.2 Heat shock protein 47 and development	11
1.4.3 The 70kDa heat shock protein family and development	12
1.4.4 The 90kDa heat shock protein family and development	16
1.4.5 Heat shock protein transcription factors (HSFs) and development	20
1.5 Introduction to apoptosis	24
1.5.1 Apoptosis occurs through two signaling pathways	25
1.5.2 Hsp70 and the inhibition of apoptosis	27
1.6 Zebrafish as a vertebrate model system	30
1.7 Eye development in zebrafish	31
1.7.1 General aspects of zebrafish eye development	31
1.7.2 Zebrafish lens development	31
1.7.3 Zebrafish retinal development	33

1.7.4 The central role of the lens in eye development	36
1.7.5 Degradation of organelles in the mature lens	37
1.8 Hypotheses and research objectives	38
2.0 Materials and Methods	41
2.1 Zebrafish embryo care, collection, and maintenance	41
2.2 Zebrafish embryo fixation and dechoriation	42
2.3 Zebrafish embryo mounting and sectioning	42
2.4 Zebrafish embryo photography	44
2.5 Zebrafish embryo eye and body measurements	44
2.6 Zebrafish embryo whole mount <i>in situ</i> hybridization	45
2.6.1 Antisense RNA probe synthesis	45
2.6.2 Probe hybridization and immunodetection	46
2.7 Microinjection of zebrafish embryos	48
2.7.1 Introduction to morpholino modified antisense oligonucleotides	49
2.7.2 Preparation of morpholino modified antisense oligonucleotides	49
2.8 Zebrafish embryo immunohistochemistry	52
2.9 Terminal deoxynucleotidyl transferase-mediated dUTP fluoroscein nick end labeling (TUNEL) analysis	54
2.10 Zebrafish embryo lens transplantation	54
2.11 Western blot analysis	56
2.12 Gel mobility shift analysis	57
2.13 Chicken egg care and incubation	58
2.14 Chick lens dissection and protein extract preparation	58
2.15 Chicken lens cell culture	59
2.16 Immunocytochemistry of chicken lens cell cultures	60

3.0 Results	
3.1 Expression analysis of the inducible <i>hsp70</i> gene under non-stress conditions in the embryonic zebrafish	62
3.2 Conserved expression of Hsp70 protein in embryonic chicken lens extracts and cell cultures	70
3.3 Functional analysis of <i>hsp70</i> during embryonic lens development in zebrafish	78
3.3.1 Morpholino modified antisense oligonucleotide mediated knockdown of <i>hsp70</i> yields small eye phenotype	78
3.3.2 Hsp70 protein levels are diminished in <i>hsp70</i> -MO injected embryos at 38 hpf under normal developmental and heat shock conditions	92
3.3.3 The small eye phenotype is characterized by an immature lens and disorganized retinal structure	95
3.3.4 The immature lens phenotype in <i>hsp70</i> -MO injected embryos is lens autonomous	101
3.3.5 Apoptotic nuclei persist in lenses of <i>hsp70</i> -MO injected embryos beyond 48 hpf	105
3.3.6 Recovery of overall lens and retinal organization in <i>hsp70</i> -MO injected embryos by 5 days post fertilization	108
3.4 Analysis of the role of HSFs in the regulation of <i>hsp70</i> expression during embryonic lens development in zebrafish	109
3.4.1 Amino acid sequence analysis of zebrafish HSFs	112
3.4.2 Morpholino modified antisense oligonucleotide mediated knockdown of HSF1 yields small eye phenotype in 2-day-old embryos	115
3.4.3 The <i>hsf1</i> -MO induced small eye phenotype is characterized by an immature and disorganized retinal structure	122

3.4.4 HSE binding activity is reduced in <i>hsf1</i> -MO injected embryos	125
3.4.5 Hsp70 protein levels are diminished in <i>hsf1</i> -MO injected embryos at 38 hpf under normal developmental and heat shock conditions	125
3.4.6 Microinjection of <i>hsf2</i> -MO or <i>hsfx</i> -MO does not phenocopy the <i>hsp70</i> -MO induced small eye phenotype	128
3.4.7 <i>hsf1</i> -MO injected embryos exhibited only partial recovery of lens and retinal organization by 5 days past fertilization	136
3.5 Analysis of thermoresistance in <i>hsp70</i> -MO and <i>hsf1</i> -MO injected	139
4.0 Discussion	143
4.1 <i>hsp70</i> is expressed during a short temporal window of lens development in zebrafish and at equivalent stages in the embryonic chicken lens	143
4.2 Morpholino modified antisense oligonucleotide mediated knockdown of <i>hsp70</i> expression results in a reproducible small eye phenotype in the embryonic zebrafish	147
4.2.1 Lens defects in the <i>hsp70</i> -MO induced small eye phenotype	148
4.2.2 Retinal defects in the <i>hsp70</i> -MO induced small eye phenotype	152
4.2.3 A model for Hsp70 function during apoptotic-like events associated with lens fibre differentiation	154
4.3 HSF1 is the major regulator of lens-specific <i>hsp70</i> expression in the embryonic zebrafish	156
4.4 Analysis of thermoresistance in <i>hsp70</i> -MO and <i>hsf1</i> -MO injected embryos	165

4.5 Thesis summary and conclusions	166
4.6 Future directions	168
References	170

## List of Tables

Table 3.1 Summary of <i>hsp70</i> -MO and control MO injection experiments	83
Table 3.2 Summary of <i>hsf1</i> -MO, <i>hsf2</i> -MO and <i>hsfx</i> -MO injection experiments	116



## List of Figures

Figure 1	Diagrammatic representation of the up-regulation of Hsp70 during the heat shock response	5
Figure 2	Zebrafish eye development	35
Figure 3	Diagrammatic representation of the functional basis of morpholino modified antisense oligonucleotides (MO)	51
Figure 4	Whole mount <i>in situ</i> hybridization analysis of <i>hsp70</i> mRNA	64
Figure 5	Diagrammatic representation of the eGFP reporter construct used to visualize <i>hsp70</i> promoter driven expression in live transgenic zebrafish embryos	67
Figure 6	Cell specific activation of the <i>hsp70</i> -eGFP transgene in a stable eGFP transgenic zebrafish line accurately mimics endogenous <i>hsp70</i> expression observed through <i>in situ</i> hybridization analysis	69
Figure 7	Histological analysis of 5.5 $\mu$ m methacrylate sections of whole mount <i>in situ</i> hybridization of <i>hsp70</i> mRNA	72
Figure 8	Western blot analysis of HSP70 in whole chick lens extracts	75
Figure 9	HSP70 protein expression as visualized by fluorescent immunocytochemistry on chicken lens cell cultures using confocal microscopy	77
Figure 10	Whole mount analysis of <i>chordin</i> -MO injected embryos.	81

Figure 11	Small eye phenotype in 52 hpf zebrafish embryos produced by microinjection of <i>hsp70</i> -MO into fertilized eggs	85
Figure 12	Bar graphs illustrating average changes in eye and pupil diameter, as well as body length, in <i>hsp70</i> -MO injected embryos relative to uninjected controls	88
Figure 13	Representative photographs of small percentage of embryos screened as non-specific phenotypes after microinjection of 3.46 $\mu\text{g}/\mu\text{l}$ <i>hsp70</i> -MO	90
Figure 14	Western blot analysis of Hsp70 knockdown in <i>hsp70</i> -MO injected embryos	94
Figure 15	Histological analysis of small eye phenotype in <i>hsp70</i> -MO injected embryos and uninjected control embryos at 52 hpf	97
Figure 16	Immunohistochemical analysis of lens and retinal protein expression in wildtype and <i>hsp70</i> -MO induced severe small eye paraffin sections	100
Figure 17	Histological analysis of lens transplant experiments at 52 hpf	104
Figure 18	Analysis of TUNEL positive nuclei and PCNA expression in uninjected control embryos and small eye phenotype embryos at 36 hpf and 52 hpf.	107
Figure 19	Histological and morphological analysis of <i>hsp70</i> -MO induced small eye phenotype and uninjected control embryo at 5 dpf	111
Figure 20	Amino acid sequence comparison of zebrafish HSFs	114
Figure 21	Small eye phenotype in 52 hpf embryos produced by microinjection of 2.25 $\mu\text{g}/\mu\text{l}$ <i>hsf1</i> -MO into fertilized eggs	118

Figure 22	Bar graphs illustrating average changes in eye and pupil diameter, as well as body length, in <i>hsf1</i> -MO injected embryos relative to uninjected controls	121
Figure 23	Histological analysis of small eye phenotype in <i>hsf1</i> -MO injected embryos and uninjected control embryos at 52 hpf	124
Figure 24	Gel mobility shift analysis of HSF1 activity in uninjected and <i>hsf1</i> -MO injected embryos under control and heat shock conditions	127
Figure 25	Western blot analysis of decrease in Hsp70 levels in <i>hsf1</i> -MO injected embryos	130
Figure 26	Histological analysis of <i>hsf2</i> -MO injected embryos at 52 hpf	133
Figure 27	Histological analysis of <i>hsfx</i> -MO injected embryos at 52 hpf	135
Figure 28	Histological and morphological analysis of <i>hsf1</i> -MO induced small eye phenotype and uninjected control embryo at 5 dpf	138
Figure 29	Analysis of thermoresistance in MO injected embryos	142

## List of Abbreviations

AIF- apoptosis inducing factor  
Apaf-1- apoptosome assembly factor  
ATP - adenosine triphosphate  
BCIP – 5-Bromo-4-chloro-3-indoyl-phosphate  
Bcl-2- b-cell lymphoma 2  
BSA – bovine serum albumin  
°C – degrees Celsius  
CARD- caspase activation and recruitment domain  
cDNA – complementary deoxyribonucleic acid  
cGMP – cyclic guanine monophosphate  
CNS – central nervous system  
cps – counts per second  
CTP – cytidine triphosphate  
DAB - diaminobenzidine  
DAPI – 4'6-diamidino-2-phenylindole  
dATP – deoxy adenosine triphosphate  
dCTP – deoxy cytidine triphosphate  
dGTP – deoxy guanosine triphosphate  
dTTP – deoxy thymidine triphosphate  
dpf- days past fertilization  
DD- death domain  
DED- death effector domain  
DEPC – diethyl pyrocarbonate  
DIABLO- direct IAP-binding protein with low pI  
Dig - Digoxigenin  
DNA – deoxyribonucleic acid

DR- death receptor  
DTT – dithiothreitol  
FADD- Fas receptor associated death domain  
ED – embryonic day  
EDTA – ethylenediamine tetraacetic acid disodium salt  
EGFP – enhanced green fluorescent protein  
ER – endoplasmic reticulum  
EtOH - ethanol  
GFP – green fluorescent protein  
Grp- glucose regulated protein  
GTP – guanosine triphosphate  
HCl – hydrochloric acid  
HEPES – N-2-hydroxyethylpiperazine-N-2-ethanesulfonic acid  
hpf – hours past fertilization  
HSE – heat shock element  
HSF – heat shock factor  
Hsc – heat shock cognate  
Hsp – heat shock protein  
IAPs- inhibitors of apoptosis  
kb - kilobases  
kDa - kiloDaltons  
M - molar  
mg - milligram  
ml - milliliter  
mM - millimolar  
mm - millimeter  
MeOH - methanol  
MO – morpholino modified antisense oligonucleotide  
mRNA – messenger ribonucleic acid  
NBT – 4-Nitro blue tetrazolium chloride  
NFZ- nuclear free zone

ng - nanogram  
nl - nanoliter  
nm – nanometer  
ORF – open reading frame  
OFZ – organelle free zone  
PBS – phosphate buffered saline  
PBST - phosphate buffered saline with 0.1% Tween-20  
PCR – polymerase chain reaction  
PCNA – proliferating cell nuclear antigen  
PFA - paraformaldehyde  
pmol - picomoles  
psi – pounds per square inch  
RNA – ribonucleic acid  
RNAi – ribonucleic acid interference  
SDS – sodium dodecylsulfate  
SDS-PAGE - sodium dodecylsulfate polyacrylamide gel electrophoresis  
sHsp – small heat shock protein  
SMP – skim milk powder  
SSC – standard saline citrate  
rRNA – transfer ribonucleic acid  
TNF- tumor necrosis factor  
TRADD- tumor necrosis factor receptor associated death domain  
TRAIL- tumor necrosis factor receptor apoptosis inducing ligand  
TUNEL - Terminal deoxynucleotidyl transferase-mediated dUTP fluoroscein nick-  
end labeling  
UTP – uridine triphosphate  
UTR – untranslated region

## 1.0 Introduction

### 1.1 General introduction

The development of the vertebrate embryo proceeds through a complex series of differentiation events and cell-cell interactions. This developmental program requires the correct synthesis, processing, translocation, and secretion of numerous transcription factors, growth factors, and cell surface receptors in a critical temporal sequence. Collectively, these processes govern the formation of the specialized cells and tissues necessary for the proper function of that organism. For example, the vertebrate eye is regarded as one of the most complex organs to arise during development, and the accurate performance of the eye requires the cooperation of many cell types with fundamentally different structures and functions, each directed by a specific genetic regime.

A revolution in molecular techniques and gene manipulation has focused developmental biology to the genetic level. In particular, the development of mutagenesis technology led to the isolation of genes that are important in development. For example, *Drosophila melanogaster* mutagenesis screens demonstrated that many genes with important functions in fly development have conserved counterparts in vertebrates, and frequently whole families of vertebrate genes were isolated by molecular screening for homology to specific *Drosophila* genes (Haffter and Nusslein-Volhard, 1996). The function of these genes could then be studied using powerful gene knockout techniques developed in rodent models (Galli-Taliadoros et al., 1995). Alternative loss of function techniques suitable for use in non-mammalian model systems, such as antisense technology like RNAi (Bosher et al., 2000) and the introduction of MO (Nasevicius and Ekker, 2000), were subsequently developed. These approaches are now commonly used in a variety of model systems.

Studies of gene function in diverse organisms have revealed that regulation at the level of mRNA and protein synthesis is an important component of an organism's developmental program. However, an understanding of the post-translational processes regulating developmental events is more limited. A number of studies have shown that the interaction of proteins with intracellular molecular chaperones, many of which have been identified as Hsps, plays an important role in the correct assembly and localization of developmentally important molecules. Although originally regarded as "housekeeping" proteins with only minimal developmental significance (Mayer and Bakau, 1998) recent evidence implicates Hsps as critical molecules in vertebrate development.

## **1.2 Introduction to heat shock proteins**

The heat shock response was first identified as the appearance of "puffs" on *Drosophila* polytene chromosomes. These puffs represent regions of increased transcription and translation following exposure of cells to elevated temperatures (Ritossa, 1962). Subsequent isolation of the genes up-regulated during the heat shock response lead to the characterization a group of proteins aptly named heat shock proteins (Hsps). Presently, Hsps are recognized as a set of highly conserved proteins, up-regulated in response to a broad range of biological stressors, including heat shock, alcohol, inhibitors of energy metabolism, heavy metals, oxidative stress, fever, or inflammation (Feder and Hoffmann, 1999). In fact, it is likely that Hsps evolved in order to allow organisms to adapt to changing cellular environments (Beere and Green, 2001).

Hsps are grouped into families based upon their approximate molecular weight. The most well characterized families include Hsp100, Hsp90, Hsp70, Hsp60, Hsp47, and the low molecular weight or small Hsps (generally ranging from 17-30 kDa). DNA and amino acid sequence analysis indicates these families are highly conserved across diverse biological phyla from bacteria to plants to higher mammals (Iwama et al., 1998). Typically, each family has several members, and each member may be targeted to different sub-cellular compartments.

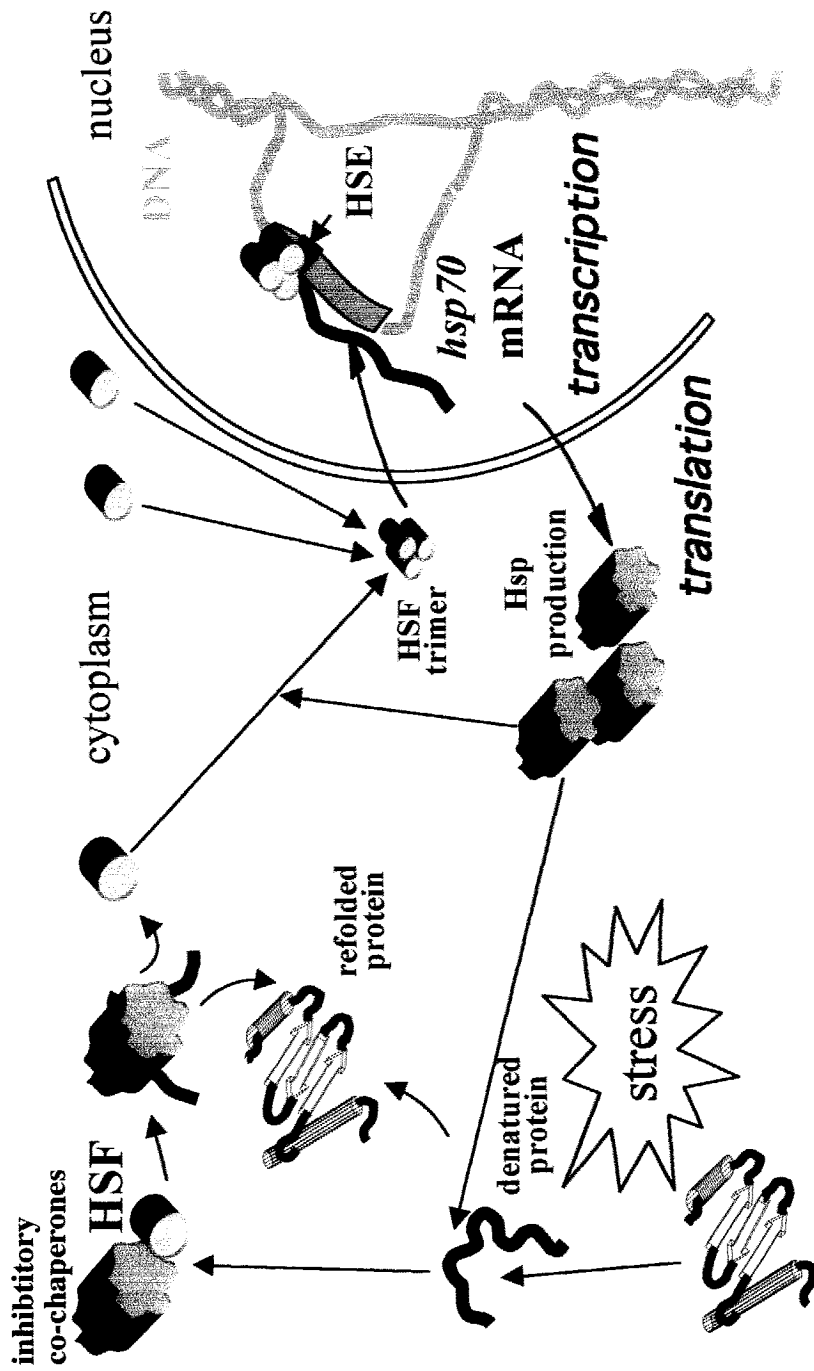


### 1.3 The heat shock response

Conditions that affect protein structure, for example heat shock, can trigger conformational changes to cellular proteins, causing the exposure of hydrophobic regions that are normally buried within the protein. Consequently, these aberrantly folded proteins aggregate and lose their function (Mosser et al., 2000). The accumulation of misfolded proteins within the cell can overwhelm the chaperoning capacity of the constitutively expressed heat shock cognate proteins (Hscs), and as a means of compensating, the inducible Hsps are up-regulated. Once present within cells, Hsps bind to denatured or non-native client proteins and assist in the systematic refolding of client proteins to their native state in order to restore proper function. For this reason, Hsps are often referred to as molecular chaperones.

The synthesis of heat shock genes following exposure to cellular stress is mediated by the binding of a transcriptional activator, HSF, to a short highly conserved sequence known as the heat shock element (HSE), found in the upstream region of the promoters of heat shock genes (Morimoto, 1998). Current models of heat shock response regulation suggest that HSF monomers form hetero-complexes with several chaperone and co-chaperone proteins in the unstressed state (reviewed in Voellmy, 2004). These molecules are believed to minimally include Hsp70, Hsp90, Hsp40, p23, and Hop. However, when cells experience proteotoxic stress, these chaperones and co-chaperones are recruited to interact with denatured or non-native client proteins, causing Hsps to become depleted within the cell. As a result the HSF heterocomplex breaks down and unbound HSF monomers are left free within the cell, where they rapidly trimerize into a transcriptionally active form. Active trimers migrate to the nucleus and bind to the HSE, subsequently leading to rapid transcription and translation of Hsps. Once all of the damaged client proteins are bound by Hsps, excess Hsps begin to once again interact with HSF, dissociating active HSF trimers, and returning HSF to the inactive, heterocomplexed form (Figure 1).

**Figure 1.** Diagrammatic representation of the up-regulation of Hsp70 during the heat shock response. In the unstressed state HSF monomers are complexed with several chaperones and co-chaperones including Hsp70 and Hsp90. As stress occurs, these chaperones are recruited to interact with denatured target proteins, releasing HSF monomers into the cytosol. HSF monomers interact to form active trimers in the cytosol and enter the nucleus. The active trimer binds to the heat shock element (HSE) found in the promoter of *hsp70* and other Hsp encoding genes, driving its transcription into mRNA. *hsp70* and other Hsp-encoding mRNAs are transported out of the nucleus, translated in the cytosol, and begin to interact with target proteins. Eventually, all denatured proteins are chaperoned and any additional chaperones produced allow for HSF monomerization.



It should be noted that the regulation of HSF activity is a far more complex process than described here. Studies have demonstrated that the activation and repression of HSF is a multistep process, and involves the step-wise interaction of several molecules with HSF at discrete intervals.

#### **1.4 Heat shock proteins and development**

The functions of Hsps are not limited specifically to the stress response. Under non-stress conditions, Hsps have multiple functions within the cell such as assisting in the folding and translocation of newly synthesized proteins. Hsps also function during the activation of specific regulatory proteins including transcription factors, replication proteins and kinases. Finally, Hsps also play roles in protein degradation, protein signaling (including steroid hormone activation) and antigen presentation (Zylicz and Wawrzynow, 2001). For this reason some Hsps have largely been considered as "housekeeping" proteins that are expressed at high levels in all cell types. However, an increasing number of studies are now demonstrating that Hsps are required for the execution of specific developmental events in a variety of organisms. These studies have shown that Hsps can function over a range of developmental processes, including tissue formation, growth, survival, and even morphological evolution. Thus, Hsps possess the capacity to function beyond those roles classified as "housekeeping".

##### **1.4.1 The small heat shock protein family and development**

Small heat shock proteins (sHsps) encompass a large family of related proteins whose molecular masses range between 15-30 kDa. The uniting factor among sHsps is a conserved 80-100 amino acid domain that is also found in vertebrate  $\alpha$ -crystallin. Indeed, vertebrate  $\alpha$ -crystallins are included in this family as studies have shown they are up-regulated by stress and possess many of the same structural and functional properties of other sHsps (Arrigo and Landry, 1994). A number of *in vivo* functions have been suggested for sHsps, including chaperone

activity, a role in actin microfilament assembly, cellular differentiation (Heikkila, 2003; Arrigo and Landry, 1994), and alleviating oxidative stress (Arrigo, 1998). While research in the past has revealed much about the functional significance of sHsps in cultured cells and in stressed states, comparatively little is known about their functions *in vivo* during normal development.

A significant amount of early information regarding the basic biochemistry and biology of sHsps has come from studies in yeast. Hsp26 is a sHsp of the budding yeast *Saccharomyces cerevisiae*. Hsp26 shares several features with higher eukaryotic sHsps, including the conserved C-terminal  $\alpha$ -crystallin domain. In addition, Hsp26 exhibits heat induced up-regulation and the ability to form large multimeric protein complexes *in vivo*. Furthermore, Hsp26 is expressed constitutively in *S. cerevisiae* during the transition from log to stationary phase, and during sporulation (Kurtz, 1986). This expression profile suggests a role for Hsp26 during very specific life cycle events. However, loss of function studies have shown no discernable consequence for the inhibition of Hsp26 (Petko and Lindquist, 1986). Specifically, the ability of *hsp26* *-/-* cells to grow or develop at high temperatures, withstand toxic effects at any point of the life cycle, or establish thermotolerance was unaffected. An effect on sporulation or cell division was also absent, despite the constitutive expression of Hsp26 during these processes.

Although loss of function studies of Hsp26 did not demonstrate a specific requirement for this molecule during the yeast life cycle, another sHsp has been shown to be critical in life cycle events of the brine shrimp (*Artemia franciscana*). *Artemia* embryos inhabit waters that are characterized by constantly fluctuating abiotic and biotic factors such as temperature and food availability. In order to cope with such variable conditions, *Artemia* has evolved the ability to disperse encysted larvae enclosed in an impermeable shell, creating a stable environment (McRae, 2003). Encysted larvae enter a genetically programmed state of dormancy called diapause, where development is arrested and metabolism significantly reduced. As a result encysted larvae can withstand severe physiological stresses such as prolonged anoxia. *Artemia* cysts exit diapause in response to the presence of favourable conditions and resume normal growth. Interestingly, the expression of large

amounts of p26, a sHsp with a conserved  $\alpha$ -crystallin domain (Liang and McRae, 1999), is associated with *Artemia* diapause. This observation implies a developmental role for p26 in encysted *Artemia* larvae. For example, p26 may be involved in inhibiting and restarting the cell cycle upon entry or exit of diapause, respectively (Day et al., 2003).

Possessing a stage in its life cycle that evolved to cope with unfavourable environments makes *Artemia* a unique model system for investigations regarding the recruitment of sHsps during development. However, traditional model systems such as *Drosophila melanogaster* and *Caenorhabditis elegans* also exhibit constitutive sHsp expression in specific tissues during normal development, and a requirement for some of these molecules during particular developmental events has been shown. In *Drosophila*, three members of the sHsp family are expressed under normal conditions. Each appears at specific stages of development in a variety of tissues and cells, suggesting *Drosophila* sHsps possess multiple functions. For example, Hsp23 is expressed in certain glial cells (Haass et al, 1990) and in salivary glands (Arrigo and Ahmed-Zadeh, 1981). Hsp23 and Hsp27 have been shown to be expressed during the third instar larvae and to be induced by the molting hormone  $\beta$ -ecdysone (Cheney and Shearn, 1983; Michaud et al., 1997). Hsp23 expression continues until the pupal stage when expression becomes reduced (Arrigo, 1987; Michaud et al., 1997). These data suggest that sHsps may also be important in *Drosophila* life cycle progression. Finally, several sHsps are localized to the male reproductive tissues. Hsp23 is constitutively expressed in somatic derived cell types such as cyst cells and epithelial cells of the seminal vesicle (Michaud et al., 1997). Hsp26 is expressed in spermatocytes, nurse cells, and epithelium (Glaser et al, 1986). Hsp27 also displays gonad specific expression in spermatocytes, cyst cells and accessory gland (Michaud et al., 1997).

The diverse expression patterns of *Drosophila* sHsps, suggests that these molecules have been recruited to perform an assortment of functions. Interestingly, it appears that one of these functions lies in the regulation of the aging process. Current theory speculates that aging is, in part, the result of the accumulation of free radicals which impair cellular functions by damaging DNA, lipids, and proteins

(Raha and Robinson, 2000; Raha and Robinson, 2001). As molecules involved in preventing proteotoxic stress, Hsps were identified as possible regulators of aging. Subsequent studies in *Drosophila* revealed that several molecular chaperones were up-regulated during aging, including the sHsps Hsp22 and Hsp23 (King and Tower, 1999; Wheeler et al., 1995). Specifically, Hsp22 is up-regulated 60-fold in the head and 16-fold in the thorax, while the level of Hsp22 is up-regulated 5-fold in the thorax (King and Tower, 1999). Overexpression of Hsp22 resulted in a 30% increase in *Drosophila* lifespan. Similarly, over-expressing Hsp23 caused a 15% increase in lifespan (Morrow and Tanguay, 2003). Finally, in the absence of Hsp22 expression in *Drosophila*, flies show a 40% decrease in lifespan (Morrow et al., 2004).

The nematode *C.elegans* has been used extensively as a model system to investigate the aging process. Research into this area has shown that sHsps also play key roles in *C. elegans* aging (Walker and Lithgow, 2003). In particular, Hsp16 was expressed at high levels in a long-lived mutant strain (Walker et al., 2001). Interestingly, Hsp16 expression may be influenced by HSF1, as HSF1 depleted worms exhibited markedly reduced life spans (Morley and Morimoto, 2004). These data confirm that sHsps are important molecules in the aging process and that their functions may be conserved. Furthermore, the correlation between lifespan and the stress response suggests that the ability to sense and respond to changing environments may be important for the regulation of aging.

In addition to their role during the aging process in *C. elegans*, sHsps are also expressed constitutively during development, and are primarily associated with the reproductive tissues. Members of the *hsp12* gene family are abundant in the spermatheca and specific vulval cells under non-stress conditions, where members of the *hsp16* gene family show a similar pattern of expression in spermathecae and vulva cells (Candido, 2002), but exhibit additional expression in intestinal cells. Comparisons of amino acid sequences show that *hsp16* has extensive homology to the sHsps of *Drosophila* and also to mammalian  $\alpha$ -crystallin (Candido, 2002). *hsp25* is also expressed in the spermathecae, but exhibits additional constitutive expression in body wall muscle (Ding and Candido, 2000). Interestingly, the small

heat shock protein, Hsp27, is localized to the developing male gonad in mice (Biggiogera et al., 1996), while *hsp25* is specifically expressed in the Sertoli cells of mice (Welsh et al., 1996). Thus, sHsps may play a conserved role in the developing reproductive system across diverse animal phyla.

As well as being associated with the male reproductive tissues in mice, several studies have correlated constitutive *hsp25* expression with the development of the heart and with cardiomyocyte differentiation (Davidson and Morange, 2000). Unexpectedly, deletion mutants of a closely related sHsp, *hspB2*, did not display any cardiac abnormalities in *hspB2* deletion mutants, despite being abundantly expressed in cardiac cells (Brady et al., 2001; Christians et al., 2003). Additionally, *hsp25* is expressed in glia and neurons, as well as during chondrogenesis, where *hsp25* becomes highly expressed during the transdifferentiation of chondrocyte to osteoblast like cells *in vivo* (Loones and Morange, 1998; Christians et al., 2003). However, its function within these tissues remains unknown.

The precise functions of sHsps during heart, CNS, and chondrogenesis has yet to be established, despite their expression in these very specific tissue types. A similar situation exists for the role of *hsp27* in the developing eye. *hsp27* expression has been observed in the developing ommatidia in *Drosophila*, (Pauli et al., 1990) and in developing rat retinal ganglion cells (Hawkes et al., 2004). Unfortunately, a specific developmental role for Hsp27 was not elucidated in either system. In contrast, investigations of  $\alpha$ -crystallins have identified specific roles for these molecules during eye development. As stated previously,  $\alpha$ -crystallins possess chaperone activity, are heat inducible, and are members of the sHsp family.  $\alpha$ A- and  $\alpha$ B-crystallin knockout mice have been generated to better understand their functions *in vivo*.  $\alpha$ A-crystallin  $-/-$  mice displayed several abnormalities in the developing ocular lens (Brady et al., 1997). Initially,  $\alpha$ A-crystallin mutant lenses appeared normal but were smaller than wildtype. However, lenses developed a progressive opacification that became apparent several weeks after birth. Lens fibre cells in  $\alpha$ A-crystallin mutants also contained an insoluble form of  $\alpha$ B-crystallin, indicating that  $\alpha$ A-crystallin may ensure lens clarity by maintaining  $\alpha$ B-crystallin (or closely associated proteins) in a soluble form. In contrast,  $\alpha$ B-crystallin



knockout mice do not result in altered lens morphology or the development of cataracts (Andley et al., 2001). Instead, lens epithelial cells are hyperproliferative and demonstrate genomic instability.  $\alpha$ -crystallins compose a third of lens fibre proteins (de Yong, 1981) and a fundamental role for both  $\alpha$ A and  $\alpha$ B-crystallin in lens development is not unexpected.

#### 1.4.2 Heat shock protein 47 and development

Hsp47 is a heat inducible glycoprotein residing in the endoplasmic reticulum (ER) (Nagata, 1989). Although heat inducible, *hsp47* also displays patterns of constitutive expression during normal embryonic development. In mouse and chick embryos, *hsp47* is expressed in fibroblasts of connective tissue of various organs, smooth muscle cells of the gastrointestinal tract, epithelium of kidneys, and the basal layer of the epidermis (Nagata et al., 1986; Nagata, 2003; Masuda et al., 1998; Miyashi et al., 1992 ). Furthermore, the expression of *hsp47* correlates with that of various types of collagen in both a spatial and temporal manner (Nagata, 1996). The constitutive expression of *hsp47* and possible interactions with proteins as fundamentally important as collagens, led researchers to investigate the role of *hsp47* in vertebrate development. In mouse, Hsp47 has been demonstrated to be a collagen specific chaperone, and is thus responsible for binding the most abundant protein in mammals (Nagata, 2003). The importance of *hsp47* in mammals is reflected in knock-out mice, which do not survive beyond 11.5 days postcoitus (Nagai et al., 2000). Prior to mortality, *hsp47* null mice (*hsp47* *-/-*) were characterized by small size and a decreased number of somites. Furthermore, the mature, propeptide form of type I collagen in mesenchyme was not observed. Maturation was partly restored by transient transfection of Hsp47 into *hsp47* *-/-* cell lines, indicating that Hsp47 is directly involved in the molecular maturation of type I collagen. Hsp47 also appears to be involved in maturing type IV collagens, as *hsp47* *-/-* embryonic stem cells show similar maturation defects, leading to abnormally formed basement membranes.

Data linking *hsp47* to collagen has also been obtained in zebrafish. In this system, *hsp47* is expressed in only a few tissues of early embryos, and the pattern of expression correlates closely both in a temporal and spatial manner with the gene encoding type II collagen, *col2a1* (Lele and Krone, 1997). In particular, the expression of these two genes is coordinate in the developing notochord of early stage embryos, while in later stage embryos, precartilagenous cells of the otic vesicle and fins also co-express the two genes. These data suggest a conserved function for *hsp47* acting as a collagen chaperone in lower vertebrates. However, not all tissues expressing the type II collagen gene also express *hsp47*. The floor plate and hypochord express *col2a1* but not *hsp47*, while the lens expresses *hsp47* but lacks *col2a1* expression. Thus, a clear understanding of the function of *hsp47* and collagens remains unknown.

#### **1.4.3 The 70kDa heat shock protein family and development**

The *hsp70* gene family includes all those stress proteins ranging in size from 66 to 77 kDa. They represent the most abundant and widely conserved group of Hsps, showing a high degree of homology across both the plant and animal kingdoms (Ryan and Hightower, 1999). In addition, members of the 70-kDa family are found in all cellular compartments including the ER, mitochondria, chloroplasts, nucleus, and cytoplasm (Morimoto et al., 1994). Mammals have at least four members: Hsc70, Hsp70 (cytoplasmic and highly stress-inducible), the mitochondrial equivalent of Hsp70, termed mt-Hsp70 or Grp75, and a glucose-regulated protein localized to the ER, Grp78 (Ryan and Hightower, 1999). The latter two proteins assist in transportation of proteins in/out of their respective organelles, while Hsp70 and Hsc70 complex with co-chaperones to facilitate proper protein folding. The protein-binding activity of Hsp70 is mediated through an interaction between the 15 kDa C-terminal peptide-binding domain, found in all members of the Hsp70 family, and exposed hydrophobic residues on unfolded or denatured proteins. Binding and release of the misfolded protein is regulated by ATP binding and hydrolysis, occurring in a 44 kDa region in the N-terminal ATPase domain. It is

this rapid series of association and disassociation cycles that allows proteins to return to their native conformations. The chaperoning activity of Hsp70 is further regulated by the binding of co-chaperones, such as Hsp40, that catalyze the binding-release cycle (Beere and Green, 2001). The following section will focus on the role of the cytoplasmic stress inducible Hsp70 genes, and their expression and function during development.

Hsp70 is the most intensely studied Hsp, and has been characterized in a range of eukaryotic systems. In *S. cerevisiae*, several homologs of the Hsp70 family have been classified into 5 subfamilies based upon structural and functional similarities and localization within the cell. Of these subfamilies, the *ssa* gene family exhibits the highest homology to mammalian *hsp70* and is predominantly expressed in the cytosol (Oka et al, 1998). The family consists of four functionally redundant members (*ssa1-ssa4*) and the effects of null alleles within these genes have been investigated. For example, targeted disruption of the *ssa1* and *ssa2* genes rendered cells temperature sensitive for growth at 35°C or higher, while adding a *ssa4* null allele did not permit growth at any temperature (Werner-Washburne, 1987).

Other organisms also express multiple *hsp70* genes. *Drosophila* has six nearly identical genes that encode members of the Hsp70 family, some of which are expressed constitutively during development. However, expression of the major heat inducible *hsp70* gene is virtually undetectable at normal growth temperatures (Parsell and Lindquist, 1994). Exactly why *hsp70* is not expressed under non-stress conditions in *Drosophila*, despite being expressed constitutively and playing critical roles in the development of several other eukaryotic organisms, is currently unknown. One possibility is that constitutive *hsp70* expression may actually be damaging to the developing fly. Several studies have revealed that *Drosophila* cells expressing Hsp70 protein at normal temperatures exhibited reduced growth and/or cell division (Feder et al., 1992). Furthermore, tissues undergoing a high rate of cell division, such as the preblastoderm, are not even capable of synthesizing Hsp70 (Parsell and Lindquist, 1994). Furthermore, a *D. melanogaster* strain from sub-equatorial Africa has a dramatically reduced ability to express *hsp70*. It is

hypothesized that this represents an adaptation to living in chronically elevated temperatures, and evolved to suppress the deleterious effects of continuous *hsp70* expression on normal growth (Zatsepina et al., 2001). Finally, genomic deletions of all *hsp70* genes of *Drosophila* had no discernable defects on flies raised at normal growth temperatures, and *hsp70* null flies were viable and fertile (Gong and Golic, 2004). Thus, evidence to date indicates that although Hsp70 is required for normal growth in yeast, Hsp70 function in *Drosophila* has evolved primarily as a stress-response mechanism.

The absence of a defined role for *hsp70* in *Drosophila* development contrasts with that of higher animals, where *hsp70* plays clearly defined, and important roles in development. Constitutive expression of stress-inducible *hsp70* genes has been detected in amphibian oocytes (Billoud et al., 1993), where it is speculated that *hsp70* may be required for oocyte maturation or be involved in activation of the zygotic genome. In mammals, several members of the *hsp70* gene family are strictly required for proper embryonic and post-embryonic development. These functions have been best described in mouse, where the *hsp70* family consists of several members. *hsp70.1* and *hsp70.3* encode the major inducible Hsp70 proteins expressed throughout the organism upon stress, but are also expressed constitutively in a temporal and spatial manner. *hsp70.1* and *hsp70.3* are first expressed in the preimplantation mouse embryo, with a peak occurring at the two-cell stage (Dix et al., 1998). Dix et al. (1998) demonstrated that inhibiting expression using antisense oligonucleotides complimentary to the start codon region of *hsp70.1* and *hsp70.3* severely disrupted normal development of blastocysts. Although blastomeres continued to divide and compact into a morula, the organization of the trophectoderm was affected, and did not expand to fill the zona pellucida as normal. Furthermore, the cells of the inner cell mass remained loose, and unconnected. The authors speculated that the early expression of *hsp70* may be required to maintain axis symmetry from blastocyst to morula, or play a role in regulating the cell cycle. A second study of *hsp70.1* and *hsp70.3* addressed their role in later embryonic and adult development (Huang et al., 2001). Huang et al (2001) generated mice deficient in *hsp70.1* and *hsp70.3* by replacing coding sequences with

an in frame sequence for  $\beta$ -galactosidase.  $\beta$ -galactosidase expression showed that *hsp70.1* and *hsp70.3* did not differ in their tissue-specific constitutive expression and were detected in the nasopharyngeal area at mid-gestation (E12.5), and later (E14) across the entire skin surface. At E17, expression of these genes was still detected over the entire epidermis, and also in the cornea, tongue, lips, gastrointestinal tract, and within the urinary system. These patterns were maintained in adult mice. Surprisingly, *hsp70.1* and *hsp70.3* null mice were viable, fertile, and did not exhibit any phenotypic abnormalities as a result of the knock-out of these genes, although defects were observed upon heat induced stress.

Hsp70 knockout mice that exhibit defects only following heat shock illustrate that developmental processes can be affected by temperature fluctuations. This concept is especially evident in tissues that are extremely temperature sensitive. For example, the testes are an externally located organ in mammals, and are maintained at temperatures 5-7°C cooler than normal body temperature. Even slight increases in temperature can induce protein denaturation and affect spermatogenesis (Christians et al., 2003; Eddy, 1999). For this reason, the testes have developed a lower activation threshold for the heat shock response, as well as testes specific chaperones, such as Hsp70.2. Hsp70.2 is found at elevated levels in developing mammalian spermatocytes, where it is associated with synaptonemal complexes (Dix et al., 1996). During the zygotene stage of meiotic prophase, axial elements of homologous chromosomes align and synapse to form synaptonemal complexes (Dix et al., 1997; Moses, 1968). Synaptonemal complexes remain synapsed in pachytene stage spermatocytes, but desynapse during diplotene as the chromosomes begin to condense. The synaptonemal complexes are required for the completion of meiotic prophase, and are thus critical to cell division. Mice deficient in Hsp70.2 lacked post-meiotic spermatids, mature sperm, and were infertile. These defects were correlated to the inability of Hsp70.2 deficient mice to desynapse their chromosomes during diplotene. As a result, spermatocytes arrested in the late pachytene stage, failed to complete meiotic prophase, and underwent apoptosis (Dix et al., 1997). Interestingly, Hsp70.2 is also a chaperone of the cell cycle protein Cdc2 in pachytene spermatocytes, and the CyclinB1/Cdc2 complex failed to form in

*hsp70.2* mutant mice (Zhu et al., 1997). Thus, it is likely that absence of the CyclinB1/Cdc2 complex is one reason for the failure of Hsp70.2 deficient spermatocytes to complete meiosis. Currently a link between the CyclinB1/Cdc2 complex and the synaptonemal complex has not been established.

Collectively, knockout studies have demonstrated that Hsp70 function is required for the post-embryonic processes involved in sperm production and fertility, as well as events associated with very early mammalian development such as cleavage of blastocysts. Thus, members of the *hsp70* gene family play critical roles in both early and late mammalian development, and their functions are required for fundamental processes such as fertility and cell division.

#### **1.4.4 The 90kDa heat shock protein family and development**

Members of the Hsp90 family of chaperones are unique among heat shock proteins in that most of their identified targets are involved in signal transduction and chromatin organization. For this reason, previous research on Hsp90 has focused on these pathways, and on *in vitro* functions. Consistent with Hsp90 mediating important cell signaling pathways, *Drosophila* Hsp90 (encoded by the *hsp83* gene) is involved in intracellular signaling events linked to compound eye formation. Mutagenesis screens revealed Hsp90 is required for proper Raf kinase and Sevenless functions, important signaling molecules involved in formation of ommatidia, the individual units comprising the compound eye. Dominant negative mutations in *hsp83* cause a reduction in the kinase activity of Raf (van der Straten et al., 1997) and reduce Sevenless (Cutforth and Rubin, 1994) signaling such that the R7 cells of the ommatidia acquire a non-neuronal fate. Although these Raf mutants are sterile, flies are viable, and do not exhibit any other significant abnormalities outside the compound eye. Such data suggest that some protein function remains in these mutants, as complete loss of function in *hsp83* has been shown to be lethal in *Drosophila*. Furthermore, the sterility of *hsp83* mutants is not surprising given recent data revealing a critical role for Hsp90 in *Drosophila* spermatogenesis (Yue et al., 1999). Using the viable, but sterile mutants identified previously (van der

Straten et al., 1997; Cutforth and Rubin, 1994), it was shown that Hsp90 was associated with microtubules, and affects all stages of spermatogenesis involving microtubule function. This result is supported by the presence of aberrantly formed microtubules in yeast *hsp90* mutants, and indicates that Hsp90 function may be conserved (Yue et al., 1999).

Although early research was dominated by investigations into the role of Hsp90 during signal transduction, more recently Hsp90 research has diverged, and novel functions for Hsp90 in a variety of cellular processes has emerged. For example, in the nematode *C. elegans*, mutation of a single allele in the *daf-21* gene encoding Hsp90 results in significant chemosensory defects, leading to the constitutive formation of the dauer larvae in the absence of normally required temperature and food inducing signals (Birnby et al., 2000). The mutant phenotype is correlated to reduced levels of cGMP, an important second messenger in signal transduction pathways, and suggests that Hsp90 is a component of these pathways. Interestingly, *C. elegans daf-21* mutants also possess defects related to fertility, and *daf-21* mutants have decreased brood sizes (Vowels and Thomas, 1994). Combined with the spermatogenic defects described in *Drosophila*, this evidence strongly suggests a role for Hsp90 in fertility. Thus Hsp90, the sHsps and Hsp70 may all function during reproductive processes. These data indicate that several families of Hsps may be critical components of an extremely important and fundamental process.

Although, mutational analysis has proven useful for analyzing Hsp90 function in *Drosophila* and *C. elegans*, expression profiling has shown Hsp90 to be expressed at several points in later embryonic development in these organisms. Analyzing Hsp90 function in late development can be challenging because traditional loss of function methodologies generally target only the first major developmental event in which a gene is involved, and in the case of *hsp90*, this typically results in early lethality. For example, Hsp90 null mutants in yeast die at all temperatures (Borkovich et al., 1989) and mutation of both alleles of the *daf-21* gene in *C. elegans* causes early larval lethality (Birnby et al., 2000). Recently, the use of an Hsp90 specific chemical inhibitor has circumvented these problems.

Geldanamycin has been shown to interact exclusively with Hsp90, and cause loss of function to a number of Hsp90 dependent signal transduction proteins (Neckers, 2002). Zebrafish embryos are very amenable to treatment using pharmacological agents, and subsequent treatment of embryos with geldanamycin prior to and during somitogenesis resulted in a reproducible short trunk and tail phenotype. The Hsp90-inhibited phenotype was correlated with a failure to form an early type of somitic muscle cell known as a muscle pioneer (Lele et al., 1999). Two *hsp90* genes, *hsp90 $\alpha$*  and *hsp90 $\beta$* , are expressed in zebrafish (as is the case in all vertebrates; Krone and Sass, 1994). The *hsp90 $\alpha$*  gene is activated specifically during striated muscle development in the somite, and the muscle pioneers are the first developing muscle cells to express the gene (Sass et al., 1996). Thus, the somitic phenotype induced by geldanamycin appears to be the result of failure of muscle pioneer formation due to inhibition of Hsp90 $\alpha$  function during its development.

An additional role for Hsp90 $\alpha$  in fish development has emerged from studies of the cavefish, *Astyanax mexicanus*. This species of teleost consists of an eyed surface dwelling form and numerous blind cave dwelling forms. Early eye structures are formed in the blind cave-dwelling form, but subsequently undergo apoptosis, arrest in development, and finally degenerate (Jeffery, 2001). The well-documented role of Hsps as regulators of apoptosis prompted an investigation into a possible link between Hsps and apoptotic degeneration of the cavefish eye (Hooven et al, 2004). *hsp70* was expressed in the lens of both cave and surface dwelling forms, and mimicked the expression observed in zebrafish. However, *hsp90 $\alpha$*  was expressed only in the degenerating lens of cave dwelling forms. *hsp90 $\alpha$*  expression peaked just prior to lens apoptosis and was reproducible in three separate cave-dwelling populations. Subsequent treatment with geldanamycin blocked TUNEL labeling for apoptosis in the lens, and suggested that *hsp90 $\alpha$*  plays a novel role in lens apoptosis and cavefish eye degeneration.

A function for the second *hsp90* gene expressed in vertebrates, *hsp90 $\beta$* , was not uncovered in fish. However, studies in mouse have revealed *hsp90 $\beta$*  is required for extraembryonic tissue development. The placenta provides essential nutrients required for fetal growth and disruption of its formation can cause major defects.



Although, several multigenic families of Hsps are expressed during placenta formation, only *hsp90 $\beta$*  has been demonstrated as essential. *hsp90 $\beta$*  null mutants developed normally until E9.5, at which point development was halted and embryos died a day later (Voss et al., 2000). Analysis of the mutant phenotype revealed allantois derived fetal blood vessels failed to expand and the trophoblast failed to differentiate into a labyrinthine trophoblast. Thus the network of blood vessels carrying maternal nutrients to the developing embryo was not established and as the yolk sac became inadequate to sustain further development, mutant embryos arrested and died a day later.

This literature review has illustrated that Hsp90 is capable of functioning within a wide range of fundamentally different processes. This point may be best exemplified by a recently described role for Hsp90 in the evolution of phenotypic diversity. Several studies in both plants (Queitsch et al., 2002) and animals (Sollars et al., 2003; Rutherford and Lindquist, 1998) have demonstrated that Hsp90 acts as a capacitor for phenotypic variation. Rutherford and Lindquist (1998) demonstrated that mutation or inhibition of Hsp90 function leads to the emergence of previously concealed phenotypes in *Drosophila*. Amazingly, the phenotypic variation occurred in seven different adult structures of the fly, discounting the possibility of a specific developmental effect. Furthermore, selection for the new variants caused the phenotypes to be assimilated into the population, and this occurred after Hsp90 levels were restored. Similar results were acquired using *Arabidopsis thaliana*, where chemical inhibition of Hsp90 produced an array of variant phenotypes. The authors propose a model whereby Hsp90 levels would become depleted through stress, leading to the uncovering of variant morphologies that are assimilated when the stress subsides and Hsp90 levels are restored. Presently, there exists evidence for both genetic and epigenetic factors leading to the assimilation of these new phenotypes (Ruden et al., 2003), but what is important is that reduction of Hsp90 can provide selectable traits that can be passed on to subsequent generations, and may have played a major role in the evolution of morphology and adaptation to new habitats across diverse phyla.

#### 1.4.5 Heat shock transcription factors (HSFs) and development

The expression of Hsps in eukaryotic cells is regulated by the binding of transcriptional activators, HSFs, to a conserved consensus sequence in the promoter regions of Hsp genes, the HSE (reviewed in Santoro, 2000; Morimoto, 1998; see Figure 1). Functional studies of HSFs have been conducted in a number of eukaryotic systems. Single copy genes encoding HSF exist in the budding yeast *S. cerevisiae*, in *C. elegans*, and in *Drosophila*. Subsequent mutation of HSF in yeast revealed that HSF expression is essential for cell viability at all growth temperatures (Sorger and Pelham, 1988). In the nematode *C. elegans*, evidence also suggests that HSF is involved in normal growth and development. In this system, RNA interference (RNAi) was used to disrupt HSF expression (Walker et al., 2003). Exposure of wildtype worms to HSF RNAi constructs resulted in developmental arrest at the L2/L3 stage at elevated temperatures. Interestingly, worms raised at normal physiological temperatures also exhibited abnormal growth, including a small and scrawny appearance, infertility, and reduced life span. A role for HSF in dauer larva formation was also suggested. Inhibition of HSF in dauer constitutive mutant backgrounds was sufficient to prevent the formation of dauer larvae (Walker et al., 2003).

The function of HSF in *Drosophila* development is more complex than in *C. elegans* and yeast. The analysis of several mutations traced to HSF reveal that HSF is required for mediating the heat shock response and for larval development and oogenesis (Jedlicka et al., 1997). Conversely, HSF appears dispensable for general cell growth or viability under normal conditions or moderate heat shock conditions. Unfortunately, the phenotypes of the HSF mutations do not provide insights into specific developmental defects, and are characterized by growth or developmental arrest without exhibiting conspicuous morphological defects. Furthermore, oogenesis and larval development represent processes characterized by extensive growth, division and differentiation events, making it difficult to identify candidate genes affected by HSF. However, developmental expression of Hsps in *Drosophila hsf* mutants is unaffected, suggesting that the target genes may not encode heat

shock proteins. These data suggest a potential novel role for HSF in regulating non-Hsp genes involved in *Drosophila* growth and development (Jedlicka et al., 1997).

Although the yeast, worm, and fly genomes encode only a single HSF protein, four related HSFs have been identified in vertebrates (HSF1-4) (Pirkkala et al., 2001). HSF1 is considered to be the functional homologue of *Drosophila* and yeast HSF, and plays a prominent role in activating the heat shock response (Morimoto, 1994). HSF3 is an avian specific HSF, and is believed to be activated following more severe cellular stresses (Tanabe et al., 1997). HSF2 and HSF4 do not respond to cellular stresses, and have been assigned largely developmental roles.

In mouse, gene-targeting approaches have provided insights into the functions of HSF1, HSF2, and HSF4. Knock-outs performed on *hsf1* in mouse confirmed this gene as the primary regulator of the Hsps during stress, as null mice (*hsf1*<sup>-/-</sup>) lacked a classical heat shock response (Xiao et al., 1999). *hsf1*<sup>-/-</sup> mice also displayed several morphological defects related to extraembryonic development and post-natal growth. Specifically, chorioallantoic placenta was abnormally developed, resulting in death in some individuals. In those surviving, the consequences of developing with a deficient placenta were manifested in post-natal development, and mice were significantly retarded in growth relative to wildtype and heterozygous individuals. In addition, *hsf1* knockout females are infertile due to the absence of essential but unknown maternal factors under the control of HSF1 (Christians et al, 2000; 2003).

In contrast to HSF1, HSF2 is not a major player in the stress response, and is typically thought to act as a regulator of heat shock gene expression during development and differentiation events. Gene expression profiles for *hsf2* suggest a role in the mammalian CNS (Rallu et al., 1997) and heart development (Eriksson et al., 2000), spermatogenesis (Sarge et al., 1994) and erythroid differentiation (Sistonen et al., 1992). However, data generated from *hsf2* knock-out mice have been contradictory in this respect. Kallio et al., (2002) reported that *hsf2* null mice suffered from defective meiotic chromosome synapsis and increased apoptosis in the testis. Specifically, developing spermatocytes were lost in a stage-specific manner and exhibited structural defects in synaptonemal complexes. These

abnormalities are likely the result of the inability of HSF2 to regulate *hsp70.2* gene expression in the testis. However, fertility problems in females were also prominent. *hsf2* null females were characterized by the production of abnormal eggs, a reduction in the number of ovarian follicles, and the presence of hemorrhagic cystic follicles. Finally, both genders displayed altered brain morphology, including an enlargement of the lateral and third ventricles, and a reduction in the hippocampus and striatum. Follow up studies by the same research group confirmed these findings (Wang et al., 2003; Wang et al., 2004). These results are in contrast to *hsf2* knockout mice generated by McMillan et al. (2002). In this study, *hsf2* null mice are reported to be viable and fertile, exhibiting normal lifespan and behavioral functions. Dissimilar phenotypes arising after the disruption of the same gene in knock-out approaches is not uncommon (Montagutelli, 2000). Factors such as genetic background and environmental conditions can influence phenotype. Despite these discrepancies in phenotype, none of these studies have reported cardiac or hematopoietic abnormalities, suggesting that HSF2 does not function in heart development or erythroid differentiation as originally speculated (Christians et al., 2003).

Similar to HSF2, HSF4 plays a prominent role in the regulation of genes under non-stress conditions, and has only minimal functions during the stress response. Although HSF4 is the most recently identified mammalian HSF, a surge of research has revealed HSF4 as an important player in mammalian development. HSF4 expression during development is restricted to certain tissues, including the eye in mice and humans (Bu et al., 2002), and several studies have investigated the role of HSF4 in mammalian eye development. In humans, a mutated DNA binding domain of *hsf4* is associated with cataract formation (Bu et al, 2002). Such a conclusion was supported in studies investigating HSF4 in murine development, where *hsf4* deletion mutants exhibited significant lens dysmorphology leading to post-natal cataracts (Min et al., 2004). The primary effect appears specific to terminal fibre cell differentiation, and may be the result of abnormal expression of *hsp25*, a known modifier of lens opacity and subsequent cataract development. In a second study, cataract formation and abnormal lens fibre differentiation were

correlated to reduced expression of  $\gamma$ -crystallin, an important factor in lens fibre cell differentiation (Fujimoto et al., 2004). Misexpression of several Hsps was also reported, suggesting the abnormal lens phenotypes may be in part due to aberrant interaction of Hsps with target proteins in the lens. Regardless, HSF4 plays a fundamental role in mammalian eye development, and HSF4 disruption is associated with relevant disease states, such as cataracts.

Currently, the avian family of HSFs does not include HSF4. However, birds have evolved a functionally distinct HSF called HSF3. HSF3 is co-expressed with HSF1 in chicken cells and tissues, suggesting that both factors are involved in mediating the stress response (Nagai and Morimoto, 1993). However, the activation thresholds of HSF3 and HSF1 appear to be unique, as HSF3 was detected predominantly in response to severe stress. In addition, the *hsf3* gene was ubiquitously expressed at high levels in early developmental stages, suggesting a function during normal embryonic development (Kawazoe et al., 1999). *hsf3* loss of function has been studied in cell cultures, where a severe reduction in heat shock response and thermotolerance was observed, despite normal levels of HSF1 (Tanabe et al., 1998). These results suggest that HSF3 may be the dominant HSF regulating the heat shock response in avian systems. Studies to date have not analyzed the role of HSF3 in the context of the whole animal, and a developmental requirement for HSF3 has not been established.

The zebrafish genome encodes at least three different HSFs. Two have been identified as HSF1 (GenBank Accession: NM\_131600; AF391099; AF159135; AF159134) and HSF2 (GenBank Accession: NM\_131867). The identity of the third zebrafish HSF has not been confirmed, but initial mRNA sequence analysis indicates that this transcript could encode a distantly divergent form of HSF4. Few studies have examined the role of HSFs under non-stress conditions in the zebrafish. Wang et al. (2001) were able to demonstrate a severe reduction in the expression of green fluorescent protein under the control of the *hsp70* promoter in heat shocked transgenic fish when injected with MO targeted to *hsf1* mRNA. The *hsf1* knockdown fish also displayed an increase in the number of apoptotic cells following heat shock, suggesting that heat shock gene function is indeed impaired.

Importantly, a specific developmental role for HSF1 in zebrafish was not suggested in this study.

## 1.5 Introduction to apoptosis

The term programmed cell death (or apoptosis) was initially used to describe cell deaths that occur in predictable places and times during development, to emphasize that the deaths were programmed into the developmental plan of that organism (Lockshin and Williams; 1964 Jacobson et al., 1997). Presently, that definition has changed, and apoptosis now refers to a cell autonomous process in which a specialized signaling pathway(s) is (are) active in killing the cell and organizing its disposal. Originally observed during amphibian metamorphosis (Vogt, 1842), apoptosis was soon discovered to occur in a variety of developing tissues in both vertebrates and invertebrates. However, it would be decades before the concept of "cellular suicide" became generally accepted, and only after genetic studies in *C. elegans* identified genes that were dedicated to the death program and its control, called *ced* genes (Horvitz et al., 1982). The argument was strengthened through the identification of *ced* homologues in mammals. Apoptosis is an extremely important process to both developing and mature organisms. For example, flies lacking a functional apoptotic pathway die early in development (Ellis et al., 1991). Furthermore, mice in which caspase-9 has been deleted by targeted gene disruption, die perinatally with a vast excess of cells in their CNS (Kuida et al., 1998).

Apoptosis serves a variety of functions during the development and maturation of eukaryotes, most of which involve the removal of unwanted cells. For example, apoptosis plays an essential role in the morphogenesis of body parts. The classical example of such a function is the removal of cells between the developing digits (Gilbert, 2000). Apoptosis is also active in hollowing out structures to form lumina, as is the case in the formation of the mouse pre-amniotic cavity (Coucouvanis and Martin, 1995). Cell death was known to occur where epithelial sheets evaginate and pinch off to form tubes and vesicles, as in the formation of the

vertebrate neural tube, lens, and palate (Glucksmann, 1951), and has since been demonstrated to occur via apoptosis. During the course of animal development many structures that are formed are later removed by apoptosis. This includes vestigial structures (such as the eyes of cavefish; Jeffery, 2001), structures that are required for one sex but not the other (such as the degeneration of the Mullerian and Wolffian ducts in male and female mammals, respectively), cells required transiently throughout development (such as subplate neurons necessary for proper cerebral cortex development), and cells originally overproduced in the developing animal (such as neurons and oligodendrocytes, which are produced in excess to ensure their numbers match that of the cells they innervate) (reviewed in Jacobson and Weil, 1997). In mature organisms, apoptosis is involved in a number of processes, including down-regulation of the immune response, menstruation, tumorigenesis, and the removal of cells with irreparable DNA damage. Thus, it is likely that cell deaths occurring in developing and mature organisms utilize the same evolutionarily conserved death program.

### **1.5.1 Apoptosis occurs through two signaling pathways**

Apoptosis can occur through two pathways, both of which are characterized by distinct changes in cell morphology including chromatin condensation, cytoplasmic shrinkage, membrane blebbing, nuclear fragmentation, and the formation of apoptotic bodies. One of these pathways is the mitochondrial or intrinsic pathway (reviewed in Garrido et al., 2001). Apoptotic signaling through this pathway is initiated in response to severe cell stress, and begins with the outer mitochondrial membrane becoming permeabilized, resulting in the release of proteins normally confined to the intermembrane space. These proteins translocate from the mitochondrion to the cytosol in a reaction that is controlled by Bcl-2 related proteins (Li et al., 1997). Membrane permeabilization is thought to arise via pore formation in the external mitochondrial membrane facilitated by proteins such as Bax and by physical disruption as a result of mitochondrial matrix swelling resulting from the formation of non-specific pores or net influx of ions or water

(Gross et al., 1999). One of the released intermembrane proteins is cytochrome c, which once in the cytosol interacts with Apaf-1 (apoptotic protease activation factor-1), where it triggers its oligomerization and exposes its CARD (caspase recruitment domain) domain. Oligomerized Apaf-1 then binds cytosolic procaspase-9, forming the apoptosome complex (Zou et al., 1999). Activated caspase-9 then triggers the proteolytic maturation of procaspase-3, initiating a caspase activation cascade responsible for cleaving and destroying cellular proteins (Wolf and Green, 1999). In some cases, other apoptotic molecules are released from the mitochondria along with cytochrome c. These include the membrane flavoprotein AIF (apoptosis inducing factor) and Smac (second mitochondrial derived activator of caspase, also called DIABLO). AIF directly translocates to the nucleus and triggers caspase independent nuclear changes (Ravagnan et al., 2001), while Smac activates apoptosis by neutralizing the inhibitory activity of IAPs (inhibitory apoptotic proteins) that associate with and hinder caspases (Verhagen and Vaux, 2002).

The second apoptotic signaling pathway is active in developmental, inflammatory, or immune system related apoptotic events and is termed the extrinsic or death receptor pathway (reviewed in Garrido et al., 2001). This pathway is mediated by plasma membrane death receptors which include TRAIL (tumor necrosis factor receptor apoptosis inducing ligand), Fas, and DR (death receptor). Death receptors contain a cytoplasmic domain called a death domain (DD). The DD is responsible for interaction with signal transducer proteins called TRADD (TNF receptor associated death domain) or FADD (Fas associated death domain). These adaptor proteins possess death effector domains (DED) that are necessary to interact with the next components of the pathway, the initiator caspases (such as procaspase 8 and 10) (Askenazi and Dixit, 1998). Their interaction promotes proteolytic autoactivation of the caspases, allowing the initiator caspases to activate their target molecules, the effector caspases. Once effector caspases are correctly cleaved, they too will activate additional caspases triggering a proteolytic caspase cascade. In an additional mechanism, active caspase-8 may cleave and activate the proapoptotic protein Bid, which translocates to the mitochondria and leads to permeabilization of



the outer mitochondrial membrane. At this point, apoptotic events are executed via the intrinsic or mitochondrial pathway (Askenazi and Dixit, 1998).

Caspases (cysteine containing aspartate specific proteases) are enzymes responsible for the degradation of key intracellular proteins, ultimately leading to the destruction of the cell (Zhivotovsky et al., 1996). The activation of sessile procaspases occurs in a hierarchical cascade. Upon activation, these caspases target downstream caspases, thereby amplifying the death signal. Alternatively, some cell death may proceed in the absence of the caspase amplification cascade. Such is the pathway involving AIF, whose activity has been shown to mediate cell death independent of caspases. Functionally, AIF dependent apoptosis appears to occur in response to certain stimuli, such as serum withdrawal. Interestingly, AIF mediated apoptosis results in the same characteristic cell death morphology. Unfortunately, how the same cell morphology is achieved in both the presence and absence of caspases is still unclear (Cande' et al., 2002).

Early experimentation on apoptotic mechanisms demonstrated that inhibitors of RNA and protein synthesis were sufficient to inhibit cell deaths that occurred during amphibian (Tata, 1966) and insect (Lockshin, 1969) development. These data suggested that apoptosis required macromolecular synthesis. Furthermore, subsequent experiments revealed that substances released from other tissues could similarly inhibit apoptosis (Liu and Stampler, 1999), indicating that the deaths were not inevitable and could apparently be suppressed by signals from other cells. More recently, evidence has accumulated indicating Hsps are capable of exerting strong anti-apoptotic effects.

### **1.5.2 Hsp70 and the inhibition of apoptosis**

Hsp70 has been shown to protect cells from a number of apoptotic stimuli, including heat shock, tumor necrosis factor, growth factor withdrawal, oxidative stress, chemotherapeutic agents, ceramide, and radiation (Mosser et al., 1992; Mailhos et al., 1993; Jaatela et al., 1992; Simon et al., 1995; Samali et al., 1996). Despite these many reports on the protective effects of Hsp70, its function within

the apoptotic pathway is not clearly defined. Hsp70 has been shown to interact with a number of components of the apoptotic pathways; however, these interactions have revealed little as to the precise mechanism underlying the inhibition of apoptosis.

The first demonstration that Hsp70 mediated suppression of cell death was by Mosser et al. (1997). Here, authors were able to show *in vivo* that stress-induced (i.e. heat shock mediated) apoptosis could be inhibited in cells expressing Hsp70, and that this resistance was associated with reduced activity of caspase-3. These data suggested that caspase processing may represent a critical target for Hsp70 under stress conditions, and that Hsp70 may promote cell survival by preventing their cleavage and subsequent activation. Subsequently, a study by Li et al., (2000) demonstrated that the addition of recombinant Hsp70 to cells undergoing heat-induced apoptosis was indeed sufficient to prevent caspase-3 activation, but unable to prevent the release of cytochrome c from the mitochondrial membrane. These data suggested that Hsp70 interacted with a component of the apoptotic pathway downstream of cytochrome c, but upstream of caspase-3 activation. The predominant event occurring downstream of cytochrome c release and up-stream of caspase-3 activation is the assembly of the apoptosome complex. Accordingly, a subsequent study demonstrated Hsp70 was able to bind to Apaf-1, a component of the apoptosome, preventing the recruitment of procaspase-9 to the apoptosome complex, and disrupt subsequent apoptotic events (Cain et al., 1999). Furthermore, it was shown that recruitment of procaspase-3 was dependent on caspase-9 activity, explaining the absence of caspase-3 activity during this process. This was the first identification of a target protein for Hsp70 within the apoptotic pathway.

Despite the identification of a specific target for Hsp70 in the cell death pathway, evidence existed suggesting that Hsp70 could also inhibit caspase-independent apoptosis. Specifically, cell lines treated with hydrogen peroxide ( $H_2O_2$ ), a known inducer of caspase-independent apoptosis, were also resistant to apoptosis when transfected with Hsp70 (Creagh et al., 2000). Therefore, if Hsp70 is capable of inhibiting caspase-independent apoptosis, Apaf-1 (whose function is to recruit initiator caspases and trigger the caspase cascade) cannot be the only target

of Hsp70 during stress induced apoptosis. This conclusion was confirmed when Hsp70 was shown to inhibit caspase-independent apoptosis in an Apaf-1 mutated cell line (Ravagnan et al., 2001). Furthermore, the same study demonstrated that Hsp70 specifically interacted with AIF, a component of caspase-independent mediated cell death. These data indicated that although Hsp70 inhibits caspase dependent apoptosis through binding of Apaf-1, it can also interact with AIF, a component of the caspase-independent apoptotic pathway to prevent apoptosis.

In the time since, a number of studies concerning the anti-apoptotic properties of Hsp70 have confirmed an ability to act as a strong inhibitor of apoptosis during a variety of cellular conditions. However, little progress has been made in identifying additional target proteins for Hsp70. Several studies have focused on pro-apoptotic members the Bcl-2 family of proteins (Gotoh et al., 2004; Stankiewicz et al., 2005). These molecules function in the mitochondrial or intrinsic pathway by regulating the release of cytochrome c from the mitochondrial membrane. Hsp70 inhibited conformational changes in the pro-apoptotic molecule Bax, required for transport to the mitochondria and subsequent activation. This inhibited the release of cytochrome c, and the mitochondrial mediated apoptotic pathway was not activated.

Much of the existing evidence seems to suggest that Hsp70 functions to suppress apoptosis with the mitochondrial-mediated or intrinsic cell death pathway. This argument is strengthened by the demonstration of a specific interaction between Hsp70 and components of the intrinsic pathway (Beere et al., 2000). Furthermore, the extrinsic or receptor mediated pathway appears unaffected by overexpression of Hsp70 (Liou et al., 1997; Creagh and Cotter, 1999). However, increasing evidence suggests that this is not an exclusive effect, and that Hsp70 may be able to interact with proteins outside the intrinsic pathway (Ravagnan et al., 2001). It is likely that the mechanism underlying Hsp70 and the inhibition of apoptosis is not a single event, and almost certainly involves multiple targets, in multiple pathways, with multiple mechanisms of regulation. Furthermore, the pleiotropic nature of Hsps as molecular chaperones easily generates the potential for

numerous points of interaction along the intrinsic, extrinsic, or caspase-independent apoptotic pathway.

## 1.6 Zebrafish as a vertebrate model system

Differences among organisms arise through specializations in how they develop, and these specializations can dramatically affect our ability to study their development. For example, the fixed number of adult cells and mosaic development of the flatworm *C. elegans*, makes it an ideal system for the study of cell lineage and cell to cell communication. The zebrafish, *Danio rerio*, is a small, tropical, freshwater fish native to the Ganges River in India. Recently, research on the zebrafish has taken advantage of several features of its development that facilitate better analysis. Most importantly, zebrafish are the first vertebrate that has proven tractable to the type of large genetic screening used so successfully in *Drosophila* (Fishman, 2001). The zebrafish mutagenesis screen was completed in 1998 and led to the isolation of 1163 mutants with defects in more than 372 genes (Haffter et al., 1996; Driever et al., 1996). As a result, mutations affecting virtually all-major organ systems are available for molecular and phenotypic characterization (Detrich et al., 1999). Furthermore, transparent embryos and external fertilization allow zebrafish mutations to be traced to the level of the individual cell in the developing embryo of a vertebrate. The transparent cells of zebrafish are also accessible for manipulative study. For example, cells can be injected with tracer dyes or be individually ablated or transplanted. Furthermore, the zebrafish embryo is organized very simply and has fewer cells than other model vertebrates, yet still exhibits strong homology to their developmental programs. Finally, the zebrafish is conducive to a research environment: individuals are cheap, easy to care for, and can be housed in large numbers. Zebrafish also produce large numbers of eggs (100-200 per mating), and develop rapidly (in about 12 hours one can visualize the establishment of a body plan that is typically vertebrate), allowing experiments to be conducted and repeated quickly. Finally, a comprehensive guide book containing valuable references on staging, embryo care, and common molecular techniques has been published

(Westerfield, 1995). Collectively, these features make the zebrafish an attractive model system to address problems in developmental genetics.

## **1.7 Eye development in zebrafish**

### **1.7.1 General aspects of zebrafish eye development**

The zebrafish model has been used extensively to address issues concerning vertebrate eye development, and several features of zebrafish eye formation have contributed to its increasing use as a model visual system (Malicki, 2000). For example, the events occurring throughout zebrafish eye morphogenesis remain conserved among other groups of vertebrates. These include such events as eye and lens morphogenesis, retinal histogenesis, and the expression of certain transcription factors (Fadool et al., 1997). Furthermore, zebrafish eye development is extremely rapid. Initial eye rudiments become delineated from the forebrain by 12 hpf, early lens rudiments by 20 hpf, and pigmented cells of the retina by 24 hpf. Retinal neurogenesis follows soon after at 28 hpf and is completed by 55 hpf. Behavioural analyses demonstrate that functional vision is acquired by the third day of development (Easter and Nichola, 1996). Thus, all major morphometric and differentiation events occur with the first three days of embryogenesis (Malicki, 2000). Finally, the rapid development of the zebrafish eye is particularly attractive for genetic screens, and has led to the characterization of dozens of zebrafish eye mutants (Gross et al., 2005). As a result, there exists extensive literature on diverse aspects of zebrafish eye development.

### **1.7.2 Zebrafish lens development**

Zebrafish lens development commences at gastrulation, when the involuting endoderm and mesoderm interact with the prospective head ectoderm to give the head ectoderm a latent lens forming bias (now called pre-lens ectoderm) (Soulez and Link, 2005). However, the activation of lens formation within the pre-lens

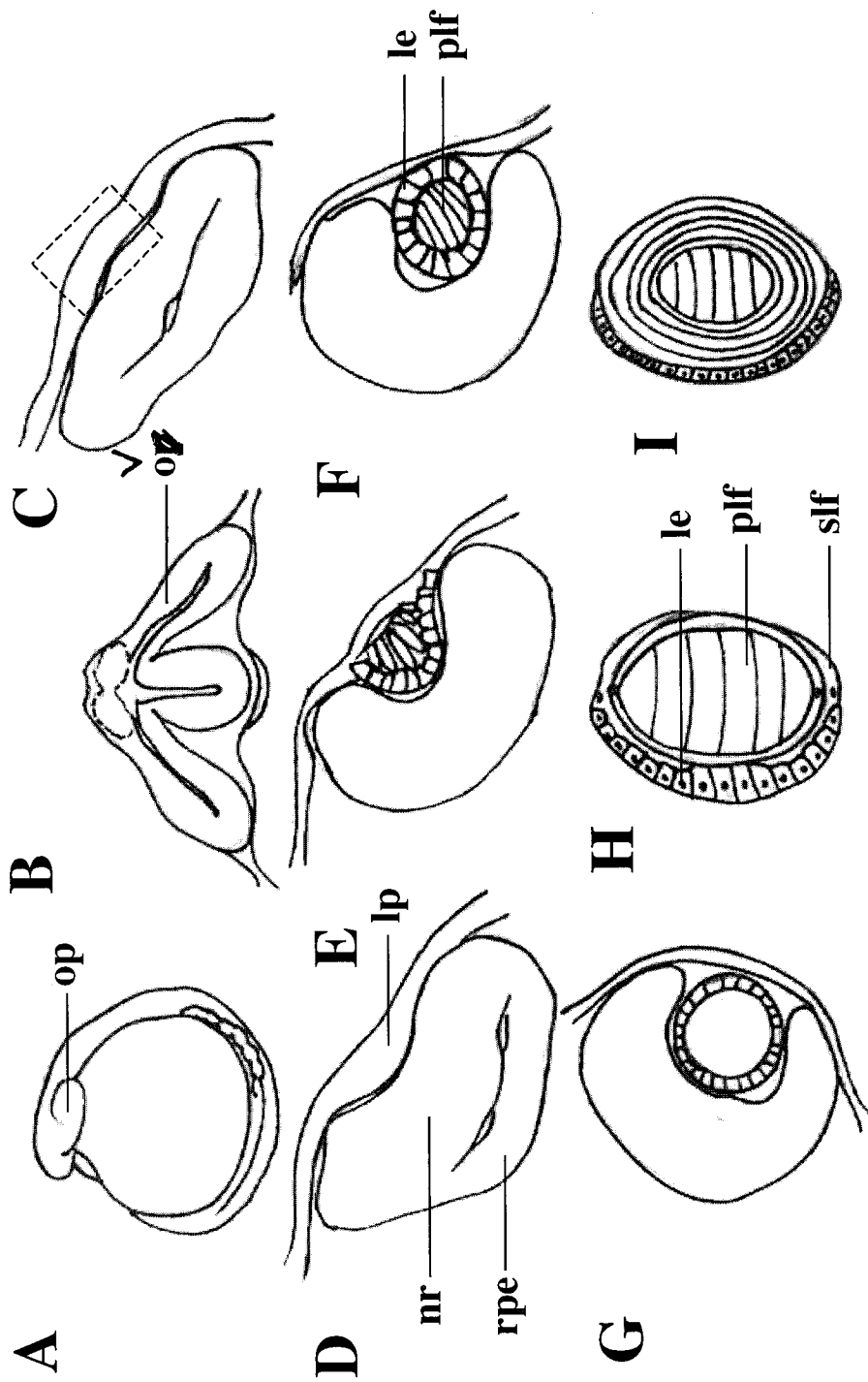
ectoderm is dependent upon an inductive event from the optic vesicles (Schmitt and Dowling, 1994). The two optic vesicles (also called optic primordia) emerge as separate projections from the anterior region of the neural keel at 13 hpf. The neural keel is analogous to the neural tube of other vertebrates, but in teleost fish forms initially from a solid mass of cells, and therefore cannot be classified as a tube (Figure 2A,B). The flattened, wing-shaped optic vesicles extend laterally until they contact the overlying pre-lens ectoderm (Figure 2C) and induce the formation of a lens placode identifiable as a thickening of the ectoderm by 20 hpf (Schmitt and Dowling, 1994; Figure 2D). Presumptive lens cells separate from the lens placode as a solid mass of cells, forming the lens vesicle by 24 hpf (Figure 2E,F). This feature of zebrafish lens development is in contrast to that of birds and mammals, where the lens vesicle arises from an invagination of the lens placode, causing the resulting lens vesicle to be hollow (Cheng et al., 2003; Easter and Nichola, 1996). Cells of the lens vesicle then differentiate into two distinct cell populations: the lateral cuboidal epithelium (equivalent to the anterior epithelium in the mammalian lens) and the primary lens fibre cells. Primary lens fibre cells lose their organelles as they differentiate and remain in the core of the lens. Secondary lens fibre cells arise later through the differentiation of cells positioned laterally in the epithelial layer (Figure 2H). Secondary fibres also lose their organelles as they differentiate, then add to the primary lens fibre cells at the core (Easter and Nichola, 1996). The process of secondary fibre differentiation occurs throughout life, and new fibres are constantly being formed and added to the lens (Piatigirosky, 1981). Consequently, the bulk of the lens consists of concentric layers of fibre cells that form an age gradient across the mature lens where the central cells are the oldest and the more peripheral cells the youngest (Bassnett and Mataic, 1997; Figure 2I).

### 1.7.3 Zebrafish retinal development

Reciprocal induction between the lens placode and optic promordia signals the invagination of the distal portion of the optic promordia to form an optic cup. The optic cup is composed of two layers (Figure 2D). Cells of the outer layer of the optic cup produce melanin and become the retinal pigmented epithelium (RPE). Cells of the inner layer of the optic cup develop into the neural retina, which will differentiate into various cell types to form the conspicuous layered appearance of the retina. These layers, in order from the RPE moving laterally toward the lens include: rods and cones of photoreceptors, cell bodies of photoreceptors, outer plexiform layer, bipolar nerve layer, inner plexiform layer, and ganglion cell layer (Easter and Nichola, 1996). As in other vertebrates, the ganglion cells are the first to be born, and the other cell types follow shortly after. Thus, differentiation is occurring medially toward the RPE, and cells at the retinal margin will remain undifferentiated as neurogenesis continues throughout the life of the organism. The majority of retinal neurogenesis occupies a narrow window of time between 27 hpf and 55 hpf, with the first neural retinal cells becoming post-mitotic by 28 hpf, and completion of the laminar pattern of the retina by 60 hpf (Malicki, 2000). Axons extending from the neural retinal layers meet at the base of the eye, and converge at the optic stalk. This stalk is the only remaining connection between the eye and the forebrain, and is termed the optic nerve. The optic nerve relays visual information from the eyes to the CNS (McDowell et al., 2004).

**Figure 2.** Zebrafish eye development. Two optic vesicles emerge from the anterior neural keel at 13hpf (A). Anterior neural keel shown in cross-section illustrates the lateral migration of optic vesicles (B). The optic vesicles migrate laterally until contacting the pre-lens ectoderm (lined box in C). The optic vesicles induce the pre-lens ectoderm to form a lens placode at 20 hpf (D). Reciprocal induction from the lens placode to the optic vesicle induces the formation of a two layered optic cup containing cells of the presumptive retinal pigmented epithelium and neural retina (D). The lens placode evaginates into the optic cup forming a lens vesicle at 24 hpf (E). Differentiation of cells within the solid lens vesicle leads to the formation of the primary lens fibre cells and lens epithelium (F), while the lens continues to expand into the optic cup (G). Secondary lens fibre cells will emerge from lateral epithelial cells and add to the primary lens fibre cells present in the lens core (H). The mature lens morphology is achieved by the third day of development (I). ov = optic vesicle; rpe = retinal pigmented epithelium; nr = neural retina; lp = lens placode; le = lens epithelium; plf = primary lens fibres; slf = secondary lens fibres. Illustrated by M. Wilm.





#### 1.7.4 The central role of the lens in vertebrate eye development

An increasing number of studies have suggested a central role for the lens in determination of several subsequent eye structures, including the retina, iris, ciliary body, trabecular meshwork and cornea. These structures are critical to the function of the eye, and are required to focus light entering the eye and to regulate intraocular pressure. Developmental defects to these structures can lead to several serious eye conditions such as glaucoma, cataracts, and corneal dystrophies (Thut et al., 2001). The lens is believed to be an important source of inductive signals that influence the formation of the above named structures. Early transplantation experiments revealed that mechanical removal (Stroeva, 1963) or toxin-induced ablation of the lens inhibits iris and ciliary body formation (Breitman et al., 1989). In addition, transplantation of an additional lens in the developing eye can cause abnormal development of the optic cup margin (Genis-Galvez, 1966). More recently, a study by Thut et al. (2001) has identified several candidate genes encoding the lens inductive signals, and the molecular mechanisms underlying the inductive properties of the lens are now being discovered. Specifically, Thut et al. (2001) demonstrated that the lens is a source of an evolutionarily conserved signal that instructs cells of the neural retina to express genes characteristic of the developing iris and ciliary body. Furthermore, suppression of lens growth by  $\alpha$ A-crystallin promoter driven expression of diphtheria toxin resulted in disruption of retinal cell organization in zebrafish (Kurita et al., 2003). Supplementary evidence for the central role of the lens has also emerged from studies of the cavefish, *Astyanax mexicanus* (Yamamoto and Jeffery, 2000). In this system, lens transplant experiments have revealed that signals originating from the lens are required for the proper degeneration of the cavefish eye. Lenses transplanted from surface-fish into cavefish are sufficient to promote proper eye development in these normally eyeless organisms, while lenses from cavefish transplanted into surface forms induce eye degeneration in eyed surface fish. To summarize, it seems likely that a signal from the lens controls tissue specification in the developing eye, and may signal a number of structures including iris, ciliary body, and neural retina.

### **1.7.5 Degradation of organelles in the mature lens**

Lens fibre cell differentiation is characterized by cellular elongation, synthesis of certain lens specific proteins, and the degradation of all membrane-bound organelles. The removal of organelles from the lens fibre cells is critical to the proper function of the mature eye, and will lead to the formation of a transparent region at the center of the lens called the organelle free zone (OFZ) (Wride, 2000). Failure of lens fibre cells to properly degrade their nuclei is characteristic of several pathological conditions, including human congenital cataracts (Zimmerman and Font, 1966). Several studies have described parallels between lens organelle degradation and classical apoptosis or programmed cell death. For example, both processes involve the systematic degradation of chromatin (Chaudun, 1994; Arruti et al., 1995; Pan and Griep, 1995; Torriglia et al., 1995). Lens denucleation is also accomplished through the use of several molecules that are integral components of the apoptotic pathways. These molecules include cytochrome c (Sanders and Parker, 2002) caspases (Ishizaki et al., 1998), and members of the Bcl-2 family (Wride et al., 1999). However, unlike the situation in apoptosis, the lens fibre cells that lose their organelles persist throughout the lifetime of that organism (Wride, 2000). These data suggest important differences between apoptotic cell death and organelle degradation in the lens. For example, during lens denucleation the cytoskeleton remains intact, while in classical apoptosis the cytoskeleton is properly degraded (Dahm et al., 1998; Bassnett and Beebe, 1992). Furthermore, nuclear degradation in lens fibre cells occurs over a much longer time period than classical apoptosis; several days instead of several hours (Bassnett and Mataic, 1997). Finally, lens fibre cells show increased resistance to classical apoptosis when treated with known apoptosis inducers such as staurosporine (Dahm et al., 1998b). A recent theory suggests that lens fibre cell organelle loss can be considered a form of attenuated apoptosis, where nuclear changes may occur independent of normal membrane changes, and complete apoptotic breakdown does not occur (Dahm, 1999).

To summarize, there exists extensive evidence for the recruitment of the components of apoptotic pathways in the apoptotic-like mechanism occurring during normal lens fibre differentiation. There also exists extensive evidence for the involvement of Hsps in modulating classical apoptotic events and protecting cells from stress induced apoptosis, and Hsp70 is capable of specifically interacting with molecules within apoptotic pathways such as Apaf-1 and AIF. However, these two areas have not yet been examined simultaneously and a role for Hsp70 in the apoptotic-like events occurring during lens fibre differentiation has not been established.

## 1.8 Hypotheses and Research Objectives

The primary objective of this thesis was to investigate the expression, function, and regulation of the stress-inducible *hsp70* gene in the normal embryonic development of the zebrafish, *Danio rerio*. A number of hypotheses and experimental approaches have been generated to address this objective:

***Hypothesis 1 – hsp70 is expressed during distinct spatiotemporal periods of embryonic zebrafish development.***

Studies in other vertebrate model systems have demonstrated that inducible members of the mouse and chicken Hsp70 family are expressed during early embryonic events. Furthermore, our lab has previously demonstrated other Hsp encoding genes such as *hsp90 $\alpha$* , *hsp90 $\beta$* , and *hsp47* are expressed during specific periods in normal zebrafish development. However, our lab had not previously examined the constitutive expression of the normally stress inducible *hsp70* gene under non-stress conditions. Thus, the first portion of this thesis presents the analysis of *hsp70* expression using *in situ* hybridization and an eGFP reporter construct.

***Hypothesis 2 - hsp70* expression is required for the proper development of the embryonic zebrafish lens.**

Our lab has previously demonstrated that constitutively expressed Hsps are important players in normal developmental events. For example, Hsp90 $\alpha$  expression in early muscle pioneers is required for subsequent muscle cell differentiation. Through the experiments outlined in hypothesis 1, it was determined that the stress inducible *hsp70* gene is constitutively expressed during a brief window of embryonic lens formation, and that this period correlated to a phase in lens development characterized by the differentiation of lens fibre cells. Therefore, *hsp70* gene expression may be required for the proper development/differentiation of the lens fibre cells in the embryonic zebrafish lens. To address this hypothesis, the expression of Hsp70 in the developing zebrafish embryo was reduced through the introduction of morpholino modified antisense oligonucleotides (MO). The resulting phenotype was characterized by using a variety of histological immunological techniques. MO represent the first viable sequence specific gene knockdown strategy in zebrafish, and have been applied successfully in many previous studies of zebrafish.

***Hypothesis 3 – Lens-specific hsp70* expression is regulated by a heat shock factor(s).**

The rapid accumulation of Hsps within the cell during stress is mediated by HSFs. However, investigations into the role of HSFs during normal vertebrate development has demonstrated that these molecules can also regulate constitutive Hsp expression under non-stress conditions. To determine whether constitutive lens-specific *hsp70* expression is regulated by an HSF, a MO based strategy was again employed. Specifically, MO targeted to the three HSFs previously identified in zebrafish, namely HSF1, HSF2, HSF $\alpha$ , were microinjected into fertilized eggs. The resulting phenotype was characterized similar to *hsp70*-MO injected embryos, and also assessed for changes in *hsp70* expression. A phenocopy of the defects observed

in *hsp70* MO knockdowns would implicate HSFs as major regulators of constitutive *hsp70* expression in the embryonic zebrafish. Currently, the function of any of these three HSFs during normal development has not been investigated using the zebrafish model.

## **2.0 Materials and Methods**

### **2.1 Zebrafish embryo care, collection, and maintenance**

Protocols for breeding, maintenance, and manipulation of zebrafish adults and embryos have been described, and are followed in this study (Westerfield, 1995). Adult wild-type (Speers Seed and Pet Store Ltd., Saskatoon) and transgenic zebrafish stocks were maintained in 5 gallon tanks housed in a stand alone Aquatic Habitats system at room temperature and a photoperiod of 14 hours daylight:10 hours darkness. Each aquarium held between 15-25 fish composed of equal numbers male and female. Adults were fed mixture of frozen bloodworms (San Francisco Bay Brand, CA) and dried flake food (Nutrafin, by Tetra) at least once per day.

Embryos were collected in accordance with procedures described in Westerfield (1995). Individual male and female fish were selected from stock tanks and placed in small 3 gallon breeding tanks lined with marbles holding a single plastic plant the evening prior to collection. Breeding tanks were maintained at 28°C. The artificial photoperiod mimics the natural day/light cycle in the wild, thus inducing the fish to continually spawn. Breeding began each morning at the start of the light cycle. Fertilized eggs were laid over the marbles, where they were subsequently collected later that morning. Breeding success was highly variable (0-2000); however most collections ranged between 50-100 eggs per aquarium.

Following their collection, embryos were divided into 25 ml sterile petri dishes (no more than 100 embryos per dish) and cleaned using filtered tap water to remove any debris that may promote the growth of mold or bacteria. Embryos were maintained in an incubator at 28°C under the same photoperiod described above. In addition, the water was changed frequently during the first 24 hpf to hinder the growth of contaminants. During early development, embryos were frequently observed under a dissecting scope to ensure proper growth and to remove dead or

unfertilized embryos. Typical mortality rates during the first 24 hours of development were approximately 15%; however occasional spawnings resulted in death rates much higher than this. Death rates dramatically decreased in embryos surviving beyond 24 hpf. All embryos raised at the standard growth temperature of 28°C were staged according to a staging guide published by Kimmel et al. (1995). In this thesis, all developmental ages refer to hours post-fertilization at 28°C, unless otherwise indicated. For heat shock treatment, embryos were collected at designated stages of development and placed in a 25 ml petri dish in filtered water, sealed using parafilm, and submerged in water bath maintained at 37°C for the desired time. Following heat shock, embryos were returned to the 28°C incubator.

## **2.2 Zebrafish embryo fixation and dechoriation**

Embryos and larvae were fixed in 1.5 ml microfuge tubes containing 4% paraformaldehyde (PFA) diluted in 1X phosphate buffered saline (PBS; 4.3 mM sodium phosphate ( $\text{Na}_2\text{HPO}_4$ ), 137 mM sodium chloride (NaCl), 2.7 mM potassium chloride (KCl), 1.4 mM potassium phosphate ( $\text{KH}_2\text{PO}_4$ )) and left at 4°C overnight. Those embryos requiring long-term storage were dehydrated through a graded series of PBS containing 0.1% Tween-20 (Sigma Laboratories; PBST/methanol (MeOH)) solutions (3:1, 1:1, 1:3) and stored at -20°C in 100% MeOH. Microfuge tubes generally contained from 5-20 embryos for all resulting experimental procedures. Following fixation, embryos were rehydrated with increasing concentrations of PBST in MeOH. Dechoriation was performed using fine forceps and a low-powered dissecting microscope.

## **2.3 Zebrafish embryo mounting and sectioning**

Embryos and larvae to be sectioned were first washed in triple distilled water, then oriented and embedded in a 1.5% agarose/water (w/v) gel. The gel was cut around the embryos and placed in 95% ethanol (EtOH) with mild agitation at 4°C overnight to allow for dehydration. This solution was changed at least once



during dehydration. The following day, the block was removed from the EtOH and processed for embedding in JB-4 methacrylate (Polysciences Inc., Warrington, PA) according to manufacturer's instructions. Specifically, agarose blocks were infiltrated using 9 mg/ml catalyst (benzoyl peroxide) dissolved in JB-4 embedding solution A (Acrylic monomer, n-Butoxyethanol) at 4°C overnight with mild agitation. Infiltrated agarose blocks were placed in plastic molds, filled with liquid JB-4 resin (a mixture of embedding solution A and solution B: N,N-dimethylaniline and polyethylene glycol), and covered with a metal chuck. The molds were placed on ice in a sealed container maintained at 4°C overnight in darkness to allow polymerization. As the JB-4 solution polymerized, blocks became adhered to the metal sectioning chucks. Polymerized blocks were sectioned to 5.5 µm thickness using a Sorvall Porter-Blum microtome with a glass knife. The resulting sections were floated on the surface of a water bath and placed on glass slides. JB-4 sections were stained with methylene blue-azure II-basic fuchsin stain (13 µg/ml methylene blue, 2 µg/ml Azure II, 1% glycerol (v/v), 1% MeOH (v/v), 1% phosphate buffer (9.078 µg/ml  $\text{KH}_2\text{PO}_4$ ;  $\text{NaHPO}_4$  11.876 µg/ml in water) (v/v) for 10 seconds at 65°C, followed by a 10 minute wash in distilled water (Humphrey and Pittman, 1974). Stained slides had coverslips mounted using a xylene based mounting media (CytoSeal XYL, Richard-Allen Scientific, Kalamazoo, MI). Alternatively, sections were stained with 4',6-diamidino-2-phenylindole (DAPI) at 10 µg/ml in PBS for 1 minute at room temperature, followed by a 5 minute wash in PBS. DAPI stained sections had cover slips mounted with CitiFluor (Marivac Inc, Montreal, Canada) and sealed with clear nail polish.

Some embryos were embedded and sectioned in paraffin wax. Embryos to be embedded in paraffin wax were encased in agarose and dehydrated in 95% ethanol as described above. The resulting blocks were infiltrated with wax using a Tissue-Tek tissue processor (Miles Scientific) overnight. The following morning wax blocks containing the embryos were oriented and placed in aluminum molds. These molds were then filled with hot paraffin wax and placed on an a refrigerated block to cool and harden. The resulting paraffin blocks were sectioned to 7 µm thickness and mounted onto coverslips coated in 1% gelatin (w/v), 0.1% chrome-

alum (w/v) in triple distilled water to improve adhesion. Paraffin sections were stored overnight at 37°C and returned to room temperature the following day. Paraffin sections were used exclusively for immunohistochemistry.

## **2.4 Zebrafish embryo photography**

Images of sections on slides and whole embryos/larvae were captured using a Nikon Coolpix digital camera and a separate camera mount housed within a Nikon Eclipse E600 photomicroscope. Whole embryos were placed in depression slides for microscopy. Fluorescence was detected using a Nikon Y-FL epifluorescence attachment. Low magnification images were taken by mounting the digital camera to the eyepiece of a Leica MZ6 dissecting scope. Post-hybridized whole mount embryos were first washed in a weak solution of hydrochloric acid (HCl) (0.05M) for two minutes in order to dissolve any magnesium-phosphate crystal artifacts precipitated in the hybridization procedure. Following the HCl wash, several changes of triple distilled water were performed before a 10 minute dehydration in 100% EtOH. All the EtOH was then removed from the microfuge tube and the embryos were allowed to air dry for approximately 1 minute. The dehydrated embryos/larvae were placed in a clearing solution containing 2:1 benzyl alcohol: benzyl benzoate for 20 minutes. Clearing solution causes the tissue to become transparent and accommodate viewing on a depression slide under the compound microscope. All images were processed using Adobe Photoshop 4.0 and arranged in Microsoft Powerpoint 9.0.

## **2.5 Zebrafish embryo eye and body measurements**

Zebrafish embryo eye diameters and pupil diameters were measured from fixed embryos previously screened as small eye from both *hsp70*-MO and *hsf1*-MO microinjections. Fixed uninjected embryos from an identical developmental stage as *hsp70*-MO and *hsf1*-MO injected embryos were measured as controls. Whole zebrafish embryos were placed in a depression slide and viewed using compound

microscopy. The length of the field of view under 40 times magnification was calculated using a histological section of known size. Eye and pupil diameters could then be estimated relative to the total field of view. Body length measurements were performed under a dissecting scope using a ruler.

## **2.6 Zebrafish embryo whole-mount *in situ* hybridization**

### **2.6.1 Antisense RNA probe synthesis**

The *hsp70* antisense probe was synthesized from a PCR amplified fragment of the gene initially isolated and cloned by Lele et al. (1997) (GenBank Accession numbers AF006006, AF158020). The plasmid containing the fragment was prepared using standard alkali lysis procedure (Jowett, 1997). Inoculated cultures of XL-Blue *E. coli* containing the plasmid vector pBluescript were incubated in YT medium (10 g/l tryptone, 5 g/l yeast extract, 5 g/l NaCl, tap water ) and ampicillin (100 µg/ml) with vigorous shaking overnight at 37°C (16-18 hrs.). Following incubation, cultures were placed on ice for 10 minutes to stop further growth. 1.5 ml of culture was transferred to a 1.5 ml microfuge tube and centrifuged for 1 minute at 12,000 rpm (maximum speed). Supernatant was aspirated and this step was repeated to double the DNA content. Cells were resuspended in 200 µl of Solution I (50 mM Tris-HCl pH 7.5, 10 mM EDTA) and incubated at room temperature for 5 minutes. Cells were then lysed in 400 µl of freshly made Solution II (0.2M NaOH, 1% SDS) by agitation and placed on ice for 5 minutes. The lysis solution was neutralized using 300 µl of ice cold Solution III (1.32 M potassium acetate pH 4.8), mixed by inversion and placed on ice for 5 minutes. This solution was then centrifuged for 5 minutes at maximum speed. The resulting supernatant was transferred a new 1.5 ml microfuge tube. To degrade remaining RNA, an RNase A (100 µg/mL) was added to this solution and incubated at room temperature for 20 minutes. A phenol/chloroform extraction was then performed. 500 µl phenol was added to the solution, the tube was vortexed, and centrifuged at maximum speed for 3 minutes. The aqueous layer was transferred to a new tube where 500 µl chloroform was

added. This tube was vortexed, and centrifuged at maximum speed for 3 minutes and the resulting aqueous layer placed in a new tube. DNA was precipitated by adding 1 ml of 95% EtOH and incubating at room temperature for 20 minutes. Tubes were centrifuged for 10 minutes at maximum speed, and ethanol was removed by aspiration. 500  $\mu$ l of ice cold 70% EtOH was then added, vortexed, and centrifuged for 5 minutes at maximum speed. The 70% EtOH was removed by aspiration and the DNA pellet allowed to air dry for 20 minutes before dissolving it in 100  $\mu$ l of triple distilled water.

A *Bss* HII digest (Invitrogen) was performed to linearize the plasmid, and an antisense RNA probe synthesized by *in vitro* transcription using the resulting cDNA fragments as template. *hsp70* antisense RNA probes were synthesized using T7 RNA polymerase according to manufacturer's instructions. Specifically, 10  $\mu$ g/ml of DNA template was added to 4  $\mu$ l of 5x T7 RNA polymerase buffer (Invitrogen), 1  $\mu$ l RNase Inhibitor (Invitrogen Technologies), 2  $\mu$ l 10 mM DTT (Invitrogen), 1  $\mu$ l T7 RNA polymerase, and 2  $\mu$ l of 10x DIG labeled nucleotide mix (10 mM ATP, CTP, GTP, 6.5 mM UTP, 3.5 mM DIG-UTP (Boehringer-Manheim)). This solution was mixed thoroughly. The reaction mix was incubated for 1 hour at 37°C, at which point an additional 1  $\mu$ l of T7 RNA polymerase was added, and the reaction mix incubated another hour. *In vitro* transcribed RNA was precipitated in 1/10 volume 0.2 M EDTA, 1/10 volume 4 M LiCl, and 2.5 times volume 95% EtOH overnight at -20°C. The following day, precipitated RNA was centrifuged for 30 minutes at 4°C, washed once in ice cold 70% EtOH and centrifuged for another 15 minutes at 4°C. EtOH was removed and the RNA allowed to air dry at room temperature for 20 minutes. RNA was dissolved in 20  $\mu$ l triple distilled DEPC water.

### **2.6.2 Probe hybridization and immunodetection**

All incubations and washes were performed in a 1.5 ml microfuge tube at a volume of 1 ml. Fixed embryos/larvae were either washed in PBST or, if stored in MeOH, were first rehydrated in a graded series of methanol:PBST solutions (3:1, 1:1, 1:3). The *in situ* hybridization protocol was performed according to Jowett

(1997) with modifications (Yoav Gothlif, personal communication). Embryos were first permeabilized using 10 µg/ml Proteinase K (Roche) in PBST for 10 minutes at room temperature. This was followed by two 5 minutes washes in PBST, and a post-fix in 4% PFA in PBS for 30 minutes at room temperature. Embryos were then incubated in pre-hybridization buffer (50% formamide, 25% 20x SSC, 1% 0.5 M EDTA, 0.5% of 20% Tween-20, 50 µg/ml heparin, 100 µg/ml tRNA in triple distilled water) for 4 to 6 hours at 65°C. Following pre-hybridization the RNA probe was heat denatured for 90 seconds at 85°C, and placed on ice for 2 minutes. Denatured probe was added to the pre-hybridization buffer at a concentration of 1 µg RNA/ml buffer. Embryos were incubated in 500 µl of this solution at 65°C for 16-20 hours. Following hybridization, a total of 11 washes were performed in order to remove any probe that was bound non-specifically. At 65°C and for 10 minutes each: 75% pre-hybridization solution / 25% 2x SSC; 50% pre-hybridization solution / 50% 2x SSC; 25% pre-hybridization solution / 75% 2x SSC; 100% 2x SSC (v/v). This series of washes was followed by two, 30 minutes washes in 0.2x SSC. Embryos were then washed 5 minutes in each of 75% 0.2x SSC / 25% PBST; 50% 0.2x SSC / 50% PBST; 25% 0.2x SSC / 75% PBST; 100% PBST (all v/v). Embryos were then incubated for 3 hours at room temperature in blocking solution (2% fetal calf serum, 2 mg/mL BSA in PBST) with light agitation. Probe was detected by an alkaline phosphatase coupled anti-digoxigenin (Dig) antibody, which interacts with the digoxigenin tag on UTPs in the probe. Embryos were incubated in a 1:5000 anti-Dig/ blocking solution mix for 3-4 hours at room temperature. Excess antibody was removed with by three, 15 minute washes in PBST at 4°C, followed by an overnight wash in PBST at 4°C. The following day, embryos were washed 15 minutes in PBST followed by two, 5 minute washes in triple distilled water. Two, 5 minute washes in staining buffer (0.1 M Tris-HCl, 0.1 M NaCl, 50 mM MgCl<sub>2</sub>, 0.1% Tween-20) were performed, followed by an incubation in staining solution (250 µg/mL BCIP, 250 µg/mL NBT, 1 mM levamisol diluted in staining buffer) at room temperature for 1-2 hours with light agitation to detect the antibody. This is followed by two, 5 minutes in PBST at room temperature and a post fix in 4% PFA in PBS for 30 minutes. Following the post-fix, embryos were washed two times in

PBST for 5 minutes at room temperature. *In situ* hybridized embryos were stored in PBS with 0.02% sodium azide at 4°C.

## 2.7 Microinjection of zebrafish embryos

Zebrafish embryos were collected as described earlier no later than 45 minutes post fertilization. Fertilized embryos were cleaned and placed in 25 ml petri dishes containing fresh filtered water. These embryos were then transferred to wellled petri dishes (one embryo per well) to ensure that the embryos would not move during the injection procedure. The wellled petri dish was placed under a Leica dissecting microscope and illuminated with an Intralux 5000-1 fiber optic light source, which does not emit heat. Custom made glass needles were utilized in the microinjection procedure. Custom glass tubes (Drummond Science Co., Broomall, PA) 100 mm in length with a diameter of 0.20 mm, were pulled into needles using a David Kopf Instruments needle puller, and trimmed to the correct length using scissors. The newly pulled needle was marked at 1 mm increments along one side to ensure that correct volumes of solution were injected with each trial, and that this procedure could be accurately repeated. The marked needle was inserted into pressurized plastic tubing attached to a Narishige 1M 300 Microinjector. The needle was pressurized to 85 psi using nitrogen gas (PraxAir, Saskatoon, SK.). Injection times were set on the microinjector and varied according to needle length, but volumes could be correlated to the 1 mm marks on the side of the needle, and thus were identical for each set of microinjections. The needle penetrated through the chorion, and solution was injected into the yolk of the embryos. Embryos were not injected beyond the 32 cell stage (1.75 hpf). Following injection, embryos were transferred to 25 ml petri dishes containing 0.00005% methylene (w/v) blue in filtered water to help prevent bacterial and fungal growth, and returned to their normal growth conditions of 28°C. The methylene blue solution was changed regularly, removing dead embryos and screening for an observable phenotype with each change. As a control, uninjected embryos were maintained in the same solution and used as a reference when screening for phenotypes.

### 2.7.1 Introduction to morpholino modified anti-sense oligonucleotides

MO are synthetic DNA analogs used as an *in vivo* gene targeting tool to eliminate the expression of a particular gene. MO possess a morpholine ring in addition to the standard ribose sugar moiety and contain a neutral charge background (Egger and Larson, 2001). MO have a high affinity for RNA and display very low cellular toxicity (Summerton, 1999). This approach makes *in vivo* targeting highly predictable and reduces non-specific effects. MO function by inhibiting translational initiation (Summerton, 1999). In this approach, an antisense sequence is targeted against the 5' leader sequence or the first 25 bases 3' to the ATG start site. Subsequent binding of the MO blocks the AUG translational start codon and prevents scanning by the 40S ribosomal subunit, and as a result, no functional protein is produced (Figure 3).

### 2.7.2 Preparation of morpholino modified anti-sense oligonucleotide

MO were designed by Gene Tools, LLC (Corvallis, OR) as a 25mer complementary to a target mRNA. Nucleotide sequences were obtained from GenBank (Accession numbers: *hsp70*: AF006006, AF158020; *hsf1*: NM131600; *hsf2*: NM131867; *hsfx*: NM001013317). The MO used in this study are shown below. The portion complementary to the start codon or portion thereof is underlined. Mismatches to the target sequence are shown in lower case.

*hsp70*-MO ( 5'-GCGATTCCTTTTGGAGAAGACCATGA-3')

*hsp70*-MO2 (5'-ATGGATTGATTTCAAGAACTGCAGG-3')

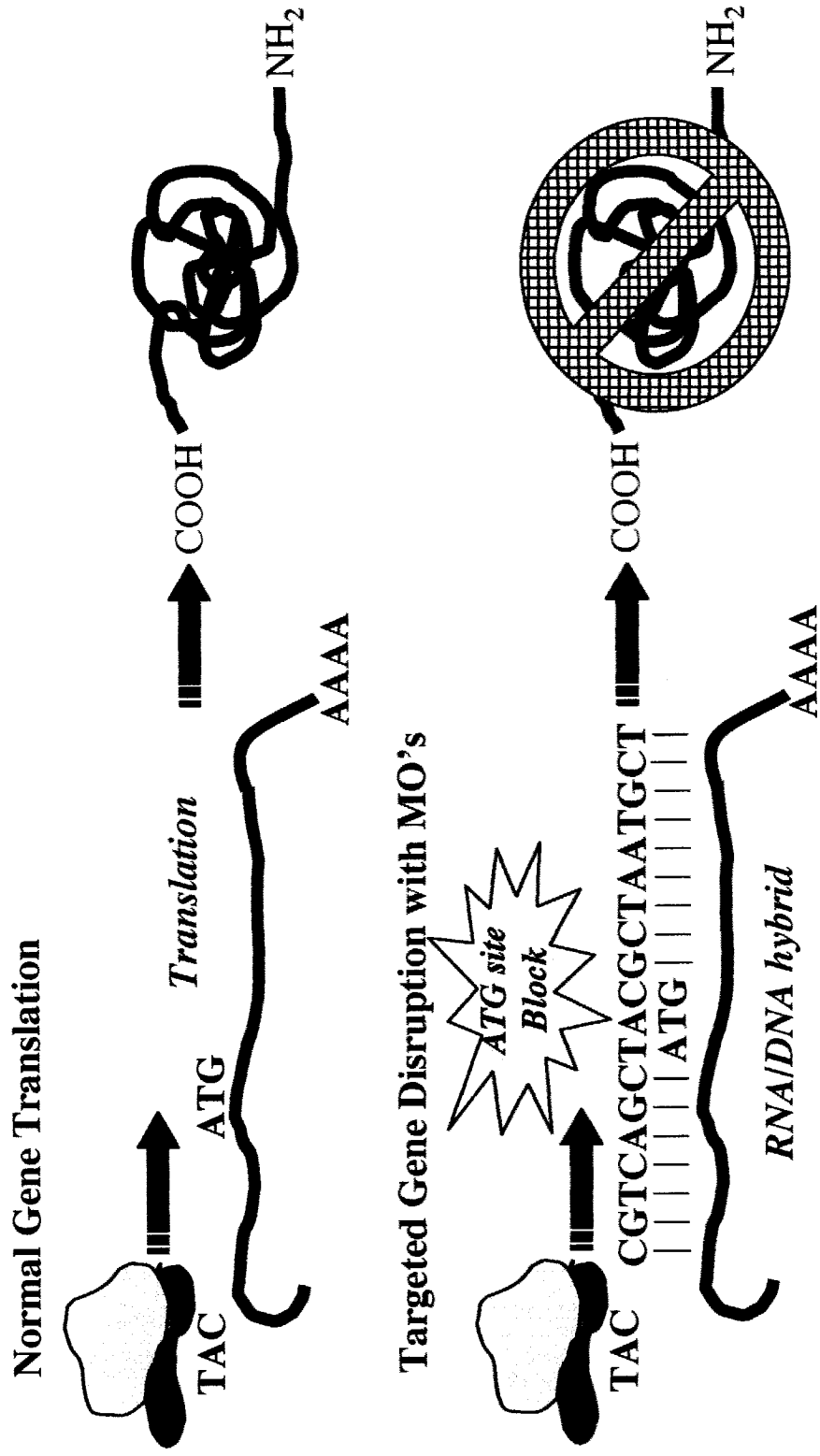
*hsf1*-MO (5'-CACGGAGAGTTTAGTGATGATTTCT-3')

*hsf2*-MO (5'-GACGTTTCGAGCTGTGTTTCATTTTG-3')

*hsfx*-MO (5'-TATAGAGCCTGGGTTCTCCTGCATG-3')

**Figure 3.** Diagrammatic representation of the functional basis of morpholino modified antisense oligonucleotides (MO). MO are DNA analogs designed and synthesized complementary to mRNA sequences of a target gene. Upon introduction into the cell, complementary base pairing results in the formation of a DNA-RNA hybrid molecule, which disrupts the ability of the ribosome to properly scan the RNA for the ATG translation start site. As a result translation is blocked, and no functional protein is produced.





standard control (5'-CCTCTTACCTCAGTTACAATTTATA-3')

*chordin* control (*chordin*-MO: 5'-ATCCACAGCAGCCCCCTCCAT 3')

*hsp70* 5bp mismatch (*hsp70*MM-MO: 5'-GCcATaCCTTTTaGAGAAcACAaGA-3')

The original concentration of the MO was 300 nM, and was subsequently diluted to a concentration of 22.5 µg/µl with triple distilled water. The resulting solution was then dispensed into 5 µl aliquots and stored at -20°C. On the day of microinjection, this stock solution was further diluted with Danieau solution (58 mM NaCl, 0.7 mM KCl, 0.4 mM MgSO<sub>4</sub>, 0.6 mM Ca(NO<sub>3</sub>)<sub>2</sub>, 5 mM HEPES pH 7.6; Nasevicius and Ekker, 2000) to the concentration indicated. MO solution was then drawn into the needle and microinjected into the embryos at 3.14 nl or 12 ng/injection as described in section 2.6. Following microinjection, embryos were transferred to a 25 ml petri dish. Both uninjected controls and injected embryos were kept at room temperature while injections were occurring. When all injections were completed, all embryos were returned to 28°C incubator. Water was replaced frequently during the first 24 hpf of development and at least once per day on the days following. During the screening process embryos were anesthetized with tricaine (0.4% 3-amino benzoic acid ethylester in 1 M Tris (pH 9.0) diluted to 0.016% in filtered fish water upon use) and visualized using a Leica dissecting scope. During the screening process control embryos were also maintained at room temperature.

## 2.8 Zebrafish embryo immunohistochemistry

The immunohistochemical technique employed is described below, and was performed on paraffin wax sections. Coverslips containing paraffin sections were loaded onto a porcelain cradle to allow for transfer to various solutions. Paraffin sections were dewaxed and rehydrated by washing 5 minutes each in: xylene, 1:1 xylene/100% EtOH, 100% EtOH, 95% EtOH, 80% EtOH, 70% EtOH (v/v). Following these steps, sections were washed 4 times for 5 minutes in 0.03 M PBS (30 mM phosphate, 200 mM NaCl). Sections were blocked for non-specific antigens

with 3% skim milk powder (w/v; SMP)/0.1% Triton-X (Sigma Laboratories; (v/v)) in PBS for 30 minutes at room temperature. Following blocking, sections were incubated in the primary antibody at 4°C overnight. Antibodies were diluted in 1% SMP/0.1% Triton-X to various concentrations depending on the antibody in use. Specifically, zl-1 (1:500), zn-5 (1:200), zns-2 (1:50), and znp-6 (1:50) were obtained from the University of Oregon Monoclonal Antibody Facility (Eugene, OR). PCNA primary antibody was used at a 1:2000 dilution and obtained from Santa Cruz Biotechnologies (Santa Cruz, CA). Sections incubated in the primary antibody were left overnight at 4°C. The following morning, unbound primary antibody was removed by washing twice for 10 minutes in 0.03 M PBS. Prior to incubation of the secondary antibody a blocking step was performed in 3% SMP/0.1% Triton-X in PBS for 30 minutes at room temperature. Biotinylated goat anti mouse secondary antibody (Vector Labs) diluted to 1:200 in 1% SMP in PBS and added to sections. Sections incubated in the secondary antibody for 30 minutes at room temperature. Following two, 10 minute washes in PBS, sections were washed in 3% H<sub>2</sub>O<sub>2</sub> in MeOH (v/v) for 15 minutes at room temperature to block endogenous peroxidases. Following two more 10 minute washes in PBS, the sections were again blocked in 3% SMP in 0.03 M PBS for 30 minutes at room temperature. Sections were incubated in ABC solution (Vector Labs) for 60 minutes according to manufacturer's instructions. Two washes of 10 minutes each in PBS followed. Sections were then washed for 10 minutes in 0.175M sodium acetate, and placed in colourmetric DAB/NiSO<sub>4</sub>/ H<sub>2</sub>O<sub>2</sub> detection solution (0.66 mg/ml DAB; 41.6 µg/ml NiSO<sub>4</sub>; 75 ml 0.175 M sodium acetate, 0.085% H<sub>2</sub>O<sub>2</sub> (v/v)) for 5 minutes under darkness. Following the colourmetric reaction, the sections were washed for 10 minutes in 0.175 M sodium acetate and then 10 minutes in 0.03 M PBS at room temperature. Sections were then dehydrated by washing 5 minutes each in: 70% EtOH, 80% EtOH, 95% EtOH, 100% EtOH, 1:1 xylene/100% EtOH, xylene. Coverslips containing sections were then mounted on slides using a xylene based mounting medium (CytoSeal XYL). Immunostaining was examined using light microscopy on a Nikon Eclipse E600 photomicroscope.

## **2.9 Terminal deoxynucleotidyl transferase-mediated dUTP fluorescein nick-end labeling (TUNEL) analysis**

The TUNEL method to detect apoptotic cells described here is from Graham (1998) with minor modifications. This procedure was performed on embryos in 1.5 ml microfuge tubes containing 5-10 embryos. Fixed embryos were washed three times for 30 minutes in PBST at room temperature. Embryos were then permeabilized in Proteinase K (10 µg/ml PBST) for 20 minutes at room temperature. The embryos were then washed twice for 5 minutes in PBST at room temperature. A post-fix in 4% PFA in PBST for 30 minutes served to stop the permeabilization reaction. Embryos were again washed twice for 5 minutes in PBST. Embryos were then washed for 5 minutes, followed by a 60 minute wash in fresh TUNEL buffer (100 mM cacodylic acid, 2.5 mM cobalt chloride, 0.1 mM DTT, 100 µg/ml BSA, 1% Triton-X, in PBST) with light agitation at 4°C. Embryos were then incubated in the TUNEL reaction mix, which contained a 9:1 ratio of TUNEL label : TUNEL enzyme (Boehringer-Manheim) for 3 hours at 37°C in darkness. As a positive control, some embryos were first incubated in 4 µg/ml pancreatic DNase in PCR buffer (500 mM KCl, 100 mM Tris-Cl pH 8.3, 15 mM MgCl<sub>2</sub>) for one hour at 37°C prior to incubation in the TUNEL reaction mix. As a negative control, embryos were incubated in the TUNEL label only. Following the TUNEL labeling reaction, embryos were washed three times for 30 minutes in PBST at room temperature and stored in PBST at 4°C in a covered canister. Fluorescent TUNEL labeled nuclei were detected using fluorescent microscopy on a Nikon Eclipse E600 photomicroscope.

## **2.10 Zebrafish lens transplantation**

The lens transplantation method is described in detail in Yamamoto and Jeffery, (2002), and was followed in this study. Embryos were prepared for transplantation approximately one hour before the operations. Transplantation can be carried out after the beginning of lens vesicle formation at approximately 22 hpf.

However, older lens are significantly stronger and respond more favorably to manipulation. Therefore, lenses in these experiments were transplanted between 31-34 hpf. The lens transplantation method consisted of three parts. First, embryos were prepared for operations by treatment with calcium free zebrafish Ringers solution (38.7 mM NaCl, 1.0 mM KCl, 1.7 mM HEPES-NaOH, pH 7.2) and embedded in agar blocks. Calcium is critical to the developing zebrafish embryo and is necessary for forming cell-to-cell adhesions. Thus, treatment with calcium free media served to loosen cell contacts and allowed the lens to be extracted with minimal damage. Embryos were then embedded in agar to immobilize them during the operations. The embryos were initially embedded in 1.2% agar (w/v) and then transferred to a glass petri dish. The agar blocks were held in place within the dish by adding a thin layer of agar below to act as an adhesive. The embedded embryos were then covered by a layer of 0.2% agar (w/v). This solution remained viscous and allowed the dissected lens to be manipulated.

Lens transplantation was conducted in the petri dish containing the immobilized embryos under a dissecting microscope. A fine gauge tungsten needle with a sharpened tip was used to remove the donor lens. First a sufficient area of 1.2% agar was removed from around the head of the donor embryo. The entire optic cup and lens were then removed as a single entity by cutting around the circumference of the eye. The lens was then isolated by carefully removing the surrounding optic cup tissue with the sharp needle. The isolated lens floated in the 0.2% agar solution surrounding the embryos. The removal of the lens from the host embryo was conducted in a similar fashion. However, the sharp tungsten needle was used to cut and remove the lens while leaving the optic cup intact within the embryo. After completing this operation, a sufficient amount of 1.2% agar was removed from around the head of the host embryo. This served to reduce the pressure on the head of the host embryos, as well as allowing the donor lens to be easily inserted into the host optic cup. This was accomplished by using the side of a blunt needle to propel the lens through the dilute agar and into the head region of the host embryo. Once the lens was in the region of the host eye primordium, the lens was pressed through the surface ectoderm into the vacant space in the optic cup.

In the final stages of transplantation the newly inserted lens was allowed to adhere to the host optic cup. In this step, the dilute 0.2% agar was gradually replaced with zebrafish Ringers solution containing calcium (38.7 mM NaCl, 1.0 mM KCl, 1.7 mM HEPES-NaOH, pH 7.2, 2.4 mM CaCl<sub>2</sub>). Incubation of embryos in this medium initiated the healing process and allowed the cell-to-cell adhesions to reform. After approximately 1 hour, the embryos had undergone sufficient healing to be removed from the 1.2% agar blocks and were returned to filtered water at 28°C. Lens transplants were analyzed under light microscopy and/or processed for JB-4 sectioning.

### **2.11 Western Blot Analysis**

Yolk proteins co-migrate with Hsp70 during SDS-PAGE. Therefore, the yolks of embryos 38 hpf were dissected out using fine forceps in PBS containing protease inhibitors (aprotinin and leupeptin at 1 µg/ml) prior to protein extract preparation. Heat shocked embryos were incubated at 37°C for 90 minutes prior to yolk dissection. Yolk-dissected embryos were placed in 1.5 ml microfuge tubes in PBST containing protease inhibitors (aprotinin and leupeptin at 1 µg/ml) and homogenized with a pestle at 4°C. The resulting slurries were further homogenized by sonication and stored at -80°C. 2x SDS sample buffer (14.5 µg/ml Tris-HCl; 4 µg/ml SDS; 20% glycerol (v/v); pH 6.8) containing 250 mM DTT was added to the protein samples, and these samples were denatured for 5 minutes at 95 °C. Denatured samples were loaded onto 8% polyacrylamide-SDS denaturing gels and covered in electrophoresis buffer (30 µg/ml Tris; 144 µg/ml glycine; 10 µg/ml SDS). Proteins were electrophoresed in a BioRad Protean II gel box at 50 volts through the stacking gel. Once proteins had migrated through the stacking gel, voltage was increased to 90 volts. Gels were electrophoresed until the visible protein marker had reached the base of the gel, and separated proteins were then electrically transferred to nitrocellulose membranes at 4°C. The membranes were washed 4 times for 5 minutes each in 3% SMP in PBST, followed by blocking for two hours in 3% SMP in PBST at room temperature with light agitation. A rabbit

polyclonal antibody raised against recombinant human Hsp70 (Stressgen Biotechnologies Corporation # SPA-812) was diluted to 1:30,000 in 3% SMP in PBST and incubated with membranes overnight at 4°C with light agitation. Following primary antibody incubation, membranes were again washed 4 times for 5 minutes each in 3% SMP in PBST, and a second one hour blocking reaction was performed in 3% SMP at room temperature with light agitation. Membranes were then incubated with a goat anti-rabbit biotin conjugated secondary antibody at 1:2000 (Vector Labs) in 3% SMP in PBST for two hours at room temperature light agitation. Following four, 5 minute washes in 3% SMP in PBST, blots were incubated in ABC kit according to manufacturer's instructions for one hour at room temperature with light agitation. Membranes were again washed four times for 5 minutes in 3% SMP in PBST. Chemiluminescence was detected using a Western Lightning kit according to manufacturer's instructions (Perkin Elmer Life Sciences), exposed to Kodak XB-1 film, and the film developed using an automatic developing machine. Resulting films were scanned into Adobe Photoshop for image processing.

## 2.12 Gel mobility shift analysis

50 pmol double stranded heat shock element (5' ctaggGAAATGGAAGCCT CGGGAA-3'; over-hanging nucleotides indicated by lower case) and CCAAT element (5'-ctaggCGA GCTCGGTGATTGGCTC-3') oligonucleotides were radio-labeled by fill-in using 5U mouse leukemia virus (MluV) reverse transcriptase (Fermentas Inc.). The labeling reaction contained 2 mM each dATP, dGTP, and dTTP; 2 µg BSA, and 20 µCi  $\alpha^{32}\text{P}$ -dCTP in a final volume of 20 µl. After incubation at 37°C for 30 minutes, reactions were diluted to 100 µl with distilled water, extracted once with phenol: chloroform (1:1) and precipitated with 1/3 volume of 7.5 M ammonium acetate and 2.5 times volume of ethanol in the presence of 1 µg carrier tRNA.

The yolks of embryos 38 hpf were dissected out using fine forceps in Buffer C (10 mM Tris-HCl pH 7.8, 50 mM NaCl, 1 mM EDTA, 1 mM DTT, and 5% glycerol) containing the protease inhibitors aprotinin and leupeptin at 1 µg/ml prior

to protein extract preparation. Heat shocked embryos were incubated at 37°C for 90 minutes prior to yolk dissection. Yolk-dissected embryos were placed in 1.5 ml microfuge tubes in Buffer C containing protease inhibitors (as above) and homogenized with a pestle at 4°C. The resulting slurries were further homogenized by sonication. DNA binding reactions contained five embryo equivalents (5 µl) lysate in Buffer C, 100 cps labeled probe, 1 µg poly deoxy-inosine-deoxy-cytosine, 10 mM Tris-HCl pH 7.8, 50 mM NaCl, 1 mM EDTA, 1 mM DTT, and 5% glycerol in a final volume of 20 µl. Reactions were incubated for 20 minutes at room temperature, then mixed with 5 µl-5x loading dye (0.25% bromophenol-blue, 0.25% w/v xylene-cyanol, 50% v/v glycerol) and immediately loaded onto non-denaturing 5% polyacrylamide gels. Samples were electrophoresed in 1x TNANA buffer (6.7 mM Tris-HCl pH 7.5, 3.3 mM sodium acetate, 1 mM EDTA) at 20°C for 2 hours at 120 volts. Following electrophoresis gels were dried onto filter paper, and exposed to Kodak XB-1 blue x-ray film overnight at -80°C with an intensifying screen.

### **2.13 Chicken egg care and incubation**

Fertilized White Leghorn hens' eggs were obtained from the Poultry Science Department at the University of Alberta and Anstey Hatchery (Saskatoon, Canada). These eggs were placed in a holder (pointed side up) and incubated at 37°C in a humid chamber containing 5% CO<sub>2</sub>. The eggs were staged according to Hamilton and Hamburger (1951). Egg entry into the incubator was staggered according to the developmental stage required, so that eggs of different age would be ready for dissection on the same day.

### **2.14 Chick lens dissection and protein extract preparation**

Eggs were removed from the incubator and left at room temperature for the remainder of the dissection. Grasping the egg in one hand, the egg was first cracked using large forceps, and finally broken open. At this point half of the broken shell was used to support the embryo. Scissors were then used to free the embryo from



the surrounding yolk and embryonic vasculature. The embryo was then transferred to a large glass petri dish containing PBS and protease inhibitors (aprotinin and leupeptin at 1  $\mu\text{g/ml}$ ). All embryos were immediately decapitated using scissors once in the dish. The bodies along with the yolk, shell, and other biological material were disposed of, while the severed heads were left in the petri dish. Fine forceps were used to cut around the periphery of the eye and separate the entire eye globe from the rest of the head. A small opening was made in the back of the eyeball exposing the vitreous humor. Using a pair of forceps to grasp the vitreous humor and a second pair to anchor the rest of the eye tissue to the petri dish, the vitreous humor was pulled out the small slit at the back of the eyeball. As the humor is extracted the lens is pulled along with it, resulting in an isolated lens still attached to the vitreous humor, but separated from the rest of the eye tissue. In the final step, fine forceps were used to pinch off the vitreous humor and any remaining retinal tissue adjacent to the lens, and the completely isolated lens was placed in a 1.5 ml microfuge tube containing cold PBS and protease inhibitors (aprotinin and leupeptin at 1  $\mu\text{g/ml}$ ). This dissection procedure was followed to isolate lenses for Western blot analyses. Isolated lenses were washed in 1.5 ml microfuge tubes with PBS plus 0.1% Tween-20 (PBST) containing protease inhibitors (aprotinin and leupeptin at 1  $\mu\text{g/ml}$ ), and homogenized with a pestle at 4°C. The resulting slurries were further homogenized by sonication at stored at -80°C.

Lenses intended for cell cultures were isolated in a similar fashion with the exception that sterile Tyrode's solution (0.8 g  $\text{CaCl}_2$ ; 0.4 g  $\text{MgCl}_2 \times 6 \text{H}_2\text{O}$ ; 0.2  $\mu\text{g/ml}$  KCl; 1  $\mu\text{g/ml}$   $\text{NaHCO}_3$ ; 8  $\mu\text{g/ml}$  NaCl; 0.05  $\mu\text{g/ml}$   $\text{NaH}_2\text{PO}_4 \times 4\text{H}_2\text{O}$ ; 1  $\mu\text{g/ml}$  glucose; pH 7.4) containing 50  $\mu\text{g/mL}$  gentamycin and 50  $\mu\text{g/mL}$  polymyxin B sulphate was used in the place of PBS.

### **2.15 Chicken lens cell culture**

To degrade extracellular proteins, dissected lenses were placed in a 1.5 mL microfuge tube containing fresh, pre-warmed (37°C) 0.1% trypsin in calcium-free Tyrode's solution plus antibiotics. Tubes were incubated at 37°C for 30 minutes and

vortexed at 5 minute intervals until dissected lenses were ruptured and in small pieces. Lens tissue was then pelleted by centrifugation for 2 minutes at 10,000 rpm. The supernatant was removed and the pellet resuspended in 500  $\mu$ l Medium 199 (Sigma-Aldrich) containing 10% fetal calf serum. The cell suspension was filtered through a 40  $\mu$ m nylon Falcon cell strainer to remove loose material. This process removed aggregations of retinal and lens fibre tissue, leaving behind only the lens epithelium cells, the precursors of lens fibre cells. The filtrate contained single cells and small clumps of cells, which were plated by spreading 45  $\mu$ l of suspension at the center of a matrigel coated coverslip. Matrigel is a commercially manufactured extracellular matrix protein preparation that is used as a substrate for the growing cells to adhere to (BD Biosciences). The gel was mixed with 50  $\mu$ l 10% fetal calf serum in 199 medium at 4°C, then plated on a coverslip at room temperature. The entire coverslip was placed in a small petri dish, and covered with the trypsin digested tissue. This cell suspension was covered with growth medium and allowed to adhere and propagate. The growth medium was changed once per day for the three day culture period. Resulting lens cultures were fixed in preparation for immunostaining. Specifically, lens cultures were first washed twice with PBS, then covered in 4% PFA for 2-3 hours at room temperature, again washed in PBS, and finally stored at 4°C until needed.

## **2.16 Immunocytochemistry of chicken lens cell cultures**

Cultures were first washed three times for 5 minutes in PBS at room temperature, followed by permeabilization in 100% acetone at -20°C for 15 minutes. Following permeabilization, the cells were again washed three times for 5 minutes in PBS and then covered in blocking solution (4% BSA in PBS) for one hour at room temperature. The cells are then covered with the Hsp70 primary antibody (StressGen Biotechnologies Corporation #SPA-812) diluted in PBS (1:200), and incubated for two hours at room temperature or overnight at 4°C. The following day the cells were again washed three times for 5 minutes in PBS, and covered in a fluorescein conjugated secondary antibody (Vector Laboratories)

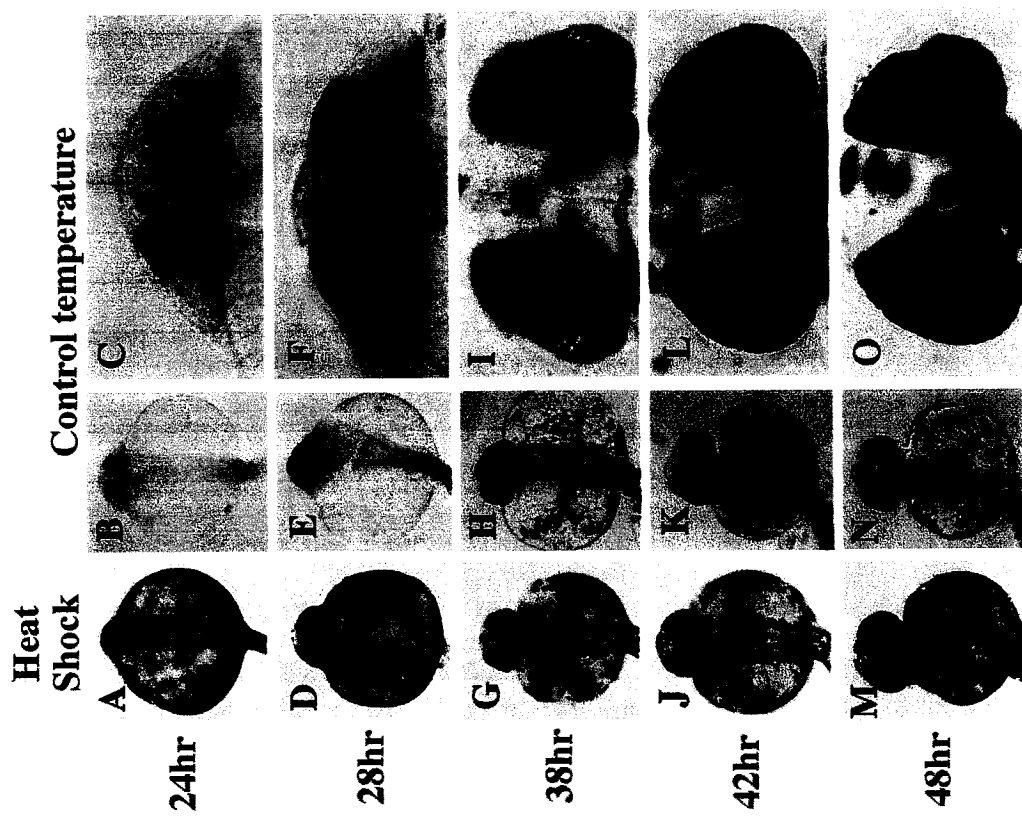
solution (1:500 in blocking solution) for one hour at room temperature. Following incubation in the secondary antibody, the cells were again washed three times for 5 minutes in PBS. The coverslips holding the cells are then mounted on slides using Vectashield (Vector Laboratories) to protect the fluorescent signal, and sealed with clear nail polish. Immunostained cells were visualized using confocal microscopy, and could be stored for several months at 4°C in the dark.

### 3.0 Results

#### 3.1 Expression analysis of the inducible *hsp70* gene under non-stress conditions in the embryonic zebrafish

Our laboratory has previously demonstrated that several normally stress-inducible Hsps are constitutively expressed under normal developmental conditions in the embryonic zebrafish (Krone et al., 2003; Krone et al., 1997). However, the precise expression pattern of *hsp70* under non-stress conditions had not been examined. Whole mount *in situ* hybridization was used to characterize *hsp70* mRNA expression *in vivo*, as well as a stable *hsp70*-eGFP reporter gene transgenic strain (Halloran et al., 2000). Whole-mount *in situ* hybridization analysis during the first 48 hours of embryogenesis revealed a short temporal window of *hsp70* expression in the lens from approximately 28-42 hpf in embryos raised at 28°C (Figure 4). The eyes are readily identifiable by the presence of pigmented epithelium by 24 hpf, and while lens development has begun by this stage of development (Li and Easter, 2000) *hsp70* expression was not yet detectable (Figure 4B,C). Over the next four hours, the eyes become more defined and *hsp70* transcripts were detected in the lens by 28 hpf (Figure 4E,F). The lens-specific expression of *hsp70* increased rapidly in intensity, and mRNA was abundant by 38 hpf (Figure 4H,I). Expression was subsequently down-regulated by 42 hpf (Figure 4K,L), and was not discernable by 48 hpf (Figure 4N,O). A weak hybridization signal was detected only sporadically in non-lens cells of the embryo at comparable stages of development. This signal was not specific to certain cell types, exhibited varying intensities in individual embryos, and was not present in all embryos assayed. In contrast, a strong hybridization signal was consistently observed throughout the embryo following a one-hour heat shock at 37°C (Figure 4A,D,G,J,M).

**Figure 4.** Whole mount in situ hybridization analysis of *hsp70* mRNA. Anterior is to the top for all figures. Dorsal/ventral views of entire embryo and enlargement of the anterior region, respectively, are shown for 24 hpf (A-,C), 28 hpf (D-F), 38 hpf (G-I), 42 hpf (I-L), and 48 hpf (M-O). Constitutive *hsp70* mRNA is first detectable in embryos raised at 28°C as weak expression in the lens at 28 hpf (E,F). Peak levels of *hsp70* mRNA are observed at 38 hpf (H,I) with significant down regulation evident by 42 hpf (K,L) and no signal present by 48 hpf (N,O,). Heat shock is a known inducer of *hsp70* expression. Upon exposure of embryos to a 90 minute heat shock at 37°C, *hsp70* mRNA is expressed ubiquitously throughout the embryos at all stages analyzed (A,D,G,J,M).



While zebrafish cultured cells and embryos raised at 28°C do not exhibit a discernable heat shock response (Krone et al., 1997), it was possible that developing lens fibres are more sensitive to temperature stress than other tissues. For example, exposure of *Xenopus* embryos to mild hyperthermia resulted in enhanced expression of *hsp70* in eye tissue (Ali and Heikkila, 2002). To address this issue, zebrafish embryos were raised at the sub-optimal growth temperature of 25°C, and assayed for *hsp70* expression via *in situ* hybridization. While developing more slowly, these embryos also exhibited lens-specific *hsp70* expression during the same relative window of lens formation (data not shown).

GFP fluorescence in a strain of zebrafish carrying 1.5 kb of the *hsp70* promoter driving expression of an eGFP reporter gene (Figure 5; Halloran et al., 2000) was used to determine whether lens specific *hsp70* expression is driven by promoter sequences, and to verify the expression pattern observed through *in situ* hybridization analysis. Tissue-specific expression of *hsp70*-eGFP accurately mimicked that of endogenous *hsp70* (Figure 6 compare A to B and C to D). However, there was a delay in when lens expression could first be detected (48 hpf) compared to the endogenous gene (28 hpf as mentioned above). This delay is likely related to the accumulation of GFP to detectable levels in the lens, although this has not been examined directly. Exposure of transgenic zebrafish carrying this reporter to a 90-minute heat shock was sufficient to induce GFP expression throughout the embryo (Figure 6D). Importantly, there was also a delay in GFP accumulation in heat shocked embryos. Maximal up-regulation of GFP occurred during a 2-4 hour lag period after heat shock, and it is likely that this delay again represents GFP accumulation in these embryos. These data indicate that the *hsp70*-eGFP reporter construct used in this study accurately reproduces *hsp70* expression patterns observed in unmanipulated laboratory fish. More importantly, the 1.5 kb of *hsp70* promoter sequences driving eGFP expression is sufficient to activate *hsp70* expression specifically in the lens, and suggests that regulation of *hsp70* expression occurs through these promoter sequences.

The developing zebrafish lens is composed of two distinct cell types, namely lens epithelial cells and lens fibre cells. Lens epithelial cells cover the outer surface

**Figure 5.** Diagrammatic representation of the eGFP reporter construct used to visualize *hsp70* promoter driven GFP expression in live transgenic zebrafish embryos. Binding of active heat shock factor 1 (HSF1) trimer to the heat shock element (HSE) found in the promoter region of the *hsp70* gene activates transcription and subsequent production of GFP, which can be visualized in live embryos via fluorescent microscopy.



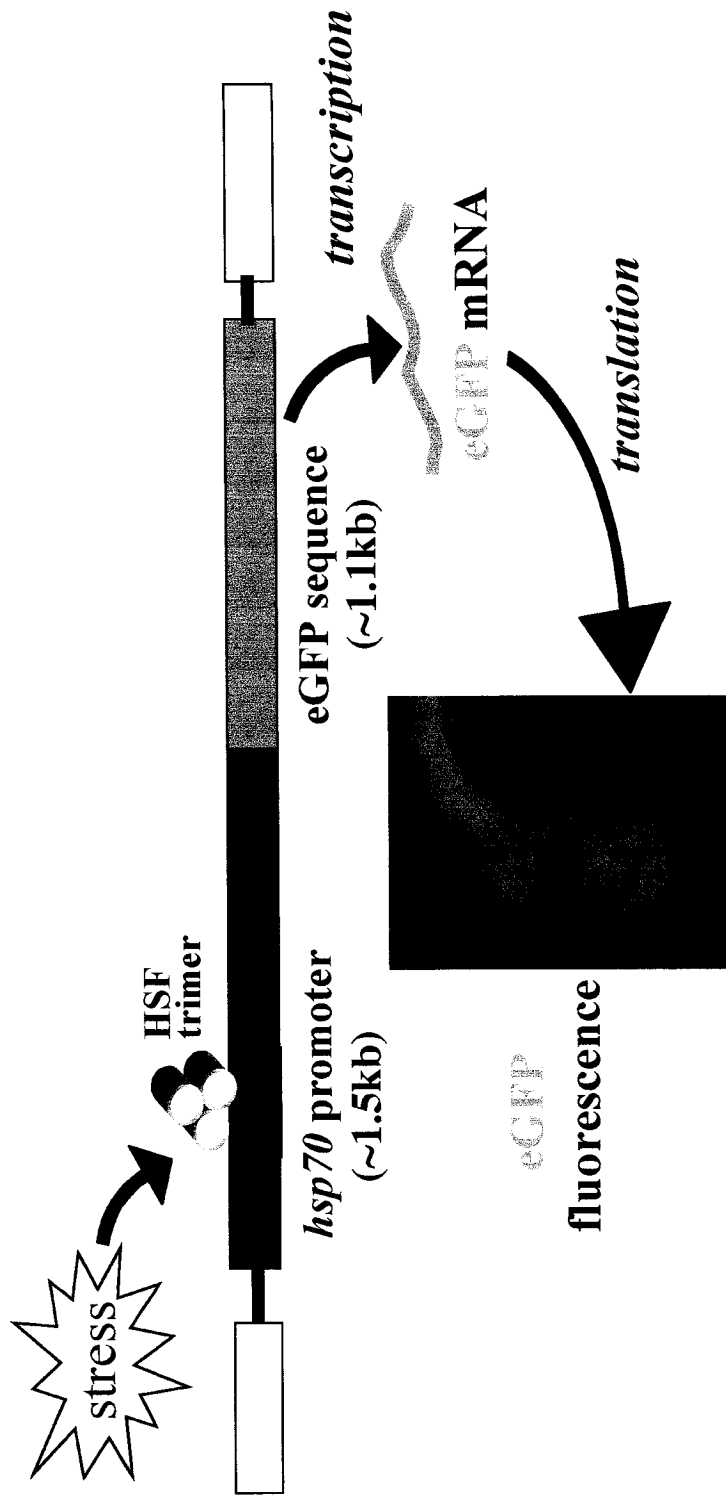
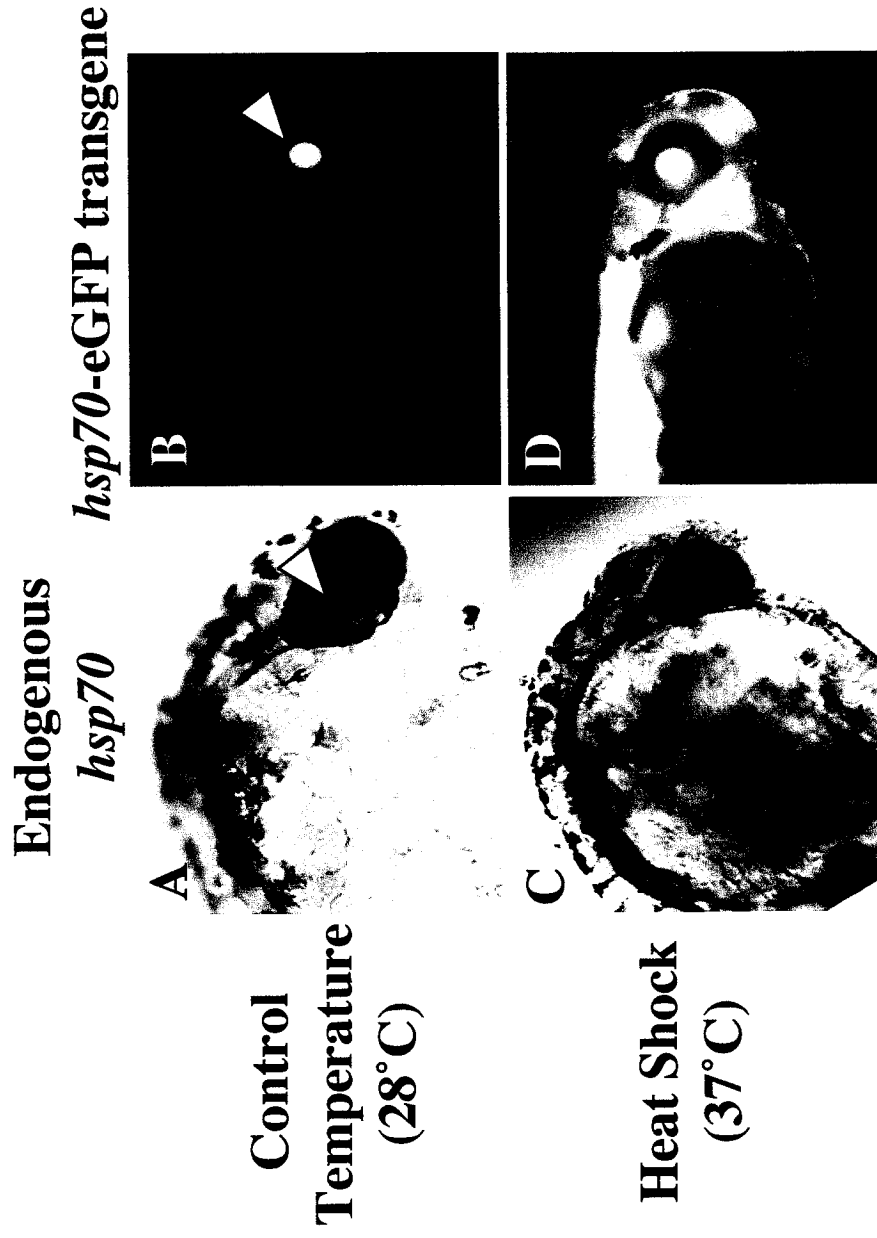


**Figure 6.** Cell specific activation of the *hsp70*-eGFP transgene in a stable eGFP transgenic zebrafish line accurately mimics endogenous *hsp70* expression observed through *in situ* hybridization analysis. *in situ* hybridization analysis of *hsp70* mRNA reveals that *hsp70* is expressed specifically in the lens (arrowhead in A) under non-shock conditions (28° C), but becomes universally expressed following a 90 minute heat shock at 37° C (C). Similarly, the stable eGFP gene product in live transgenic embryos carrying an *hsp70*/eGFP reporter gene occurs only in the lens under non-shock (arrowhead in B) conditions, but is again expressed ubiquitously throughout the embryo following heat shock (D).



of the lens, and as development proceeds, cells within this layer differentiate into fibre cells which are displaced inward to form the core of the lens (Easter and Nichola, 1996). To determine which of these lens cell types are expressing *hsp70*, histological analyses of embryonic eyes at 38 hpf, when peak levels of *hsp70* expression occur, and 48 hpf, when *hsp70* is no longer detectable were performed (Figure 7). Cross sections of the eye at 38 hpf revealed that *hsp70* expression was restricted primarily to the developing lens, with only weak expression detected in the retina and extra-ocular tissue (Figure 7A). Retinal and extra-ocular expression was highly variable among individual embryos, but always extremely weak in intensity when compared to lens expression. Lens specific *hsp70* expression was concentrated to both the developing lens fibre cells and the surrounding epithelial cells. As observed in intact embryos, *hsp70* expression was not detected in sections at 48 hpf (Figure 7B).

### **3.2 Conserved expression of inducible Hsp70 protein under non-stress conditions in embryonic chicken lens cell extracts and cultures**

The data presented here show that the zebrafish *hsp70* gene is strongly expressed during formation of the embryonic lens, and is directed to the lens by sequences within the *hsp70* promoter. Lens specific expression of *hsp70* may be more widespread in vertebrates, since chicken *hsp70* mRNA has been detected in cultured lens explants using RNA blot analysis (Dash et al., 1994), and by immunoblotting (Bagchi et al., 2001). Thus, *hsp70* expression may represent a conserved feature of lens developmental programs in vertebrates. However, the exact temporal expression of *hsp70* in chicken has not been reported, and it remains unknown whether chicken *hsp70* is expressed during similar stages of lens development as observed in zebrafish. Interestingly, our laboratory has previously demonstrated that *hsp90 $\alpha$*  gene expression present in a small subset of cells within the developing somites is conserved between fish and chicken (Sass and Krone, 1997).

**Figure 7.** Histological analysis of 5.5  $\mu\text{m}$  methacrylate sections of whole mount embryos after *in situ* hybridization with an antisense *hsp70* RNA probe. Intact embryos were analyzed via *in situ* hybridization and then embedded in agar and processed for sectioning. At 38hpf *hsp70* mRNA is restricted exclusively in the developing lens, and is present in both lens fibre and lens epithelial cells (A). In contrast, expression is no longer detectable in the lens by 48 hpf (B).

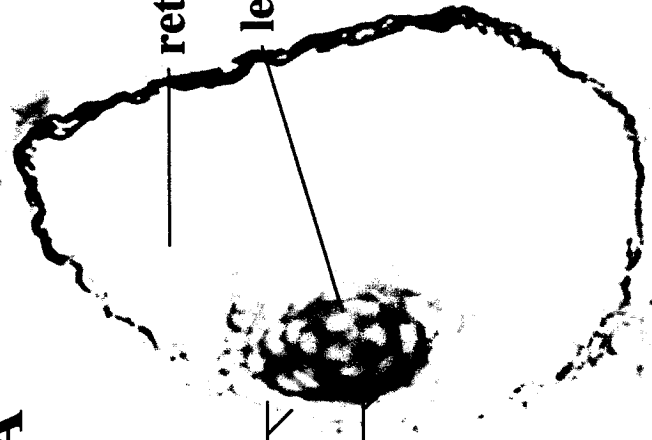
48hpf

B



38hpf

A



lens  
epithelial  
cells  
lens  
fibre  
cells

To address whether lens specific *hsp70* expression is conserved in chicken, Hsp70 protein was analyzed via Western blot analysis in whole lens extracts from embryonic day (ED) 6 to ED 18 (Figure 8). Membranes probed with an antibody specifically recognizing the heat inducible Hsp70 (StressGen Biotechnologies Corporation # SPA-812) revealed expression occurs throughout lens development (Figure 8A). Peak levels of expression were observed early in lens development at ED 6. During this stage of lens development, epithelial cells are committed to forming the initial population of primary lens fibre cells. Expression was reduced slightly by ED 8, and decreased further until ED 10. Hsp70 levels remained lower at consistent and detectable levels at stages ED10 through ED 14. This period of lens development is characterized by the differentiation of secondary lens fibre cells from the lateral lens epithelium. A period of enhanced Hsp70 accumulation was observed at ED16, but by ED 18, Hsp70 was down-regulated and no longer detectable in our assay. Equal protein loading was confirmed via Coomassie staining of SDS-PAGE gels (Figure 8B).

Lens specific expression of *hsp70* was further investigated using a lens cell culture system developed by our colleagues at the University of Alberta. In this system, lens cells proceed through similar division and differentiation events as in the whole animal (Sanders and Parker, 2002). Specifically, lens epithelial cells proliferate to form a lawn of cells. Lens fibre cells then emerge from within this lawn of epithelial cells, and begin to stack upon one another as more and more differentiate. These stacks are referred to as lentoids. Immunocytochemistry performed on lens cultures revealed strong Hsp70 expression specifically in lentoids, while the underlying epithelium exhibited only minor expression (Figure 9). These data suggest that Hsp70 expression may be greatest in the differentiating fibre cells.

**Figure 8.** Western blot analysis of HSP70 in whole chick lens extracts. HSP70 expression is detectable at embryonic day (ED) 6 through ED16. An antibody (StressGen Biotechnologies Corporation # SPA-812) specifically recognizing the inducible form of HSP70 was used in all trials. Peak levels of expression occur early in lens fibre development at ED 6 and ED8. By ED 10 levels have decreased significantly, though HSP70 was still detectable through to ED14. Enhanced levels of HSP70 were detected at ED16, however HSP70 was not detected at ED18 (A). Equivalent protein loading was confirmed by coomassie blue staining of lens extracts following SDS-PAGE (B).

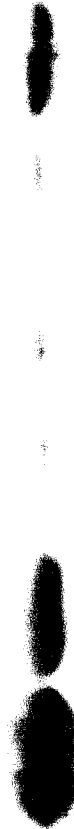


Embryonic day

**A**

6 8 10 12 14 16 18

Hsp70 →

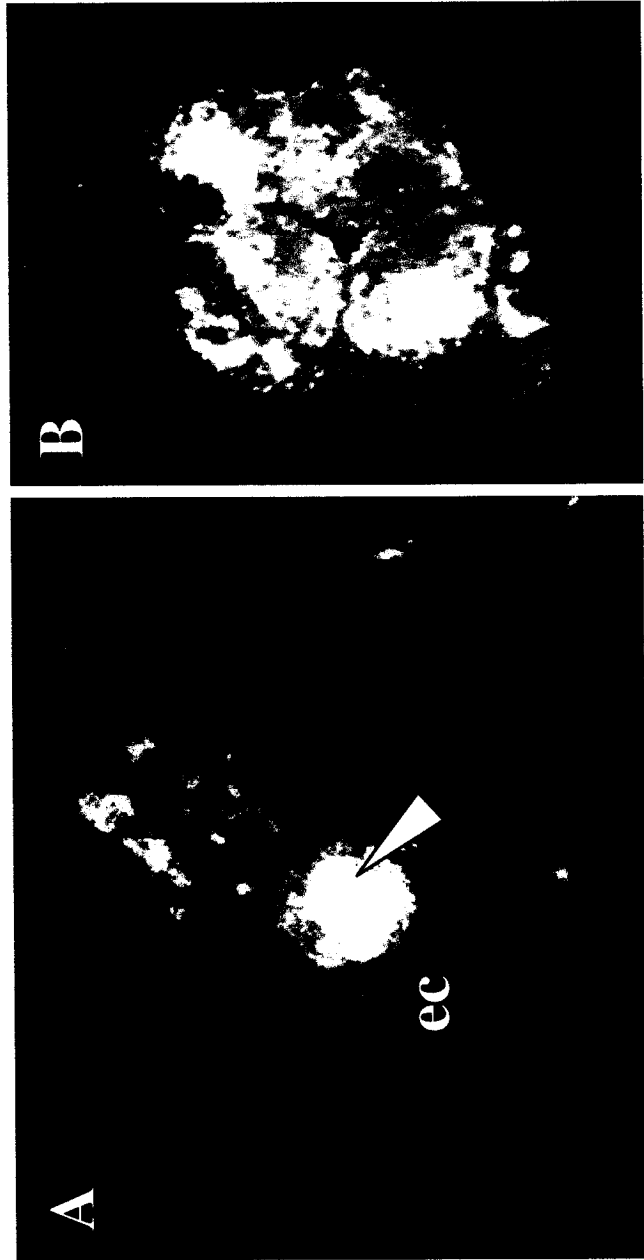


**B**

Coomassie  
Blue



**Figure 9.** HSP70 protein expression as visualized by fluorescent immunocytochemistry on chicken lens cell cultures using confocal microscopy. Cells from whole lens extracts dissected at ED8 were cultured until ED12. Lens cell cultures were then fixed and processed for immunocytochemistry. An antibody specifically recognizing the inducible HSP70 was used in all trials. In culture, lens fibre cells differentiate from an underlying lawn of lens epithelial cells (ec) and stack upon one another forming structures called lentoids (arrowhead in A). High magnification analysis of lentoids (B) show HSP70 is expressed in these cells during lens fibre differentiation.



These analyses indicate that there exists a specific temporal pattern for *hsp70* expression in chicken, and that this expression pattern is similar to that observed in zebrafish. Additionally, histology and immunocytochemistry revealed that Hsp70 protein levels are greatest in the developing fibre cells, and implies that Hsp70 may be required for the development of this specific cell type. Furthermore, these data provide evidence that lens specific expression of *hsp70* occurs in distantly related classes of animals, namely birds and fish, and therefore may be a conserved event among vertebrates.

### **3.3 Functional analysis of *hsp70* during embryonic lens development in zebrafish**

#### **3.3.1 Morpholino modified antisense oligonucleotide mediated knockdown of *hsp70* yields small eye phenotype**

The data presented thus far demonstrate that the normally stress-inducible *hsp70* gene is expressed during a short temporal window of embryonic lens development in the zebrafish. Furthermore, *hsp70* expression is greatest in the lens fibre cells and this expression may be conserved among vertebrates. These data indicate that *hsp70* is expressed as a component of embryonic lens developmental programs, but whether *hsp70* function is required for lens development remains unresolved. Our laboratory has previously shown that constitutively expressed Hsps perform important developmental functions in a variety of tissues and cell types (reviewed in Krone et al., 2003). Therefore, the observed lens-specific expression of *hsp70* may play a fundamental role in embryonic lens development. To address this hypothesis, MO targeted to *hsp70* were injected into early stage zebrafish embryos to eliminate the translation of *hsp70* mRNA, and deplete the embryos of a functional protein product (Figure 3). MO have been widely used as an *in vivo* gene targeting tool to reduce expression of particular genes in zebrafish and other organisms (e.g. Summerton 1999; Nasevicius and Ekker 2000; Ekker and Larson 2001).

In order to establish the effectiveness of the MO microinjection procedure, initial MO microinjection experiments were performed using *chordin*-MO. This MO is targeted to the mRNA of the *chordin* gene. Mutations in *chordin* are manifested during gastrulation, and the phenotype is typified by the absence of dorsal structures, whereby the tail is enlarged at the expense of the head and anterior region of the trunk. The *chordin* mutation was characterized during the original zebrafish mutagenesis screen (Hammerschmidt et al., 1998), and as a result has been well documented. Microinjection of *chordin*-MO resulted in a concentration dependent phenocopy of the typical *chordin* mutant phenotype (Figure 10) ranging from moderate (Figure 10A) to severe (Figure 10B) in 24 hpf embryos. The *chordin*-MO used in these experiments was covalently modified with a fluorescein tag, allowing the distribution of the MO within the embryo to be visualized under fluorescence microscopy (Figure 10C,D). Analysis of *chordin*-MO distribution indicated that the MO is dispersed evenly throughout the developing embryo, and indicates that all tissues within the embryos will receive the MO using this injection procedure.

Given the above data demonstrating the procedure for the microinjection of MO into early zebrafish embryos is effective, MO targeted to *hsp70* were microinjected. Two *hsp70* targeting MO were designed, one against the 5'-ORF (*hsp70*-MO) and the other against the 5'-UTR, (*hsp70*-MO2). The majority of studies utilizing MO in zebrafish have focused on genes expressed during the first day of development, and have normally required microinjection of anywhere from 0.5 to 5 ng per embryo in order to produce a consistent phenotype (Nasevicius and Ekker, 2000). However, it was expected that injection of higher amounts of *hsp70*-MO would be required since further MO degradation/dilution occurring between 1 and 2 days of development would reduce the effective concentration during the period of *hsp70* expression. Thus, optimal injection concentrations of MO were initially determined (Table 1). All embryos in these experiments were raised at the non-heat shock, normal growth temperature of 28°C. Embryos microinjected with a concentration of 3.46  $\mu\text{g}/\mu\text{l}$  *hsp70*-MO (10.9 ng/injection) were indistinguishable from control embryos at 24 hpf, whereas 63% of the 486 assayed embryos displayed

**Figure 10.** Whole mount analysis of *chordin*-MO injected embryos. Microinjection of *chordin*-MO reproduces the well-characterized *chordin* mutation (Hammerschmidt et al., 1998), and serves as a positive control MO in this study. The microinjection procedure used in this study was sufficient to accurately reproduce *chordin* (A) and severe *chordin* (B) phenotypes. This *chordin*-MO is modified with a fluorescein tag on each base pair allowing the visualization of MO distribution throughout the embryo. In both *chordin* (C) and severe *chordin* (D) phenocopies, *chordin*-MO is evenly distributed through the developing embryo.



a characteristic small eye phenotype at 52 hpf (Table 3.1). Similarly, injection of *hsp70*-MO2 resulted in 53% of embryos displaying an identical, small eye phenotype at 52 hpf. The slightly lower potency of *hsp70*-MO2 is most likely related to the low GC content of this MO (36%) compared with *hsp70*-MO (44%). In all cases the number of embryos displaying a small eye phenotype differed significantly from controls as determined by Fischer's exact test. Diagnosis of a small eye phenotype was confirmed independently by a second researcher using a blind lineup of both small eye and non-small eye injected embryos. Furthermore, standard error of percentages of injected embryos displaying small eye phenotype between trials was  $\pm 2.4$ , indicating that the small eye phenotype was produced and assessed consistently between trials. The majority of embryos displayed the severe small eye phenotype shown in Figure 11A, although some variation in severity was observed. A minority of the embryos displayed a range of eye sizes between a severe small eye and moderate small eye phenotype (Figure 11B) relative to uninjected embryos (Figure 11C). Microscopic analysis revealed that the overall eye diameter is significantly reduced in small eye phenotype embryos, with eye diameters ranging from 43  $\mu\text{m}$  to 110  $\mu\text{m}$ . Thus, all embryos screened as small eye fell within this range of eye diameters, and represents a decrease in eye diameter large enough to be easily screened using a dissecting microscope. The variability among small eye phenotypes is most likely due to differences in the distribution of the MO in individual embryos by this stage of development, and is a common occurrence in studies using MO (Heasman, 2002). Furthermore the two lot numbers of *hsp70*-MO and one of *hsp70*-MO2 were all synthesized at different times, eliminating the possibility of any batch specific contaminants, and the phenotype was consistently produced using different microinjection systems and different operators at both the University of Saskatchewan and the University of Maryland. Small eye phenotype embryos did not display any other significant abnormalities, although slight reductions in pigmentation in a proportion of these embryos was observed. Overall growth and development was somewhat affected, and *hsp70*-MO injected embryos showed a slight reduction on overall body length.



**Table 3.1** Summary of *hsp70*-MO and control MO injection experiments

Solution Injected	Solution concentration <sup>1</sup>	Number of embryos	Survivors displaying small eye phenotype <sup>2</sup>	Survival rate at 52 hours
<i>chordin</i> -MO	2.25 $\mu\text{g}/\mu\text{l}$	54	0% (75%) <sup>3</sup>	N/A
Standard Sequence MO	3.46 $\mu\text{g}/\mu\text{l}$	86	0%	61%
Danieau Solution	N/A	175	0%	57%
<i>hsp70</i> -MO	2.25 $\mu\text{g}/\mu\text{l}$	123	13%*	58%
<i>hsp70</i> -MO	4.50 $\mu\text{g}/\mu\text{l}$	107	16%* <sup>4</sup>	23%
<i>hsp70</i> -MO	3.46 $\mu\text{g}/\mu\text{l}$	486	63%*	58%
<i>hsp70</i> -MO2	3.46 $\mu\text{g}/\mu\text{l}$	107	53%*	54%
<i>hsp70MM</i> -MO	3.46 $\mu\text{g}/\mu\text{l}$	109	0%	63%

1. 3.14 nl injected per embryo in all experiments
2. In all embryos, both eyes are affected equally
3. Bracketed numbers refer to percent embryos displaying typical *chordin* mutant phenotype
4. Majority of embryos injected with 4.50  $\mu\text{g}/\mu\text{l}$  *hsp70*-MO concentration displayed non-specific defects and death as indicated in Results, and do not appear in these counts

\* = statistically different from control embryos as determined by Fischer's exact test: *hsp70*-MO 2.25  $\mu\text{g}/\mu\text{l}$   $p=0.0067$ ; *hsp70*-MO 4.50  $\mu\text{g}/\mu\text{l}$   $p=0.0016$ ; *hsp70*-MO 3.46  $\mu\text{g}/\mu\text{l}$  and *hsp70*-MO2 3.46  $\mu\text{g}/\mu\text{l}$   $p<0.0001$

**Figure 11.** Small eye phenotype in 52 hpf zebrafish embryos produced by microinjection of 3.46  $\mu\text{g}/\mu\text{l}$  *hsp70*-MO into fertilized eggs. Severe small eye phenotype (A) and a more moderate small eye phenotype (B) are shown relative to an uninjected control embryo (C). All embryos screened as small eye phenotype lie within this phenotypic range. No other major phenotypic abnormalities are apparent in the *hsp70*-MO injected embryos, although a slight reduction in pigmentation and body length was observed.

**Severe  
Small Eye**

**A**



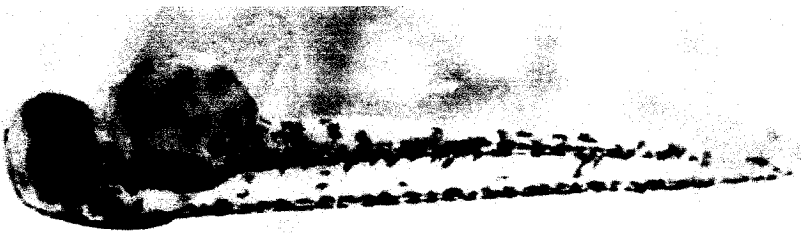
**Small Eye**

**B**



**Uninjected**

**C**



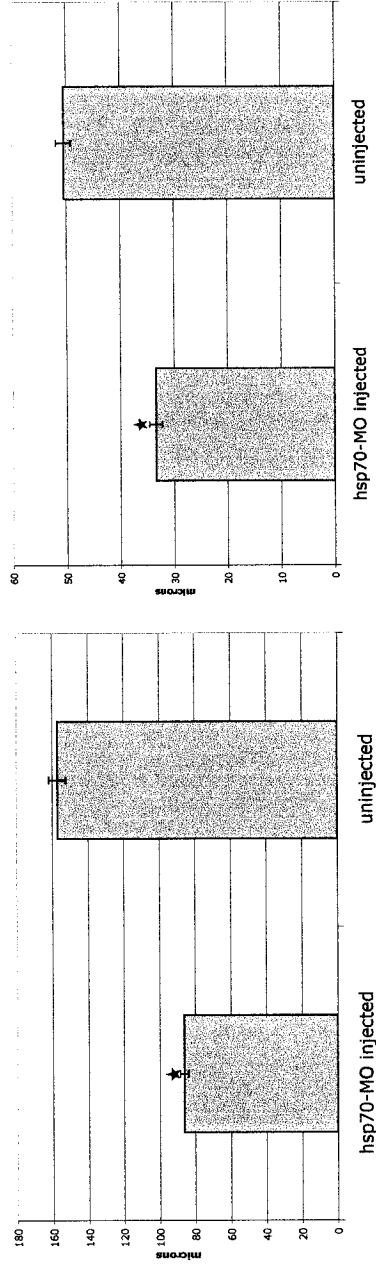
To better quantify the small eye phenotype, average eye and pupil diameters, as well as body length were calculated among fixed embryos screened as small eye, and compared to uninjected control embryos (Figure 12). Average eye diameter in small eye embryos decreased to 86  $\mu\text{m}$  as compared to an average diameter of 157  $\mu\text{m}$  for control embryos (Figure 12A). This represented an average decrease in eye diameter of 45%. An estimation of the reduction in lens size can be inferred by calculating pupil diameter in whole embryos. Average pupil diameter was 33  $\mu\text{m}$  among small eye embryos, as compared to a diameter of 50  $\mu\text{m}$  observed in uninjected controls (Figure 12B). This represented an average decrease in pupil diameter of 34%. Small eye embryos also exhibited slight reductions in overall body length (Figure 12C); however, these differences were quite minor relative to the effects observed in the eye. In all cases (overall eye diameter, pupil diameter, and body length), small eye embryos differed significantly from control embryos as determined by statistical analyses (unpaired t test,  $p < 0.0001$ ).

Embryos injected with a concentration of 2.25  $\mu\text{g}/\mu\text{l}$  *hsp70*-MO showed a much lower penetrance of the small eye phenotype, whereas those injected with 4.50  $\mu\text{g}/\mu\text{l}$  exhibited numerous inconsistent toxic effects, including developmental abnormalities and increased death rate, comparable to those seen when negative control MO were injected at this higher concentration. However, the number of small eye embryos produced in these experiments still differed significantly from control embryos, as determined by Fischer's exact test. Given these results, all subsequent experiments utilized 3.14 nl MO per injection at a concentration of 3.46  $\mu\text{g}/\mu\text{l}$  (10.9 ng/injection).

Injected embryos not displaying the characteristic small eye phenotype in *hsp70*-MO injection experiments deviated from the wildtype condition in only 5.7% of the cases, and these embryos developed a variety of severe and inconsistent defects (Figure 13). Non-specific phenotypes ranged from embryos exhibiting relatively minor defects such as slight edema and abnormal tail curvature (Figure 13A), to loss of prominent anterior structures such as the eye or parts of the brain (Figure 13B), to extremely severe developmental defects resulting in an undifferentiated mass of cells with little or no identifiable anatomical structures

**Figure 12.** Bar graphs illustrating average changes in eye and pupil diameter, as well as body length, in *hsp70*-MO injected embryos relative to uninjected controls. Average eye diameter decreased from 157  $\mu\text{m}$  in control embryos (n=27) to 86  $\mu\text{m}$  in *hsp70*-MO injected embryos (n=32) (A). Pupil diameter, used to infer decreases in lens diameter, was reduced from 50  $\mu\text{m}$  in control embryos (n=27) to 33  $\mu\text{m}$  in *hsp70*-MO injected embryos (n=30) (B). Body length of *hsp70*-MO injected embryos (n=22) also decreased slightly from control embryos (n=27) (C). Reductions in eye diameter, pupil diameter, and body length all differed significantly from control embryos (indicated as star on graphs) as determined by statistical analyses (unpaired t test  $p < 0.0001$ ). Standard error of means are shown for each data set.

**A** hsp70-MO injected embryos: average eye diameter **B** hsp70-MO injected embryos: average pupil diameter



**C** hsp70-MO injected embryos: average body length

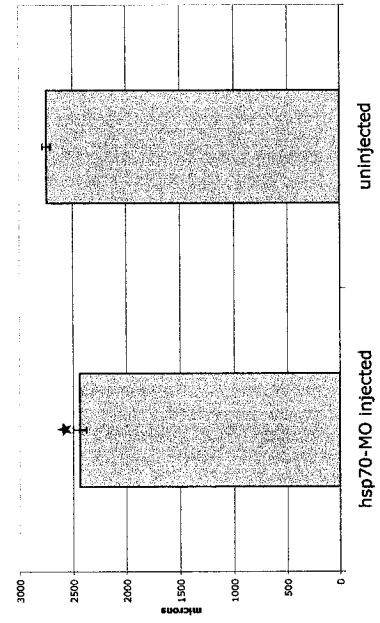


**Figure 13.** Representative photographs of small percentage of embryos screened as non-specific phenotypes after microinjection of 3.46  $\mu\text{g}/\mu\text{l}$  *hsp70*-MO. Phenotypes range from embryos showing defects in the yolk sac, tail, and anterior regions, including edema (A), to those exhibiting major defects throughout the embryo, including severe edema and failure to develop important anatomical structures including the eye (B). Extreme dysmorphology also appeared and was characterized by the absence of many anatomical landmarks and severe edema (C).





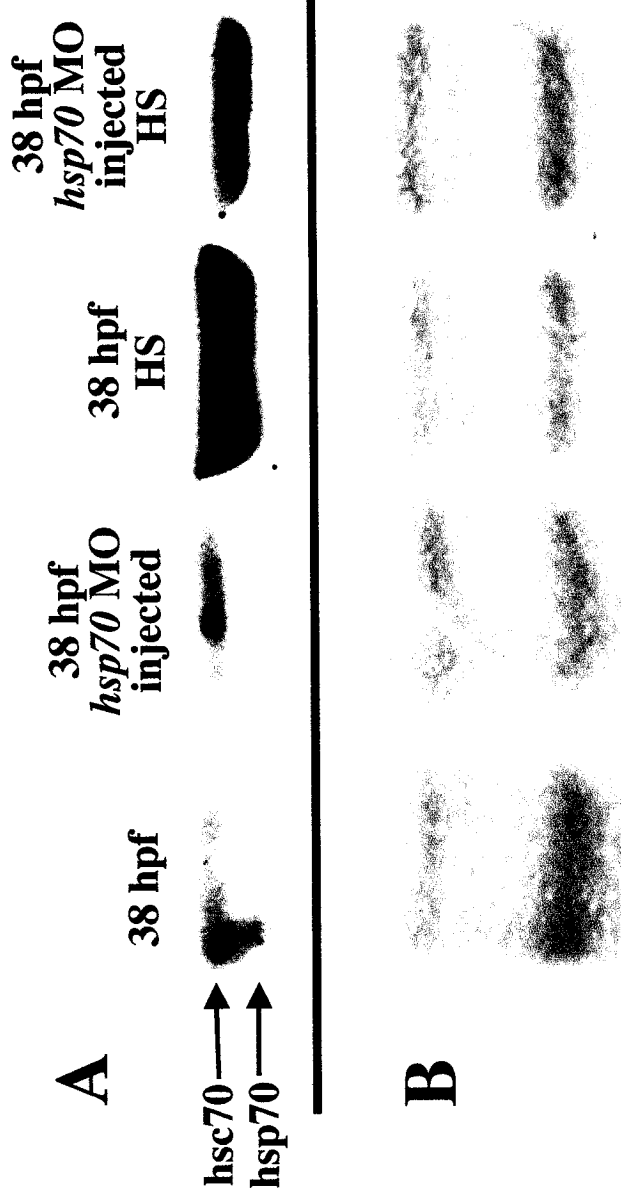
(Figure 13C). Such defects occurred in only a small proportion of embryos, and phenotypes were highly variable within single injection trials, indicating that the effect is not specific to the MO itself.

To ensure the observed small eye phenotype was exclusive to MO targeting *hsp70*, microinjections were performed using several negative controls. Firstly, the standard sequence MO is designed by the manufacturer such that its sequence does not target any known mRNA in zebrafish, and does not induce a phenotype. The standard sequence MO has been used in a number of previous studies employing MO in zebrafish (Nasevicius and Ekker 2000). Secondly, a MO based on the *hsp70*-MO sequence, but where 5 of the 25 base pairs in the oligo have been mismatched was designed. These mismatches should be sufficient to prevent the MO from inhibiting the translation of *hsp70* mRNA. Importantly, the mismatches also preserve the G/C content (known to affect MO activity) of the original MO sequence. Finally, zebrafish embryos were microinjected with Danieau solution, an isotonic solution used to dissolve the MO to their respective concentrations. Danieau solution injections served as an additional negative control and provided valuable information on expected survival rates from the microinjection procedure itself. Injection of either standard sequence MO or the 5 bp mismatch *hsp70*MM-MO at the same 3.46  $\mu\text{g}/\mu\text{l}$  concentration sufficient to induce a small eye phenotype in *hsp70* targeted MO, did not give rise to any embryos displaying the small eye phenotype (Table 3.1). Importantly, these injections still resulted in a similar small percentage of embryos displaying severe and inconsistent defects as observed for *hsp70*-MO and *hsp70*-MO2 (Figure 13). Thus, the small eye phenotype is specific only for the *hsp70* targeting MO, whereas the other defects observed in a small number of embryos are non-specific. Survival rates of embryos in these experiments, regardless of the identity of the MO, did not differ from those observed by injection of Danieau solution alone. Microinjection of Danieau solution did not result in embryos displaying a small eye phenotype (Table 3.1).

### 3.3.2 Hsp70 protein levels are diminished in *hsp70*-MO injected embryos at 38 hpf under normal and heat shock temperatures

The microinjection of MO targeted to *hsp70* gives rise to a reproducible small eye phenotype. MO function by inhibiting scanning of a target mRNA by the ribosome complex, thereby blocking its translation and depleting the cell of a functional protein product. Therefore, in order to confirm that *hsp70*-MO was effectively inhibiting the production of Hsp70 protein, Western blot analyses on injected and uninjected embryos at 38 hpf under normal and heat shock conditions were performed (Figure 14). Extracts were prepared at 38 hpf because this stage represented peak levels of *hsp70* expression, while heat shock treatments were used not only to investigate the effect of *hsp70*-MO on the heat shock response, but also as a positive control for antibody recognition. Injection of *hsp70*-MO resulted in the disappearance of Hsp70 under normal, non-heat shock growth temperature at which these experiments were carried out (Figure 14A). While the antibody cross-reacts with Hsc70, resulting in two closely spaced bands in these blots, Hsp70 can be easily distinguished from Hsc70 as it is a slightly smaller protein (72 kDa versus 73 kDa for Hsc70; Santa Cruz et al., 1997) and thus has a slightly greater relative mobility within SDS-polyacrylamide gel electrophoresis. Analysis of heat-shocked embryos revealed that the *hsp70*-MO also caused a reduction in the heat inducible up-regulation of Hsp70 expression. Under these conditions the MO cannot completely eliminate the Hsp70 band, a result that is not surprising considering both the amount of protein synthesized throughout the embryo after heat shock, and the fact that some MO degradation and dilution has occurred by this point in development. Equal protein loading was confirmed by Coomassie staining of SDS-PAGE gels (Figure 14B).

**Figure 14.** Western blot analysis of Hsp70 knockdown in *hsp70*-MO injected embryos. Embryos were allowed to develop until 36.5 hpf and then heat shocked at 37°C for 90 minutes, or maintained at 28°C for an additional 90 minutes. Hsp70 is a slightly smaller protein than Hsc70, and can be distinguished as a unique band with a slightly greater relative mobility than Hsc70. *hsp70*-MO injection caused a significant reduction in the constitutive expression of *hsp70* (compare lane 1 and lane 2 in A). Decreases in the amount of Hsp70 synthesized after heat shock, a extremely strong and rapid inducer of *hsp70* expression, was also evident (compare lanes 3 and lanes 4 in A). Equivalent protein loading was confirmed by coomassie blue staining of embryo extracts following SDS-PAGE (B).



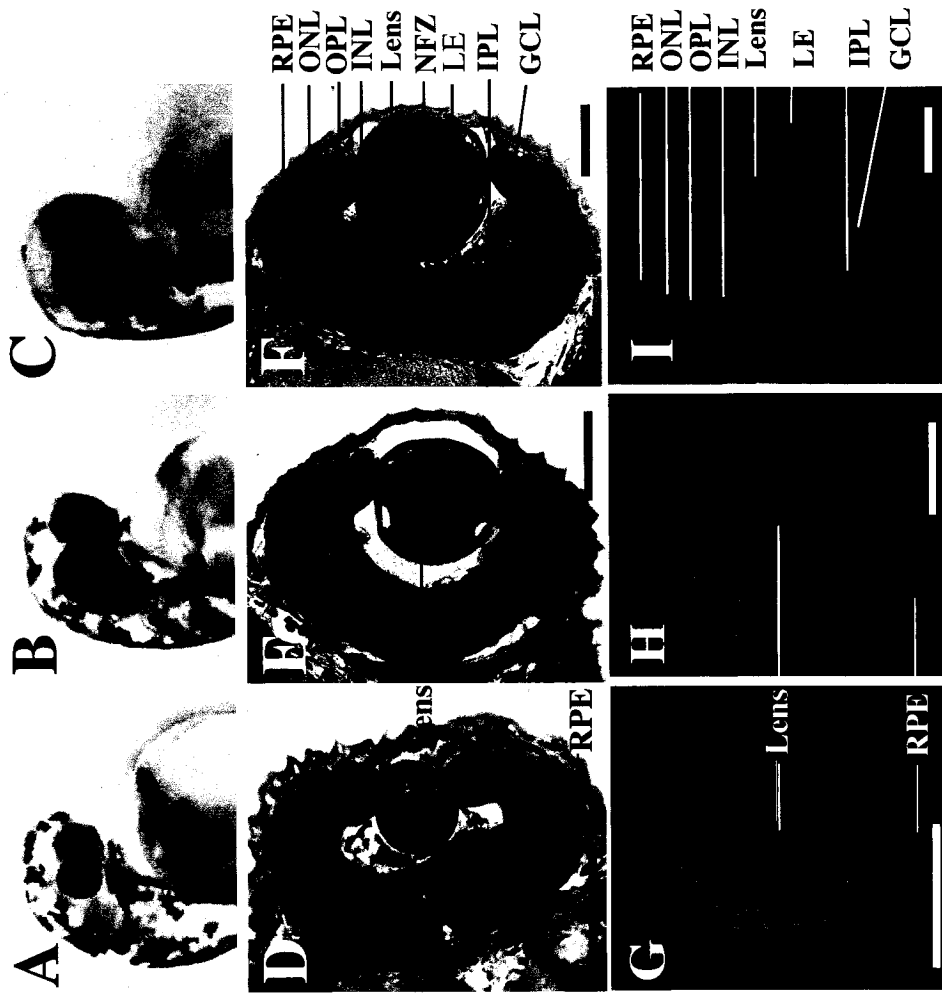
### **3.3.3 The small eye phenotype is characterized by an immature lens and disorganized retinal structure**

Microinjection of *hsp70*-MO depletes embryos of Hsp70 protein and results in a characteristic small eye phenotype, where eye diameter is typically 45% smaller than in control embryos. To permit a detailed assessment of the small eye phenotype, histological analysis was performed on small eye embryos at 52 hpf. Histology revealed that the small eye phenotype is characterized by an under-developed lens (Figure 15). Specifically, the lens is greatly reduced in size: severe small eye lenses are approximately 30  $\mu\text{m}$  (Figure 15D) in diameter, while more moderate small eye lenses had a diameter of 60  $\mu\text{m}$  (Figure 15E) at their widest location. Lenses of uninjected control embryos were approximately 90  $\mu\text{m}$  in diameter (Figure 15F). Thus, *hsp70*-MO injection resulted in lenses that were typically between 33% and 67% smaller than control lenses, and confirm lens reductions inferred through pupil measurements in whole embryos.

Normal zebrafish lens formation begins between 16-20 hpf, with the optic vesicle contacting the overlying head ectoderm. By 24-26 hpf the lens vesicle has developed (Schmitt and Dowling, 1994, Easter and Nicola, 1996; Li et al, 2000). The concentric organization of lens fibre cells becomes apparent by 36 hpf, and the central core of the lens appears significantly different from the cuboidal epithelium lining the lens periphery. By 48 hpf differentiated primary fibres that have lost their nuclei and organelles have begun to appear at the lens core. However, the cellular structure of small eye lenses in *hsp70*-MO injected embryos most closely resembled lenses of earlier stages of development. This morphology is most noticeable in those embryos displaying the severe small eye phenotype (Figure 15A,D,G). Severe small eye embryos had an extremely small lens, did not display the concentric fibre organization characteristic of lenses at this age, and clear separation of the lens epithelium and lens core was just becoming apparent. However, these lenses do express the early lens marker, *zl-1* (first detectable between 21-22 hpf; Vihtelic et al., 2001), suggesting that some of the earlier events in lens formation are occurring in these embryos (Figure 16E). The proportion of *hsp70*-MO injected embryos that

**Figure 15.** Histological analysis of small eye phenotype in *hsp70*-MO injected embryos and uninjected control embryos at 52 hpf. A,D,G; severe small eye phenotype. B,E,H; moderate small eye phenotype. C,F,I; uninjected control embryos. A-C: unstained whole embryos. D-F; methylene blue-azure II-basic fuchsin stained 5.5  $\mu\text{m}$  thick methacrylate cross-sections. G-H; DAPI stained 5.5  $\mu\text{m}$  thick methacrylate cross sections viewed through a fluorescence microscope to visualize nuclei. The immature structure of the lens and retina are readily apparent in the small eye embryos (D,E,G,H) relative to uninjected control embryos (F,I). Note that the nuclear free zone has begun to appear in the uninjected embryos, but is not present in the small eye lens. RPE=retinal pigmented epithelium; ONL=outer nuclear layer; OPL=outer plexiform layer; INL=inner nuclear layer; IPL=inner plexiform layer; GCL=ganglion cell layer. NFZ=developing nuclear free zone. Scale bar = 50  $\mu\text{m}$

*hsp70*-MO Injected      Uninjected

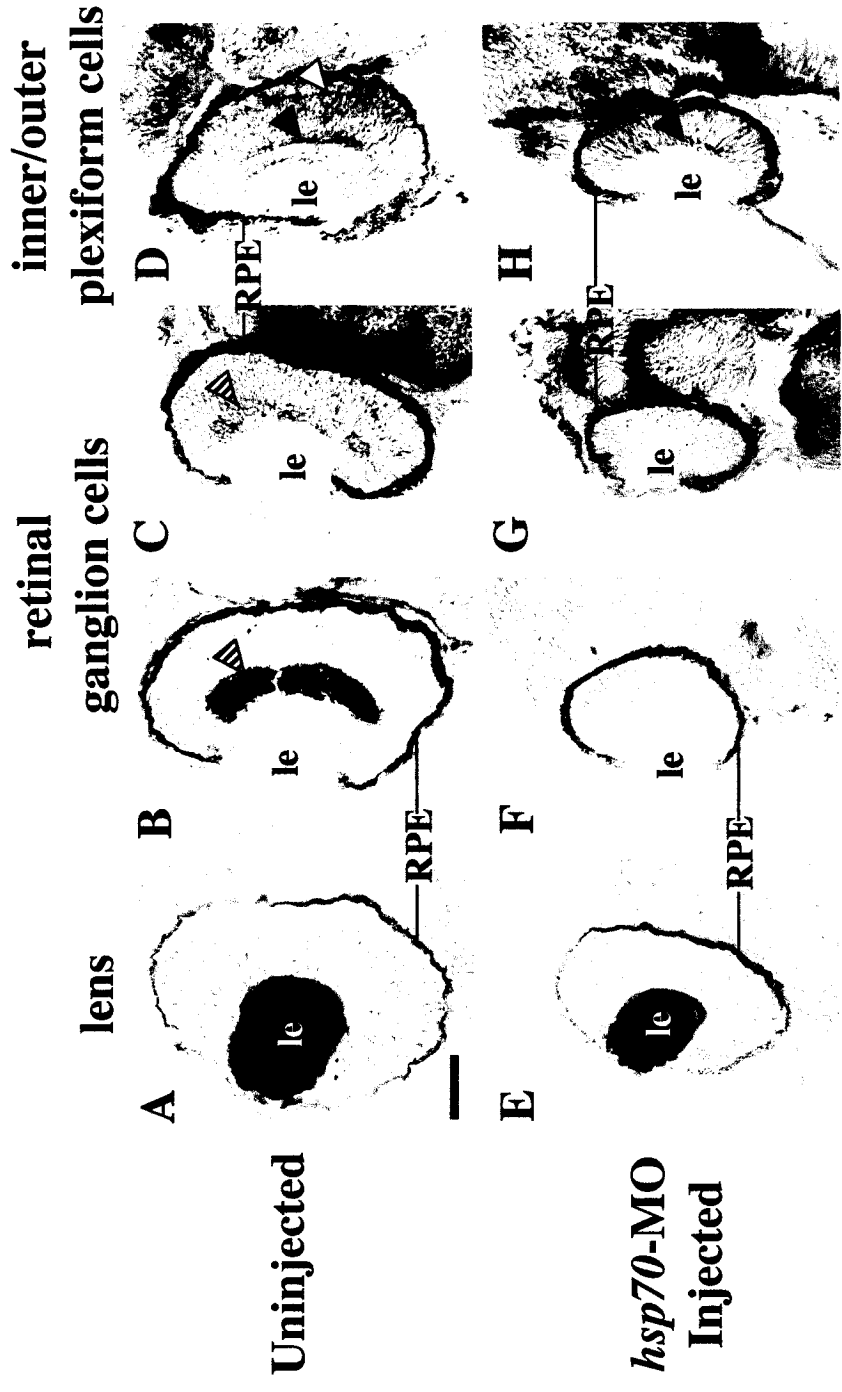


displayed a more moderate phenotype (Figure 15B,E,H) exhibited some features of more mature lenses. However, they were still significantly smaller in size, there was no central zone of denucleation yet apparent, there were fewer cells within the lens epithelium and core, and the lens epithelial cells were larger and more cuboidal than is normally expected for a 52 hpf embryo.

The retinal organization of *hsp70*-MO injected embryos was also disrupted, and the retinal structure appeared underdeveloped at 52 hpf. Normally, the bulk of retinal neurogenesis occurs from 27-55 hpf (Schmitt and Dowling, 1994, Easter and Nicola, 1996; Fadool et al 1997; Li et al, 2000). The initial population of retinal ganglion cells begins to appear at approximately 30 hpf. Postmitotic interneurons forming the inner nuclear layer appear by 38 hpf, while neurons in the outer nuclear layer are evident by 43 hpf. By 50 hpf, the normal retina exhibits the typical laminated structure, and most cell types can be identified morphologically (Figure 15F,I). Finally, between 55-60 hpf photoreceptor cell outer segments differentiate, and by 60-80 hpf, behavioural analyses reveal that the retina is functional. The *hsp70*-MO induced small eye phenotype retinas lacked the characteristic laminated structure of uninjected embryos at 52 hpf (Figure 15D,E,G,H). Retinal size was also reduced relative to control embryos. Severe small eye retinas were approximately 25  $\mu\text{m}$  thick, while moderate small eye retinas were approximately 45  $\mu\text{m}$  in thickness. Relative to a retinal thickness of 70  $\mu\text{m}$  observed in control embryos, *hsp70*-MO injected embryos have retinas between 36% and 64% smaller than uninjected embryos. Immunostaining further confirmed the disruption of retinal formation (Figure 16). Normal retinal ganglion cells appear to be completely absent or severely under-developed in *hsp70*-MO injected embryos, as retinal cells are not expressing the retinal ganglion cell markers *zn-5* (compare Figure 16B to F) or *znp-6* (compare Figure 16C to G). Staining with *zns-2*, a marker of the inner and outer plexiform layers, was also abnormal in that the two recognizable stripes of expression were not present in the *hsp70*-MO injected embryos, although some weak staining was apparent immediately adjacent to the lens in some embryos (Figure 16 compare D to H). This suggests that formation of the inner plexiform



**Figure 16.** Immunohistochemical analysis of lens and retinal protein expression in wildtype (A-D) and *hsp70*-MO induced severe small eye (E-H) paraffin sections. Lens protein *zl-1* is expressed in both wildtype (A) and small eye (E) lens. Retinal ganglion cells (striped arrowheads), visualized by immunostaining with either *zn-5* (B,F) or *znp-6* (C,G) are not expressing either of these proteins in small eye embryos (F,G), but are readily apparent in the eye from uninjected embryos (B,C). Similarly, both inner plexiform (black arrowheads) and outer plexiform (white arrowhead) layers are stained with *zns-2* in wildtype sections (D), but a similar pattern is not apparent in the eyes of microinjected embryos with the small eye phenotype (H). Staining was visualized using an ABC kit (A-H). Dorsal is to top. Scale bar = 50  $\mu$ m



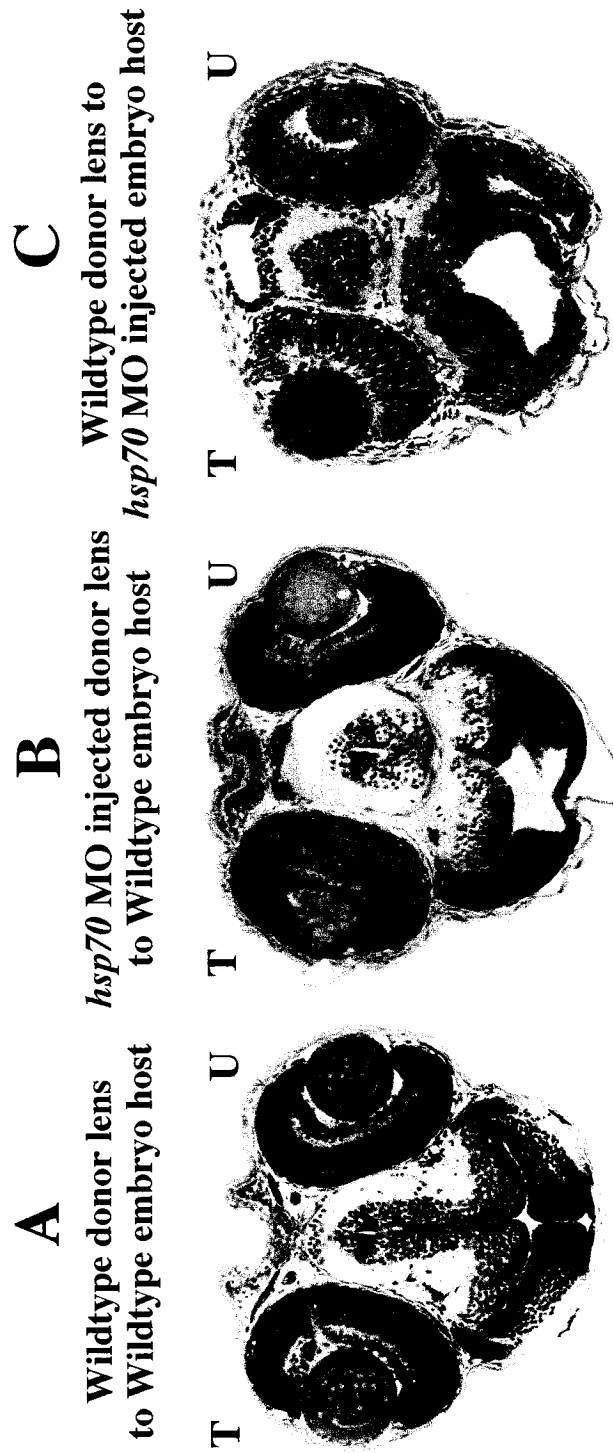
layer, although delayed, was beginning to occur in microinjected embryos at this age.

### **3.3.4 The immature lens phenotype in *hsp70*-MO injected embryos is lens autonomous**

Since *hsp70* expression has only been detected in the lens under non-stress conditions, it was predicted that the small lens phenotype described in this thesis would be lens autonomous. This hypothesis was tested using lens transplantation. Recent studies performed on the Mexican cavefish, *Astyanax mexicanus*, which has both a surface dwelling and an eyeless cave dwelling form, have demonstrated a central role for the lens in teleost fish eye development. In this system, lens transplant experiments revealed that signals originating from the lens play a critical role in eye formation (Yamamoto and Jeffery, 2000). The lens transplant technique developed in this system is transferable to zebrafish, and zebrafish lens transplantation experiments have been used to demonstrate the autonomy of lens defects in zebrafish mutants (e.g. Vihtelic et al., 2001). Lenses isolated from one eye of *hsp70*-MO injected embryos (donors) were transplanted into the optic cup of uninjected, wildtype embryos (hosts) at 30-34 hpf, and transplant embryos were allowed to develop to 52 hpf. Since the *hsp70*-MO small eye phenotype is not visibly discernable at 34 hpf, all donor embryos were also allowed to develop to 52 hpf, and development of their remaining lens in the untouched contralateral eye was assessed. Only those host embryos receiving lenses from donor microinjected embryos that displayed a typical small eye phenotype in their remaining eye at 52 hpf were assessed further. Initial whole-embryo analysis revealed that transplanted lenses in host embryos were extremely small, and hardly visible within the surrounding optic cup. In contrast, the contralateral control eye on the host embryos exhibited normal eye morphology at 52 hpf. Sections through transplant embryos at 52 hpf revealed that the lens retained the cellular characteristics of the small eye phenotype (Figure 17). Transplanted lenses were extremely small, did not show the same degree of lens fibre differentiation and lamination that was evident in lenses

on the non-transplanted control side, nor the clear definition between lens epithelium and core (Figure 17B). In contrast, control transplants where a lens from an uninjected embryo was removed and reinserted into the optic cup of a second uninjected embryo, revealed normal lens and retinal morphology (Figure 17A). Thus, the presence of a wild-type retina could not rescue the *hsp70*-MO dependent lens phenotype, suggesting that the lens phenotype is indeed lens autonomous. However, it was possible that the underdeveloped retina in microinjected embryos was the source of a long-lasting inhibitory signal that stunted lens development, and that the transplanted lens contained enough of this signal to prevent recovery following transplant to the wild type retina. In order to address this possibility, reciprocal transplants in which wild type lenses from uninjected embryos were transplanted into the retinas of *hsp70*-MO injected embryos were performed. If there was a lens inhibitory signal produced by these retinas, it would be expected to act on the wild-type lens and stunt its development. However, the lens from an uninjected donor continued to develop normally within the *hsp70*-MO injected host retina, confirming the lens autonomy of the immature lens phenotype (Figure 17C). Interestingly, the wildtype lens is unable to induce normal retinal patterning in *hsp70*-MO injected, and retinas continued to exhibit the disrupted retinal structure characteristic of small eye embryos. This occurrence may be related to the developmental stage of embryos when transplants were performed (see Discussion). Brain morphology also appears disrupted in small eye host embryo in Figure 17C. However, these abnormalities are not consistently observed in small eye embryos in these or other experiments. In addition, a proportion of wildtype embryos appeared similar in cross section (Figure 17B) suggesting that the observed brain morphology is an artifact related to the plane of sectioning.

**Figure 17.** Histological analysis of lens transplant experiments at 52 hpf. Lenses were isolated from donor embryos and inserted into the optic cup of host embryos between 30-34 hours of age. The left eye received the transplanted lens while the right side served as an unmanipulated control in all cases. Lens transplants are shown relative to wildtype lens into wildtype optic cup control transplants (A). Note that transplanted lenses from *hsp70*-MO injected donor embryos still exhibit characteristics of small eye phenotype including extremely small size and immature lens organization following transplant into a wild type retina (B). Reciprocal transplants of wildtype lenses transplanted into *hsp70* morpholino injected optic cups maintain normal morphology, and are unable to revert the *hsp70* morpholino induced knockdown retinal phenotype to the wildtype condition (C). T; transplant side. U; unmanipulated control side.



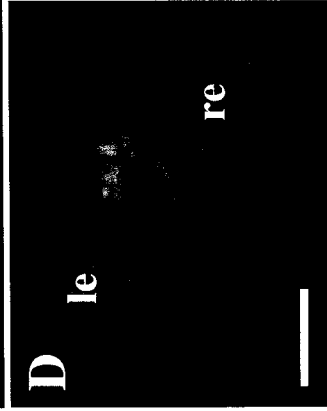
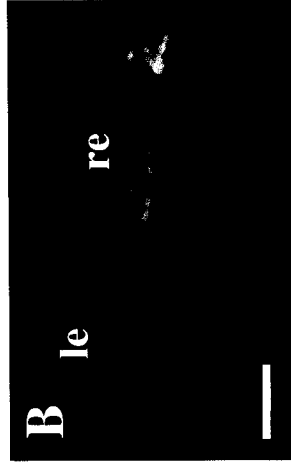
### 3.3.5 Apoptotic nuclei persist in lenses of *hsp70*-MO injected embryos beyond 48 hpf

During lens development, cell differentiation leads to the formation of primary and secondary lens fibres. In order to ensure the optical clarity of the lens, lens fibres must degrade cellular organelles, including the nucleus, but maintain overall cellular integrity. Recent evidence suggests that the process of organelle degradation within differentiating lens fibre cells shares several common features with classical apoptotic events. For example, both events involve the degradation of chromatin leading to the presence of so-called “DNA ladders” (Appleby and Modak, 1977; Bassnett and Mataic, 1997; Ishazaki et al, 1998), and the fragmented DNA is amenable to labeling via TUNEL analysis (Ishazaki et al, 1998). Cole and Ross (2001) previously showed that the developing zebrafish lens exhibits apoptotic-like nuclei, with the peak number occurring during the fibre differentiation phase of 30-40 hpf. Following this time, apoptotic nuclei become significantly reduced and by 48 hpf they are no longer detectable in the lens. Importantly, this corresponds with the time period during which: 1) primary and secondary fibre differentiation occurs, 2) *hsp70* expression occurs, and 3) the small eye phenotype of *hsp70*-MO injected embryos becomes apparent. Thus, a similar analysis was performed on both uninjected and *hsp70*-MO injected embryos at both 36 and 52 hpf (Figure 18A-D). In agreement with the data of Cole and Ross (2001), numerous apoptotic nuclei were detected using TUNEL analysis within the lens of uninjected embryos at 36 hpf (Figure 18A), but were not detected in the lens by 52 hpf (Figure 18C). However, *hsp70*-MO injected embryos continued to exhibit TUNEL-labeled nuclei within the lens at 52 hpf (Figure 18D), in addition to the normal peak at 36 hpf (Figure 18B). In all cases, the TUNEL-labeled nuclei were located specifically within the lens fibres, and labeling was absent from the surrounding lens epithelium. The retinas of small eye and uninjected embryos contained a comparable number of TUNEL labeled nuclei (Figure 18A-D), and these levels were in agreement with those reported by Cole and Ross (2001) to occur during normal development. The small lens of *hsp70*-MO injected embryos does not appear to be correlated with a

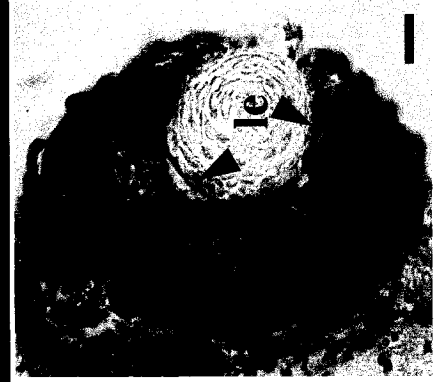
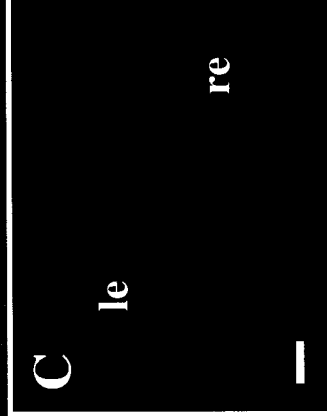
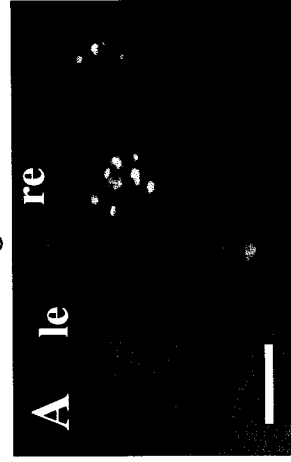
**Figure 18.** Analysis of TUNEL positive nuclei and PCNA expression in uninjected control embryos (A,C,E) and small eye phenotype embryos (B,D,F) at 36 hpf (A,B) and 52 hpf (C-F). Notice the presence of apoptotic nuclei in the developing lens and retina at 36 hpf (A,B). Basal level of apoptosis seen in both injected and control embryos agrees with the number of apoptotic nuclei described by Cole and Ross (2001) in the normal development of the eye at 36hpf. However, by 52 hpf, apoptotic nuclei are no longer apparent in the lens of uninjected control embryos (C) as expected (Cole and Ross, 2001), but continue to appear in the small eye phenotype lens (D). Again, normal developmental apoptosis is observed in the retina of *hsp70*-MO injected embryos (B,D) and control embryos (A,C) at 36 hpf (A,B) and 52 hpf (C,D). Immunostaining of Proliferating Cell Nuclear Antigen (PCNA) in wildtype (E) and small eye (F) 7  $\mu$ m paraffin sections at 52 hpf. Although the small eye lens contains significantly less cells than wildtype controls, this does not appear to be caused by a loss of proliferative capability of lens fibre precursors originating from the lens epithelium (arrowheads). PCNA levels immediately drop when these cells exit the cell cycle and enter the lens vesicle as expected. le=lens; re=retina. Scale bar = 50  $\mu$ m



*hsp70*-MO Injected



Uninjected



36hpf

52hpf

52hpf

loss of proliferative capability within the lens epithelial cells, since staining for proliferating cell nuclear antigen (PCNA) was comparable within the lens of both injected and uninjected embryos (Figure 18E,F). PCNA is a highly conserved protein essential for cellular DNA synthesis, and a well-established marker of proliferating cells in fish and other vertebrates (Cid et al, 2002). As expected, PCNA levels dropped immediately following exit of lens epithelial cells from the cell cycle as they are recruited to the region of fibre differentiation within the lens.

### **3.3.6 Recovery of overall lens and retinal organization in *hsp70*-MO injected embryos by 5 days post fertilization**

The data to this point have revealed that normal lens and retinal development is disrupted in *hsp70*-MO injected embryos, that the effect is lens autonomous, and that it is correlated with an extension of the time period over which TUNEL-positive nuclei appear during the process of fibre differentiation within the lens core. However, whether the *hsp70*-MO induced phenotype is permanent, or if the lenses of these embryos can recover following degradation/dilution of the MO later in development was unknown. Although MO have been shown to successfully phenocopy mutations not expressed until 48 hpf (Nasevicius and Ekker, 2000) and that such phenotypes can be expressed up to 4 dpf (Baat et al., 2001; Heasman, 2002), there has been no evidence of MO remaining stable for periods longer than this. If the *hsp70*-MO disrupts fibre differentiation subsequent to the exit of lens epithelial cells from the cell cycle as data from this thesis suggests, but does not affect earlier inductive events in the lens formation pathway such that lens organization can be properly specified, then one would expect embryos to recover from the phenotype once the MO has been degraded/diluted during development after 52 hpf. Alternatively, if the *hsp70*-MO disrupts earlier patterning events that occur only during discrete spatial and temporal windows of early embryogenesis, and that are required to give rise to a properly organized lens, then MO dilution would not be expected to allow for further lens maturation if this window of development has passed. *hsp70*-MO injected embryos that displayed the typical

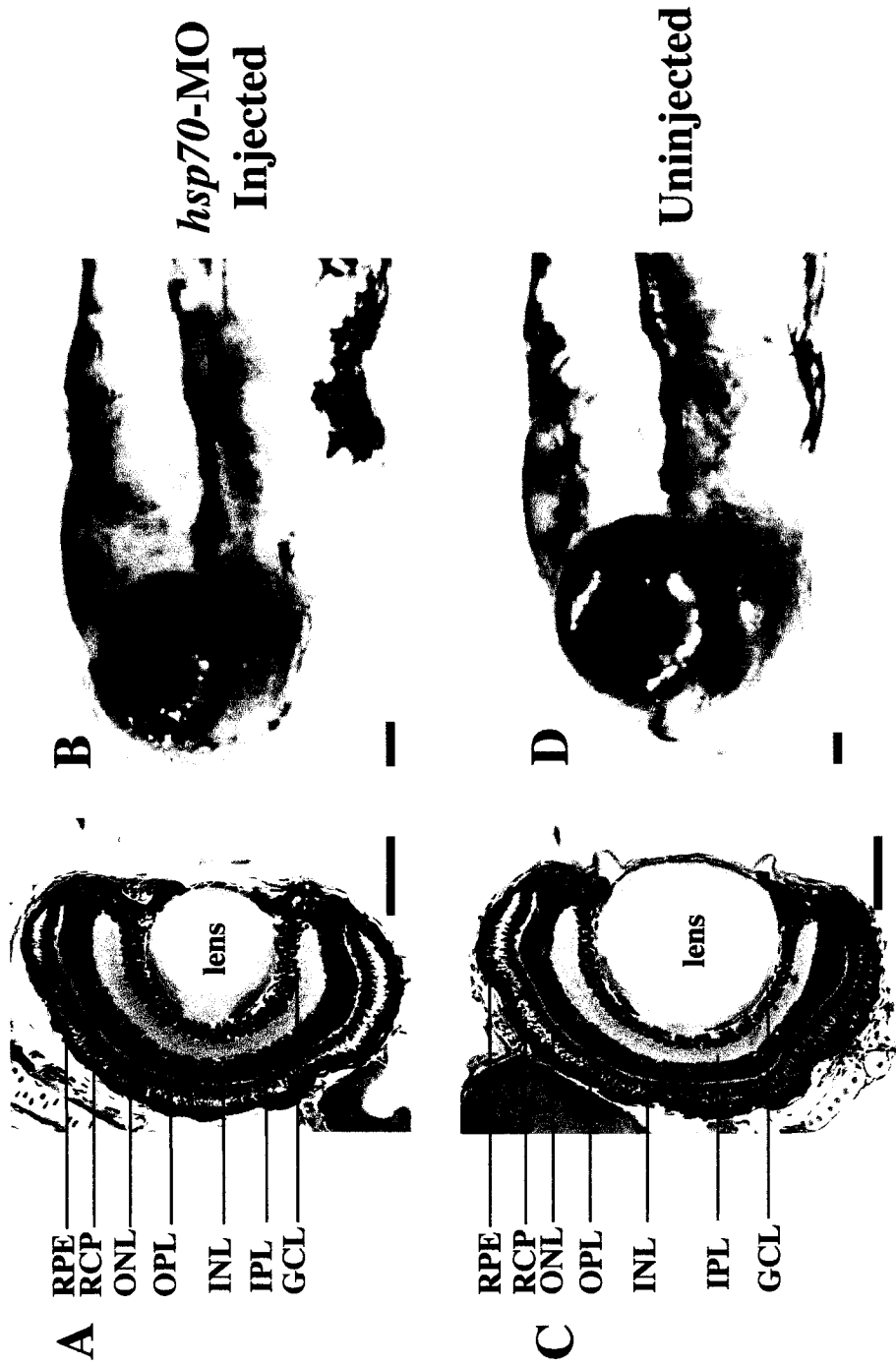
small eye-phenotype at 52 hpf were allowed to develop until 5 dpf, after which histological analysis was performed. Sections from injected embryos at this age revealed that overall lens and retinal organization of *hsp70*-MO injected embryos is comparable to uninjected embryos (Figure 19). Although the lens is slightly smaller than in uninjected control embryos at 5 dpf, its organizational structure and the degree of fibre differentiation was indistinguishable from that of a mature lens (Figure 19A,C).

The observed recovery in *hsp70*-MO injected embryos is associated with degradation/dilution of the *hsp70*-MO. Microinjection *hsp70*-MO that contained a 3' fluoroscein tag visualized by fluorescent microscopy was used to analyze the stability of this *hsp70*-MO within the embryo. In embryos injected with fluoroscein tagged *hsp70*-MO, fluorescence was detected in 90% of animals at 48 hpf. However, only 26% of embryos showed fluorescence at 3 dpf, and by 4 dpf fluorescence was no longer detectable in any of the injected embryos (data not shown). These data suggest that the recovery observed in *hsp70*-MO injected embryos at 5 dpf is closely correlated with dilution/degradation of the MO below an effective concentration (Heasman, 2002).

#### **3.4 Analysis of the role of HSFs in the regulation of *hsp70* expression during embryonic lens development in zebrafish**

Studies investigating a possible role for HSFs during development have demonstrated these molecules are critical players in a variety of developmental events, and several of these studies have demonstrated significant reductions in constitutive Hsp expression when one or more HSFs have been disrupted (Xiao et al., 1999). In particular, the lens specific HSF4 was shown to play a fundamental role in mammalian eye development, and was required for the proper differentiation of lens fibre cells (Min et al., 2004). However, the developmental significance of HSFs in non-mammalian vertebrates remains unresolved, including the possible role of HSFs in the regulation of lens-specific *hsp70* expression. In zebrafish, few studies have examined the function of HSFs in development, and none of these

**Figure 19.** Histological and morphological analysis of *hsp70*-MO induced small eye phenotype (A,B) and uninjected control embryo (C,D) at 5 dpf. 5.5  $\mu\text{m}$  thick methacrylate cross sections through the developing eye of small eye phenotype embryos (A,C) reveal that the eye and related structures remain smaller than uninjected controls (B,D), but recover proper lens and retinal morphology characteristic of this stage. RPE=retinal pigmented epithelium; RCP=rods and cones of photoreceptors; ONL=outer nuclear layer; OPL=outer plexiform layer; INL=inner nuclear layer; IPL=inner plexiform layer; GCL=ganglion cell layer. Scale bar = 50  $\mu\text{m}$ .



studies have yet identified a specific role for these molecules during normal embryonic development. Thus, in the present study the three HSFs identified in zebrafish were analyzed for their role in the normal embryonic development. HSFs may be responsible for regulating lens-specific expression of *hsp70*, and several lines of experiments were performed to address this hypothesis.

### **3.4.1 Amino acid sequence analysis of zebrafish HSFs**

All members of the HSF family share common structural features, including a highly conserved DNA binding domain and a transactivation domain (HR-A/B) involved in translocation to the nucleus and activation induced trimerization (Pirkkala, 2001). Vertebrate HSF1 and HSF2 also possess a carboxyl-terminal inhibition of trimerization domain (HR-C) involved in the dissociation of HSF trimers. In contrast, mammalian HSF4 lacks a HR-C domain, and HSF4 binds DNA constitutively (Pirkkala, 2001).

The zebrafish genome encodes at least three HSFs (Figure 20). Two of these molecules have been previously identified as HSF1 (GenBank Accession: NM\_131600) and HSF2 (GenBank Accession: NM\_131867). The third has recently been identified in a zebrafish embryonic EST screen, and is here designated as HSFX (GenBank Accession: NM\_001013317). Predicted amino acid sequence comparisons between all three of these zebrafish HSFs confirm the identity of HSF1 and HSF2, as these two molecules possess the HR-C domain, in addition to the highly conserved DNA binding and HR-A/B domains. Interestingly, and similar to mammalian HSF4, HSFX lacks the HR-C domain associated with the inhibition of trimerization. This suggests that HSFX may bind DNA constitutively, and could represent the ancestral gene that gave rise to mammalian HSF4. However, in contrast to HSF4 and all other known HSFs, HSFX is truncated at the C-terminal, resulting in a much shorter protein. Regardless, zebrafish HSFX represents a unique vertebrate heat shock factor expressed during development.

**Figure 20.** Amino acid sequence comparison of zebrafish HSFs. All members of the HSF family share common structural features, including a highly conserved DNA binding domain (red), and a transactivation domain (HR-A/B) (green) involved in translocation to the nucleus and activation-induced trimerization. Vertebrate HSF1 and HSF2 also possess a carboxyl-terminal inhibition of trimerization domain (HR-C) (blue) involved in the dissociation of HSF trimers. Similar to mammalian HSF4, HSFX lacks the HR-C domain associated with the inhibition of trimerization. This suggests that HSFX may bind DNA constitutively, and could represent the ancestral gene that gave rise to mammalian HSF4. However, in contrast to HSF4 and all other known HSFs, HSFX is truncated at the C-terminal, resulting in a much shorter protein.

```

1
HSF1 MEYHSVGPGGVVVVTGNNVPAFLTKLWTLVEDPDTDPLICWSPNGTSHFVFDQGRFSKEVL
HSF2 -MKHSS-----NVPFAFLTKLWTLVEDSDTNEFICWSQEGNSFLVLDEQRFAKEIL
HSFX MQENPGSIGVDGGYASNVPFAFLTKLWTLVEDPETNHLICWSATGTSHFVFDQGRFAKEVL
      .                ***** . *      **** * . ** * * . ** . ** . *

61
HSF1 PKYFKHNNMASFVRQLNMYGFRKVVHIEQGGLVKPEKDD-TEFQHPYFIRGQEQLLLENIK
HSF2 PKFFKHNNMASFVRQLNMYGFRKVMHIDSG-IVKQERDGPVEFQHPYFKHGQDDLLENIK
HSFX PKYFKHNNMASFVRQLNMYGFRKVVNIEQSGLVKPERDD-TEFQHLIFLQGHLEHLEHIK
      ** . ***** . * . . . ** * . *      **** * * . * . . ** . **

121
HSF1 RKVTTVSNIKHEDVRFSTPDAVFKGILAVFEMFGKQESITSSLSLXZRHHEMLVFEVAFGR
HSF2 RKVS---NARPEEENIQDQDLSFLLPSVLSVNFQANNQARLATQEFENHAIWTELSDLA
HSFX RKVS---IVKSEETKVSQEDLTKLNLVYVLRQGENREEMQYQDMQYQHTVWVWVWVSLR
      *** . . * . * . * . ** . . . ** * . . . * . * . ** * . **

181
HSF1 QKHSQQQKVVNKLIQFLITLARSNR--VLGVKRMPLMLNDSSSAHSMKFSRQYSLESP
HSF2 KVHVQQQVVIKELVQFIFTLVQNNR--LLNLKRKRPLALNING---KKSKEFHQLFEETPI
HSFX QNHTQQQKVMNKLIFLFSQMQSNPSTVGMKRKPLMLDDGCSTPPASKFSHNHSMESL
      . * *** . * . * . . . * . . . ** * * *      * * . . *

241
HSF1 APSSTAFTGTGVFSSESPVKTGPIISDITELAQSSPVATD--EWIEDRTSPLVHIKEEPS
HSF2 DHSKTTVNGLKNNSD---ISDDVVICDITDED---PEVTDGIVPDEEDAEIVEITYE-S
HSFX QESFYIQSPSTESAS-----CSTSSVMTGGPIISD-----VTEIPQS-S
      * . . . . * . *      . * *

301
HSF1 SPAHSPEVEEVCPEVEVEGAGSDLPVDTPLSPTTFINSILQSEPVFRPDSAPSEQKCLS
HSF2 SPKTVQQDSANGTIVNSTAHQEAEPKTTHDVSTT--NSALQLNK-----PS-----
HSFX SMALQMQAEEER-----
      *

361
HSF1 VACLNDNYPQSEITRFLFSGFSTSSLHLRPHSGTELHDHLESIDSGLENLQQILNAQSINF
HSF2 --CLSLEDPMKLMDSILSENGAISQININLLGKVELMDYLDSDIDCSLEDFQAMLYGKQFNI
HSFX -----

421
HSF1 DSSPLFDIFSSAASDVDLDSLASIQDLLSPDPVKETESGVDTDSGKQLVQYTSQPSFSPI
HSF2 DP----DIIIEETISETKNNNSKANKENLDSE-----NTD--KQLIQYTT----CPL
HSFX -----

481
HSF1 PFSTDSSSTDLPMLLELQD--DSYFSSEPTEDPTIALLNQFVPEPDSRTRIGDPCFKLK
HSF2 MAFLDGCPTLTPSDPQPEDPPDLLDESLEMKTPRSSLRLEPLTEAEANEATLFYLCELN
HSFX -----

541
HSF1 KESKR-----
HSF2 SDLPNADTPPLDI
HSFX -----

```



### 3.4.2 Morpholino modified antisense oligonucleotide mediated knockdown of *hsf1* yields small eye phenotype in 2-day-old embryos

A MO based strategy was used to analyze the role of *hsf1*, *hsf2*, and *hsfx* in embryonic zebrafish development, with initial experiments examining *hsfx*. The same microinjection procedures described previously for *hsp70*-MO were used in these experiments. Positive and negative control injections were performed previously, and not repeated here. As with *hsp70*-MO, optimal injection concentrations of each MO were initially determined (Table 3.2). Microinjected embryos were subject to the same screening procedure described for *hsp70*-MO injections. Embryos microinjected with *hsf1*-MO at a concentration of 2.25  $\mu\text{g}/\mu\text{l}$  were indistinguishable from control embryos at 24 hpf, whereas 55% of the 263 assayed embryos displayed a characteristic small-eye phenotype apparent during the second day of development. A much lower potency was observed in embryos where *hsf1*-MO was injected at a concentration of 3.46  $\mu\text{g}/\mu\text{l}$ . Although the number of *hsf1*-MO injected embryos displaying a small eye phenotype still differed significantly from controls at both of these concentrations, as determined by Fischer's exact test ( $p < 0.0001$ ). However, the 3.46  $\mu\text{g}/\mu\text{l}$  MO concentration was also associated with an increase in non-specific defects (30% of the 408 injected embryos) not observed in the 2.25  $\mu\text{g}/\mu\text{l}$  injections. Thus, a MO concentration of 2.25  $\mu\text{g}/\mu\text{l}$  was used in all subsequent experiments (Table 2). The majority of embryos displayed the small eye phenotype shown in Figure 21A, although some variation in severity was observed, with a minority of the embryos displaying a range of eye sizes between the small eye and moderate small eye phenotype (Figure 21B) relative to uninjected embryos (Figure 21C). This is most likely due to variation in the distribution of MO in individual embryos. Importantly, the phenotype was consistent, easily distinguishable from control-injected embryos, and reproducible in eight separate injection trials. *hsf1*-MO induced small eye embryos did not exhibit defects in any other anatomical structures, with the exception of slight reductions in pigmentation similar to that observed in the *hsp70*-MO induced small eye phenotype.

**Table 3.2** Summary of *hsf1*-MO, *hsf2*-MO and *hsfx*-MO injection experiments

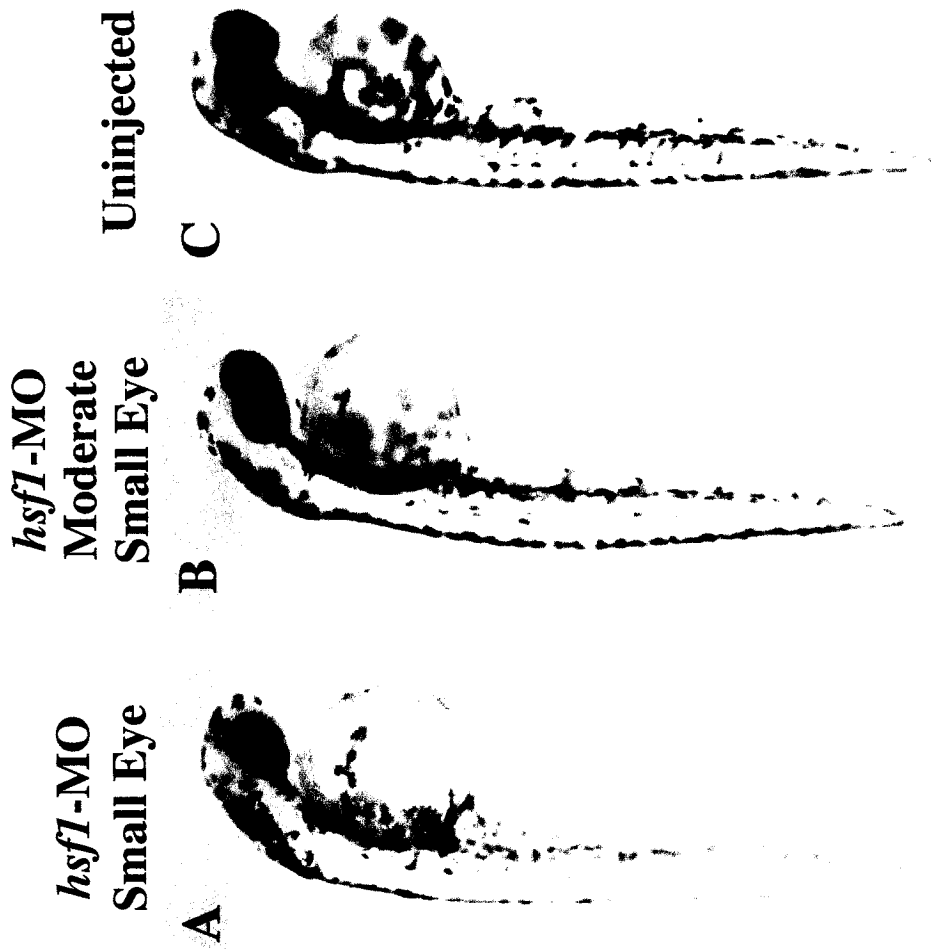
Solution Injected	Solution concentration <sup>1</sup>	Number of embryos	Survivors displaying small eye phenotype <sup>2</sup>	Survival rate at 52 hours
<i>hsf1</i> -MO	2.25 µg/µl	263	55%*	58%
<i>hsf1</i> -MO	3.46 µg/µl	408	33%*	55%
<i>hsf2</i> -MO	2.25 µg/µl	180	5%	49%
<i>hsf2</i> -MO	3.46 µg/µl	178	5%	66%
<i>hsf2</i> -MO	4.50 µg/µl	157	0%	10%
<i>hsfx</i> -MO	2.25 µg/µl	390	16%*	53%
<i>hsfx</i> -MO	3.46 µg/µl	311	2%	36%
<i>hsfx</i> -MO	4.50 µg/µl	202	5%	11%

1. 3.14 nl injected per embryo in all experiments

2. In all embryos, both eyes were affected equally

\* = statistically different from control embryos as determined by Fischer's exact test: *hsf1*-MO 2.25 µg/µl and 3.46 µg/µl  $p < 0.0001$ ; *hsfx*-MO 2.25 µg/µl  $p = 0.0004$

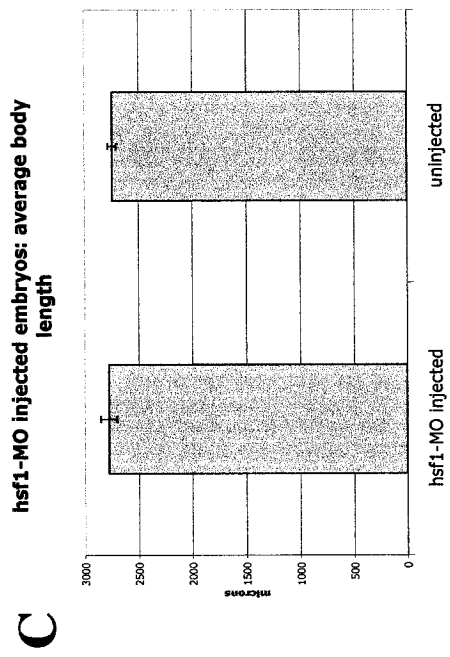
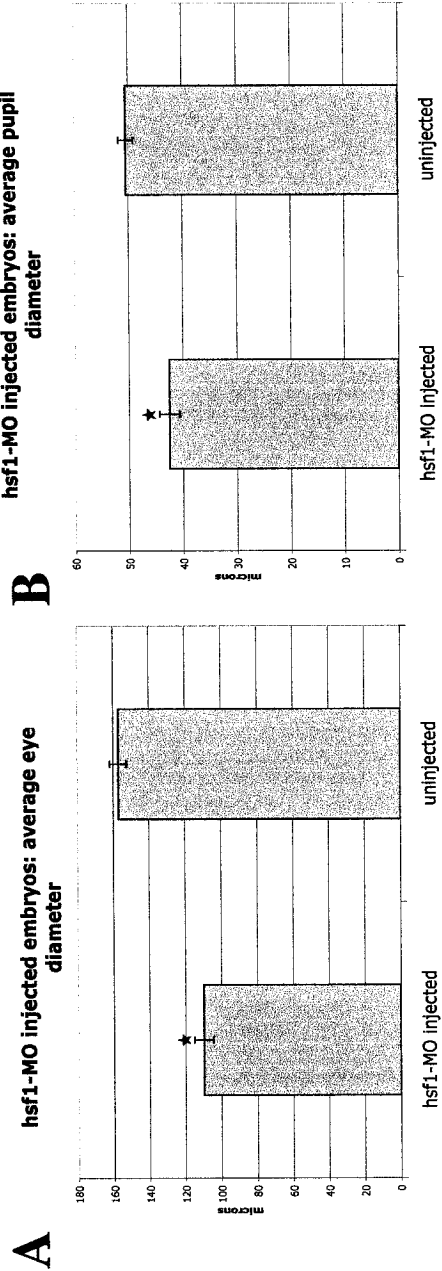
**Figure 21.** Small eye phenotype in 52 hpf embryos produced by microinjection of 2.25  $\mu\text{g}/\mu\text{l}$  *hsf1*-MO into fertilized eggs. Small eye phenotypes exhibited a phenotypic range from a more severe (A) to a more moderate (B) small eye phenotype, and are shown relative to an uninjected control embryo (C). All embryos screened as small eye phenotype lie within this phenotypic range. No other major phenotypic abnormalities are apparent in the *hsf1*-MO injected embryos, although a slight reduction in pigmentation was observed.



Microscopic analysis revealed that the overall eye diameter is significantly reduced in small eye phenotype embryos. Individual eye diameters ranged from 86  $\mu\text{m}$  to 146  $\mu\text{m}$ , and represents a reduction in eye diameter large enough to be easily screened for the presence of a phenotype using a dissecting microscope. Furthermore, standard error of percentages of injected embryos displaying small eye phenotype between trials was  $\pm 11.5$ , indicating that the small eye phenotype was produced and assessed consistently between trials. Embryos not displaying the characteristic small-eye phenotype deviated from the wildtype condition in only 9% of the cases, and in these cases the embryos developed a variety of severe and inconsistent defects, similar to those observed in *hsp70*-MO and control injections (Figure 13).

To better quantify the *hsf1*-MO induced small eye phenotype, average eye and pupil diameters, as well as body length among fixed embryos screened as small eye were calculated, and compared to the same uninjected control embryos measured previously (Figure 22). Average eye diameter in small eye embryos decreased to 109  $\mu\text{m}$  as compared to an average diameter of 157  $\mu\text{m}$  for control embryos (Figure 22A). This represented an average decrease in eye diameter of 33%. Average pupil diameter was 42  $\mu\text{m}$  among small eye embryos, as compared to a diameter of 50  $\mu\text{m}$  observed in uninjected controls (Figure 22B). This represented an average decrease in pupil size of 16%. Statistical analyses show that both eye diameter and pupil diameter differ significantly from control embryos (unpaired t test  $p < 0.0001$ ). Statistical analysis also revealed that overall growth was unaffected, as overall body length did not differ significantly from control embryos (unpaired t test  $p = 0.14$ ; Figure 22C).

**Figure 22.** Bar graphs illustrating average changes in eye and pupil diameter, as well as body length, in *hsf1*-MO injected embryos relative to uninjected controls. Average eye diameter decreased from 157  $\mu\text{m}$  in control embryos (n=27) to 109  $\mu\text{m}$  in *hsf1*-MO injected embryos (n=12) (A). Pupil diameter, used to infer decreases in lens diameter, was reduced from 50  $\mu\text{m}$  in control embryos (n=27) to 42  $\mu\text{m}$  in *hsf1*-MO injected embryos (n=12) (B). Body length of *hsf1*-MO injected (n=18) remained similar to uninjected control embryos (n=27) (C). Reductions in eye diameter and pupil diameter differed significantly from control embryos (indicated as star on graphs) as determined by statistical analyses (unpaired t test  $p < 0.0001$ ). Similar tests reveal that body length of *hsf1*-MO injected embryos did not differ significantly from control embryos ( $p=0.14$ ). Standard error of means are shown for each data set.



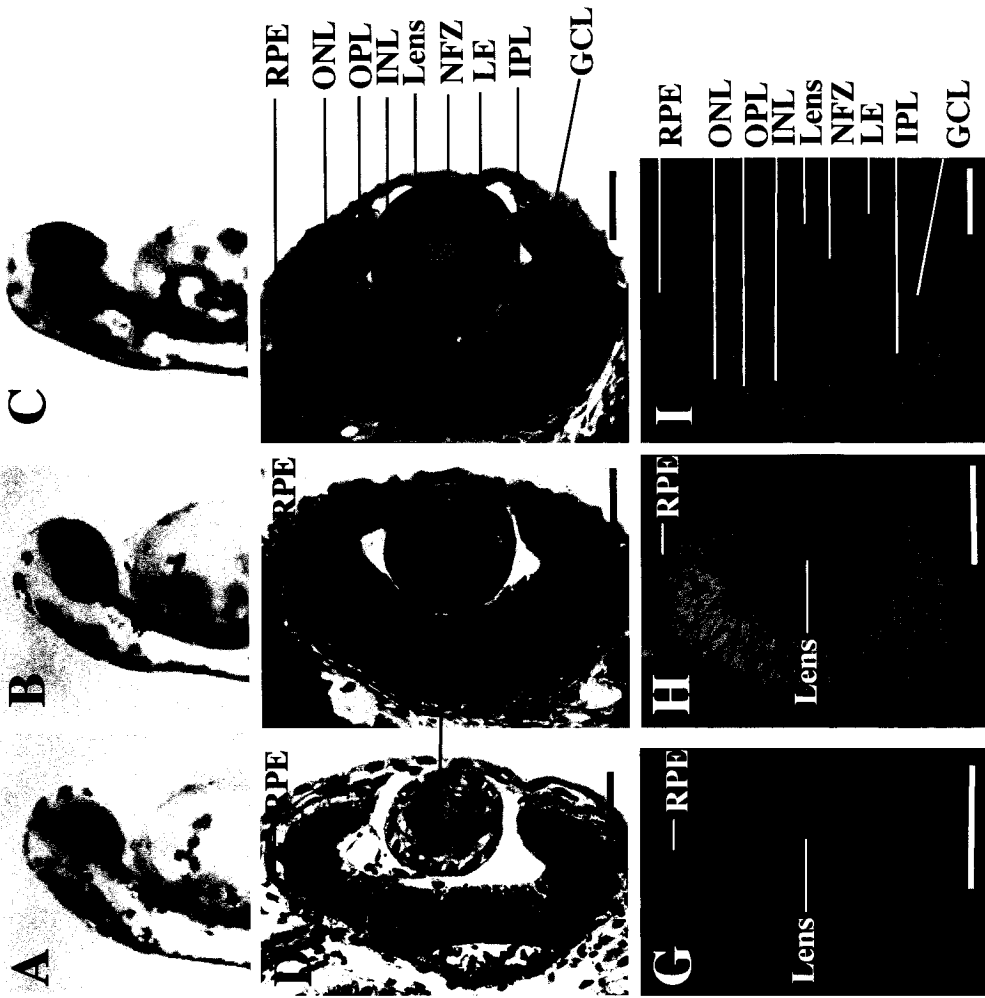
### 3.4.3 The *hsf1*-MO induced small eye phenotype is characterized by an immature lens and disorganized retinal structure

Microinjection of *hsf1*-MO resulted in a reproducible small eye phenotype. In order to analyze the *hsf1*-MO induced small eye phenotype at the cellular level, histological analysis of *hsf1*-MO injected and uninjected control embryos at 52 hpf was performed (Figure 23). Similar to the *hsp70*-MO, histology revealed that the *hsf1*-MO induced small eye phenotype is characterized by an immature lens and a disrupted retinal structure. The lens is significantly reduced in size and its cellular structure is reminiscent of an earlier developmental stage (Easter and Nichola, 1996). Small eye embryos possessed an extremely small lens, characterized by fibres that did not display the concentric organization representative of lenses at this stage, and a distinct separation of lens core and lens epithelial cells was not yet apparent (Figure 23D,G). The proportion of embryos that exhibited more moderate small eye phenotypes displayed features of more mature lenses (Figure 23B,E,H). However, lenses were still considerably smaller than control embryos, there was no central zone of denucleation, and there were still fewer cells in the lens core and epithelium. The retina of *hsf1*-MO injected embryos was also disrupted relative to control embryos. *hsf1*-MO induced small eye embryos lacked the characteristic laminated pattern of retinal cell layers at this stage. Histological analysis revealed that retinal patterning is abnormal across the spectrum of *hsf1*-MO induced small eye phenotypes, and several of the retinal cell types present in control embryos, such as retinal ganglion cells or plexiform layers cannot be identified (compare Figure 23 panels D,E to F and G,H to I). Such lens and retinal defects are strikingly similar to those observed in *hsp70*-MO induced small eye phenotypes, and provide supporting evidence that HSF1 is regulating *hsp70* expression in the zebrafish lens.



**Figure 23.** Histological analysis of small eye phenotype in *hsf1*-MO injected embryos and uninjected control embryos at 52 hpf. A,D,G; more severe small eye phenotype. B,E,H; more moderate small eye phenotype. C,F,I; uninjected embryos. A-C: unstained whole embryos. D-F; methylene blue-azure II-basic fuchsin stained 5.5  $\mu\text{m}$  thick methacrylate cross-sections. G-I; DAPI stained 5.5  $\mu\text{m}$  thick methacrylate cross-sections viewed through a fluorescence microscope to visualize nuclei. The immature structure of the lens and retina are readily apparent in the small eye embryos (D,E,G,H) relative to uninjected control embryos (F,I). Note that there are more nuclei present in the core of small eye lenses, indicating that lens fibre cell differentiation may be abnormal in *hsf1*-MO injected embryos. RPE=retinal pigmented epithelium; ONL=outer nuclear layer; OPL=outer plexiform layer; INL=inner nuclear layer; IPL=inner plexiform layer; GCL=ganglion cell layer. NFZ=developing nuclear free zone. Scale bar = 50  $\mu\text{m}$ .

*hsf1*-MO injected                      uninjected



#### **3.4.4 HSE binding activity is reduced in *hsf1*-MO injected embryos**

HSE binding activity in *hsf1*-MO injected and control embryos was assayed using gel mobility shift assays under normal and following heat shock conditions (Figure 24). The resulting gels demonstrate a significant reduction in HSE binding activity using protein extracts from *hsf1*-MO injected embryos under heat shock conditions (Figure 24A). Binding activity of radiolabeled CCAAT-box transcription factor (CBTF) was slightly increased in *hsf1*-MO injected heat shock extracts (Figure 24B), however, a significant decrease in HSE binding activity from the same extracts was still observed. A change in HSE binding activity under non-stress conditions was not detected in these assays. This may be due to the interaction of HSFs other than HSF1 with the radiolabeled HSE. Nonetheless, these results indicate that *hsf1*-MO injected at a concentration of 2.25  $\mu\text{g}/\mu\text{l}$  is sufficient to decrease HSE binding activity using our microinjection procedure.

#### **3.4.5 Hsp70 protein levels are diminished in *hsf1*-MO injected embryos at 38 hpf under normal developmental and heat shock temperatures**

Data presented thus far indicate the anatomical defects associated with both *hsp70*-MO and *hsf1*-MO small eye phenotypes parallel each other. These similarities, as well as the reduction in HSE binding activity among *hsf1*-MO injected embryos, prompted an investigation into whether HSF1 may be regulating *hsp70* expression in the lens. To address this question, Hsp70 protein levels in *hsf1*-MO injected embryos were quantified using Western blot analysis (Figure 25). Injection of *hsf1*-MO resulted in the reduction of both Hsp70 and Hsc70 protein at control temperatures (Figure 25A). Hsc70 also contains an HSE within its promoter sequences (Santa Cruz et al., 1997), and a reduction in Hsc70 levels is not unexpected. Following heat shock both Hsp70 and Hsc70 show a dramatic increase in expression, while *hsf1*-MO injected heat shocked embryos show a significant reduction in the accumulation of both Hsp70 and Hsc70 (Figure 25C). Although, the

**Figure 24.** Gel mobility shift analysis of HSF1 activity in uninjected and *hsf1*-MO injected embryos under control and heat shock conditions. Embryos were allowed to develop until 36.5 hpf and then heat shocked at 37°C for 90 minutes, or maintained at 28°C for an additional 90 minutes. Heat shock leads to a significant increase in the ability of HSF1 to bind radiolabeled heat shock elements (lane 2 in A). However, HSE binding activity is greatly inhibited by the introduction of *hsf1*-MO in heat shocked embryos (lane 4 in A). Our assay was unable to detect decreases in HSE binding activity under normal developmental temperatures (28°C; lanes 1 and 3 in A). Quantification of protein loading was visualized by CBTF binding activity (B).

38hpf      38 hpf HS      38 hpf HS + morph      38 hpf HS + morph

**A**

**HSF1-HSE Complex** →



**B**

**CBTF-CAAT Box Complex** →

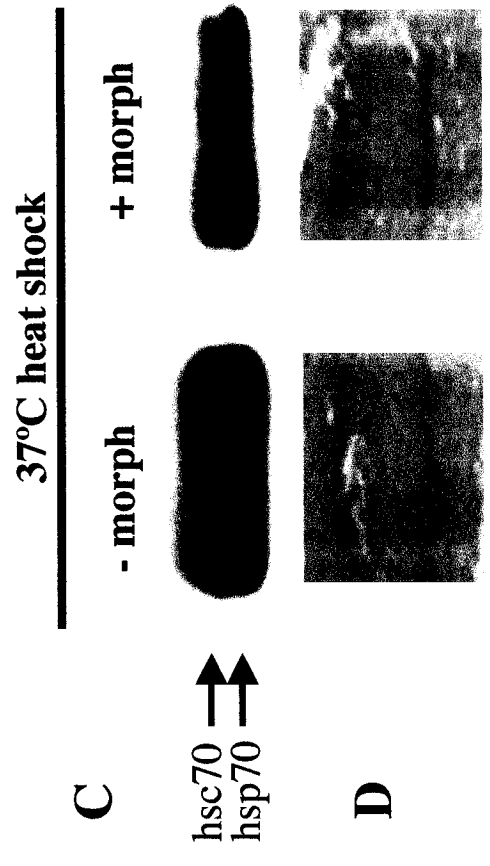
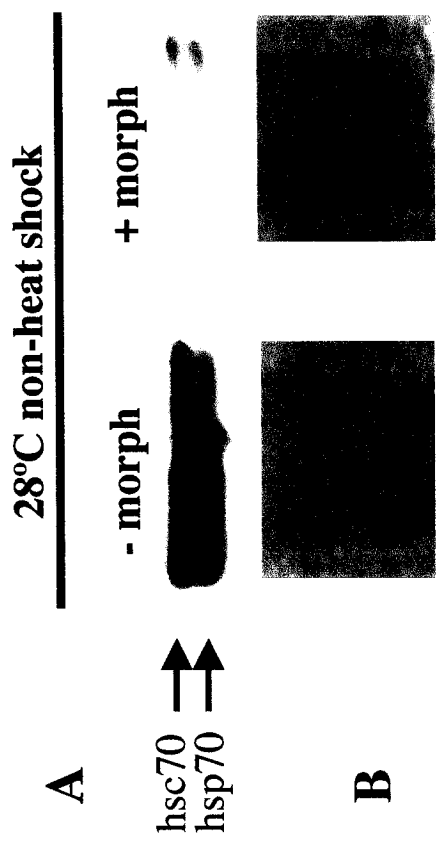


*hsf1*-MO cannot completely eliminate Hsp70 or Hsc70 under these conditions, such a result is not surprising considering both the large amount of protein synthesized after heat shock, and the fact that some MO degradation and dilution will have occurred by this stage of development. Equal protein loading was confirmed by Coomassie staining of SDS-PAGE gels for both non-heat shock (Figure 25B) and heat shock (Figure 25D) extracts. Thus, microinjection of *hsf1*-MO is sufficient to reduce Hsp70 protein expression in these embryos, and provides additional evidence that HSF1 is responsible for regulating constitutive *hsp70* expression in the zebrafish lens. Furthermore, inhibition of *hsp70* expression through the introduction of MO targeted to either *hsp70* or *hsf1* disrupts *hsp70* expression, and results in a characteristic small eye phenotype.

#### **3.4.6 Microinjection of MO targeting *hsf2* or *hsfx* does not fully phenocopy the *hsp70*-MO induced small eye phenotype**

Two other HSFs have been identified in zebrafish. To address a possible developmental role for HSF2 and HSFX, MO targeting these molecules were microinjected into fertilized zebrafish eggs. As in *hsf1*-MO, *hsf2*-MO and *hsfx*-MO were injected at several concentrations and assayed for survival rate and presence of a phenotype (Table 3.2). When injected at 2.25  $\mu\text{g}/\mu\text{l}$ , a concentration sufficient to induce a small-eye phenotype using *hsf1* MO, only 5% of *hsf2*-MO injected embryos displayed a comparable phenotype. At a concentration of 3.46  $\mu\text{g}/\mu\text{l}$ , once again only 5% of *hsf2*-MO injected embryos displayed a small-eye phenotype, while at the highest concentration of 4.50  $\mu\text{g}/\mu\text{l}$ , 0% of injected embryos displayed a small eye phenotype, and survival rate decreased to 10%. Subsequent statistical analyses revealed that the numbers of small eye embryos observed among *hsf2*-MO injected embryos did not differ significantly from control embryos at all three concentrations assayed (Fischer's exact test; *hsf2*-MO 2.25  $\mu\text{g}/\mu\text{l}$   $p=0.17$ ; *hsf2*-MO 3.46  $\mu\text{g}/\mu\text{l}$   $p=0.21$ ). Therefore, no effort was made to further investigate those embryos displaying this small eye phenotype.

**Figure 25.** Western blot analysis of decrease in Hsp70 levels in *hsf1*-MO injected embryos. StressGen Biotechnologies Corporation # SPA-812 antibody was used in these experiments. Embryos were allowed to develop until 36.5 hpf and then heat shocked at 37°C for 90 minutes, or maintained at 28°C for an additional 90 minutes. Hsp70 is a slightly smaller protein than Hsc70 and can be distinguished as a unique band with a slightly greater relative mobility than Hsc70. Microinjection of *hsf1*-MO results in a significant reduction of both Hsp70 and Hsc70 under non-heat shock conditions (A) Similarly, the amount of both Hsp70 and Hsc70 is significantly reduced in *hsf1*-MO injected embryos exposed to a 90 minute heat shock (C). Equivalent protein loading was confirmed by coomassie blue staining of embryo extracts following SDS-PAGE for 28°C non-shock extracts (B) and 37°C heat shock extracts (D).



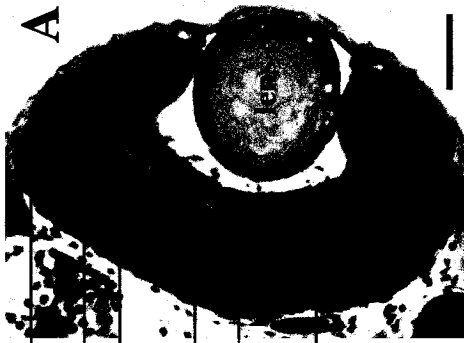


A similar injection procedure was utilized to investigate the requirement for HSF $\alpha$  in embryonic eye development. Interestingly, 16% of *hsfx*-MO injected embryos displayed a small eye phenotype when injected at a concentration of 2.25  $\mu\text{g}/\mu\text{l}$ . This number decreased to 2% when injecting *hsfx*-MO at 3.46  $\mu\text{g}/\mu\text{l}$ . Finally at 4.50  $\mu\text{g}/\mu\text{l}$ , *hsfx*-MO injected embryos displayed a small-eye phenotype in 5% of assayed embryos, while survival rate once again dramatically decreased to only 11% (Table 3.2). Statistical analyses revealed that small eye embryos observed with injection of *hsfx*-MO at 3.46  $\mu\text{g}/\mu\text{l}$  or 4.50  $\mu\text{g}/\mu\text{l}$  concentrations did not differ significantly from controls as determined by Fischers exact test (*hsfx*-MO 3.46  $\mu\text{g}/\mu\text{l}$   $p = 1.0$ ; *hsfx*-MO 4.50  $\mu\text{g}/\mu\text{l}$   $p = 0.22$ ). However, the 16% small eye frequency observed at 2.25  $\mu\text{g}/\mu\text{l}$  was deemed significant from controls ( $p = 0.0004$ ). Histological analyses revealed that *hsfx*-MO injected embryos screened as small eye displayed phenotypes equivalent to the most moderate small eye phenotypes observed in *hsf1*-MO or *hsp70*-MO injected embryos. These embryos exhibited only minor reductions in lens size and retinal patterning was clearly visible (data not shown). Major reductions in eye size or severe disruptions to lens or retinal structure comparable to those observed in *hsf1*-MO or *hsp70*-MO injected embryos were not observed. Consequently, over a range of MO concentrations, neither *hsf2*-MO nor *hsfx*-MO injected embryos were able to reproduce a severe small eye phenotype comparable to those observed in both *hsf1*-MO and *hsp70*-MO injections.

To ensure that those embryos screened as non-small eye in *hsf2*-MO and *hsfx*-MO injections do not possess any significant eye defects at the cellular level, histological analyses of *hsf2*-MO (Figure 26) and *hsfx*-MO (Figure 27) embryos screened as non-small eye were performed. Importantly, these embryos were injected at the same 2.25  $\mu\text{g}/\mu\text{l}$  concentration sufficient to induce a small eye phenotype using *hsf1*-MO. Histology confirmed gross morphological analysis, in that no significant differences between *hsf2*/*hsfx*-MO injected and uninjected embryos were observed (compare panels A to B and C to D in Figures 26,27 respectively). In particular, the lenses were at a comparable developmental stage relative to uninjected control embryos. Retinal development appeared only minorly

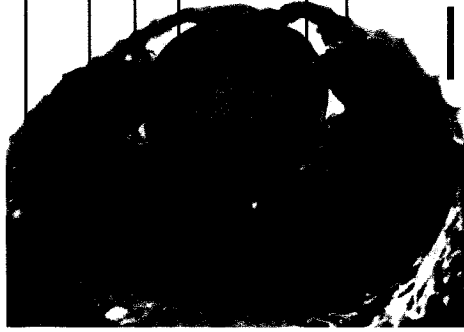
**Figure 26.** Histological analysis of *hsf2*-MO injected embryos at 52 hpf. *hsf2*-MO injected (A,C); uninjected control (B,D); methylene blue-azure II fuchsin stained 5.5  $\mu\text{m}$  thick methacrylate cross-sections (A,B); DAPI stained 5.5  $\mu\text{m}$  methacrylate cross-sections viewed through a fluorescence microscope to visualize nuclei (C,D). Lens and retinal structure appeared minorly affected in *hsf2*-MO injected embryos. Equivalent retinal layers can be identified in both *hsf2*-MO injected and uninjected control embryos. Similarly, lens morphology is unaffected in both *hsf2*-MO injected and uninjected control embryos. RPE=retinal pigmented epithelium; ONL=outer nuclear layer; OPL=outer plexiform layer; INL=inner nuclear layer; IPL=inner plexiform layer; GCL=ganglion cell layer. Scale bar = 50  $\mu\text{m}$ .

*hsf2*-MO  
Injected

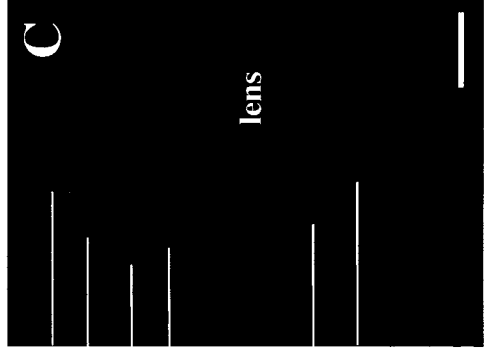


RPE  
ONL  
OPL  
INL  
IPL  
GCL

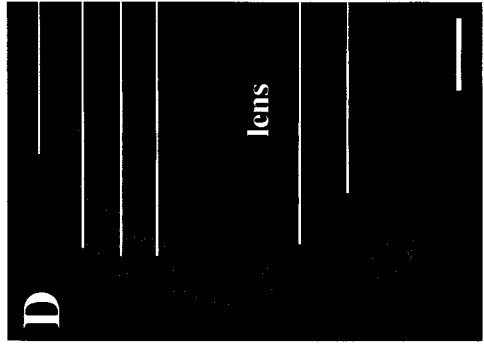
Uninjected



RPE  
ONL  
OPL  
INL  
IPL  
GCL



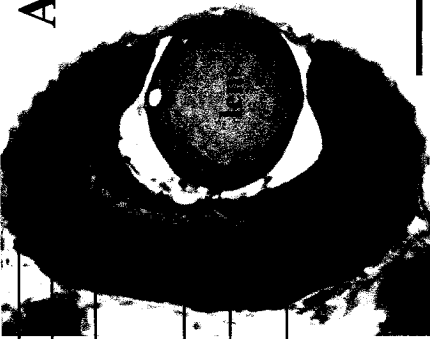
RPE  
ONL  
OPL  
INL  
IPL  
GCL



RPE  
ONL  
OPL  
INL  
IPL  
GCL

**Figure 27.** Histological analysis of *hsfx*-MO injected embryos at 52 hpf. *hsfx*-MO injected (A,C); uninjected control (B,D); methylene blue-azure II fuchsin stained 5.5  $\mu\text{m}$  thick methacrylate cross-sections (A,B); DAPI stained 5.5  $\mu\text{m}$  methacrylate cross-sections viewed through a fluorescence microscope to visualize nuclei (C,D). Lens and retinal structure appeared minorly affected in *hsfx*-MO injected embryos. Equivalent retinal layers can be identified in both *hsfx*-MO injected and uninjected control embryos. Similarly, lens morphology is unaffected in both *hsfx*-MO injected and uninjected control embryos. RPE=retinal pigmented epithelium; ONL=outer nuclear layer; OPL=outer plexiform layer; INL=inner nuclear layer; IPL=inner plexiform layer; GCL=ganglion cell layer. Scale bar = 50  $\mu\text{m}$ .

*hsfx-MO*  
Injected

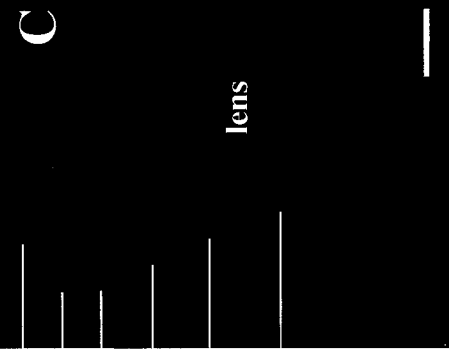


RPE  
ONL  
OPL  
INL  
IPL  
GCL

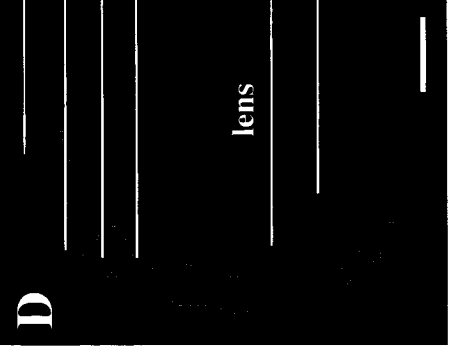
Uninjected



RPE  
ONL  
OPL  
INL  
IPL  
GCL



RPE  
ONL  
OPL  
INL  
IPL  
GCL



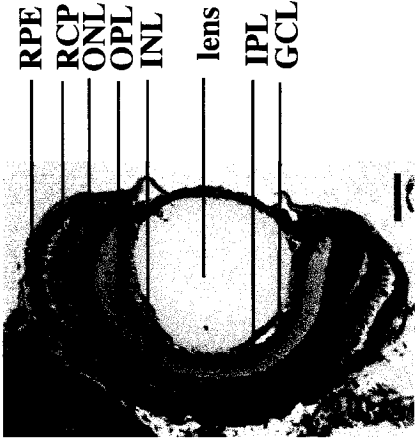
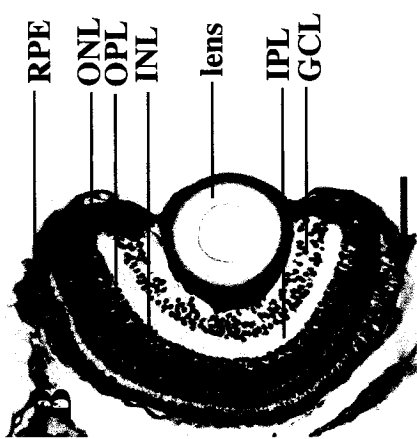
RPE  
ONL  
OPL  
INL  
IPL  
GCL

affected. The characteristic laminated retina was visible, and equivalent cell layers could be identified in both injected and control embryos. Injected embryos did exhibit slight differences in the extent of development in each retinal cell layer, but retinas remained in sharp contrast to the total absence of patterning observed in *hsf1*-MO injected embryos. These data suggest that the screening procedure accurately identified those embryos possessing an eye defect, and that the small eye phenotype observed in *hsf1*-MO injected embryos is a specific and exclusive effect. In addition, HSF2 and HSFX do not appear to be molecules critical for proper early eye development of the embryonic zebrafish.

#### **3.4.7 *hsf1*-MO injected embryos exhibit only partial recovery of lens and retinal organization by 5 days post-fertilization**

Given the phenotypic similarities between *hsf1*-MO and *hsp70*-MO induced small eye phenotypes, *hsf1*-MO injected embryos may also regain normal eye morphology after degradation and dilution of the MO later in development. Microinjection of fluorescein tagged MO in previous experiments demonstrated that MO are not detectable in embryos beyond 4 dpf. In accordance with these data, morphological and histological analysis on *hsf1*-MO and control injected embryos at 5 dpf were performed (Figure 28). Gross morphological analysis revealed that the eye remains considerably smaller than uninjected control embryos at this stage (Figure 28A,C). Subsequent histology revealed that the lens was significantly smaller than uninjected embryos (Figure 28B,D). However, unlike the lenses of *hsp70*-MO injected embryos, the cellular structure of lenses in *hsf1*-MO injected embryos remains significantly disrupted. Although prominent events in lens fibre differentiation such as denucleation appear to have occurred, the core of the lens is occluded with cellular aggregates resembling cataracts. Retinal structure also had not completely recovered (Figure 28B,D). The characteristic laminated appearance of the retina is apparent and specific cell types can be identified; however, there are notable differences between the retinas of *hsf1*-MO injected and uninjected controls. Namely, photoreceptor cells, the last cell type to differentiate within the retina,

**Figure 28.** Histological and morphological analysis of *hsf1*-MO induced small eye phenotype (A,B) and uninjected control embryo (C,D) at 5 dpf. Morphological analysis revealed the eye of *hsf1*-MO injected embryos (A) remained significantly smaller than control embryos (C). Cross sections through the developing eye of small eye phenotype embryos confirm that the eye and related structures (B) remain significantly smaller than uninjected controls (D) and contain cell occlusions that resemble cataracts. Cell numbers in retinal layers are reduced and photoreceptors are absent in *hsf1*-MO injected embryos, suggesting the *hsf1*-MO has a long term effect on eye development. RPE=retinal pigmented epithelium; RCP=rods and cones of photoreceptors; ONL=outer nuclear layer; OPL=outer plexiform layer; INL=inner nuclear layer; IPL=inner plexiform layer; GCL=ganglion cell layer. Scale bar = 50  $\mu$ m.



*hsf1*-MO  
injected

Uninjected



cannot be identified in these sections. Several cell types also appear to be underdeveloped. For example, retinal ganglion cells, the first cell type to differentiate, are not as tightly associated as in control embryos, and appear fewer in number. The same may be said for the inner nuclear layer, where cells appear more loosely associated. Thus, the absence of photoreceptor cells and deficient cell associations and fewer total cells within the retinal ganglion cells and inner nuclear cells, may represent an overall delay in the recovery of the retina, or a permanent effect of the MO on their development.

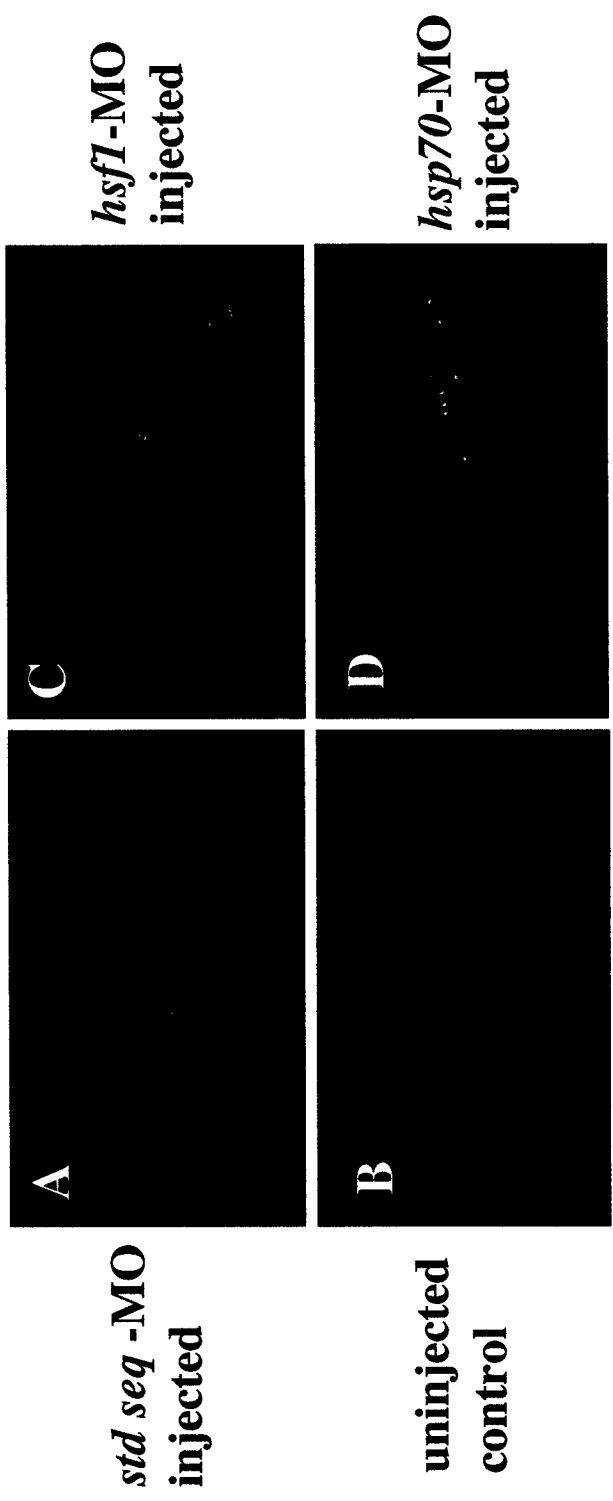
### **3.5 Analysis of thermoresistance in *hsp70*-MO and *hsf1*-MO injected embryos**

In this thesis, the normal developmental role for two key components of the stress pathway were investigated. Hsp70 is the most temperature sensitive of the Hsps, and usually exhibits the highest increase in expression following heat shock, while HSF1 is responsible for activating transcription of Hsps during the heat shock response (Nollen and Morimoto, 2002). Although the MO based strategy provided insight as to the role these molecules played during development, it is possible that inhibiting the production of two molecules critical to a cells ability to cope with stress would have detrimental effects during changes to the cellular environment. To address this issue, 24 hpf *hsp70*-MO and *hsf1*-MO injected embryos were exposed to heat shock conditions and monitored for effects. Surprisingly, gross morphological analysis of embryos injected with either *hsp70*-MO or *hsf1*-MO did not result in any noticeable abnormalities, even when maintained at heat shock conditions continuously for a full 8 hours (data not shown).

Although *hsp70*-MO and *hsf1*-MO injected embryos did not exhibit any gross morphological defects, damage at the cellular level may still have occurred. To analyze the cellular effect of heat shock on *hsp70*-MO and *hsf1*-MO embryos, TUNEL assays for cell death following a 90-minute heat shock were performed (Figure 29). Specifically, 24 hpf injected embryos were heat shocked for 90 minutes, and allowed to develop at the normal growth temperature until 52 hpf. In addition to *hsp70*-MO (Figure 29D) and *hsf1*-MO (Figure 29C) injected embryos,

standard control-MO injected (Figure 29A) and uninjected control (Figure 29B) embryos were assayed to assess cell death arising non-specifically from MO or the injection procedure itself. Entire embryos were screened for TUNEL labeled nuclei; however, only TUNEL positive nuclei appearing in the tail region of these embryos are shown to allow for clearer presentation. TUNEL positive nuclei are easily visible with the thin cellular structure of the tail. In all cases, the number of TUNEL labeled cells occurring throughout the embryo was accurately represented in the tail. Whole embryo analysis of TUNEL assays revealed no significant increases in cell death in standard control-MO injected or uninjected embryos (Figure 29A,B). However, significant increases in cell death were observed in both *hsf1*-MO (Figure 29C) and *hsp70*-MO (Figure 29D) injected embryos exposed to a 90-minute heat shock. These data reveal that although no visible morphological changes occurred during heat shock, the heat shock response was compromised with a considerable number of cells in *hsp70*-MO and *hsf1*-MO injected embryos undergoing cell death.

**Figure 29.** Analysis of thermoresistance in MO injected embryos. TUNEL analysis in the tail region of MO injected and heat shocked embryos at 52 hpf. Fertilized eggs injected with standard sequence-MO (A), *hsf1*-MO (C), or *hsp70*-MO (D) are shown relative to uninjected embryos (B). All embryos in this assay were heat shocked at 37°C for 90 minutes at 24 hpf, then allowed to develop at 28°C until 52 hpf. TUNEL analysis reveals considerably more cell death in *hsf1*-MO (C) and *hsp70*-MO (D) than in *std seq*-MO (A) and uninjected controls (B).



## 4.0 Discussion

The focus of this thesis was the expression, function, and regulation of the normally stress-inducible *hsp70* gene during the normal embryonic development of the zebrafish. Expression analysis revealed that *hsp70* is expressed exclusively in the embryonic zebrafish lens during a short temporal window of normal development characterized by the differentiation of lens fibre cells. Hsp70 protein was also detected during equivalent stages of chick lens development, which suggests that lens-specific *hsp70* expression may be a conserved event. The possible function of *hsp70* during lens development was addressed by reducing levels of Hsp70 in zebrafish embryos through the microinjection of MO targeting *hsp70* mRNA. *hsp70*-MO injected embryos exhibited a consistent and reproducible small eye phenotype, characterized by a small, immature lens and disrupted retinal structure. Further analysis of this defect suggested it occurs predominantly at the level of post-mitotic fibre differentiation. Microinjection of *hsf1*-MO resulted in a consistent and reproducible small eye phenotype, with lens and retinal defects similar to those observed in *hsp70*-MO. Furthermore, Hsp70 protein levels are markedly reduced in *hsf1*-MO injected embryos. These data suggest that *hsp70* expression may be regulated by HSF1.

### **4.1 *hsp70* is expressed during a short temporal window of lens development in the embryonic zebrafish and at equivalent stages in the embryonic chicken lens**

Members of the *hsp70* gene family are the most temperature sensitive Hsps and exhibit the greatest increase in expression during the heat shock response in a variety of organisms (Nollen and Morimoto, 2002). For this reason, their functions as chaperones during cellular stress have been widely studied. However, studies investigating a potential role for *hsp70* under non-stress conditions are few, with no

studies examining this in zebrafish. In this thesis, experiments aimed at characterizing the expression pattern of the stress inducible *hsp70* at normal growth temperatures in the embryonic zebrafish were performed. Our laboratory has been particularly interested in the expression and possible function of Hsps as molecular chaperones during normal developmental processes. To this end, we have made extensive use of *in situ* hybridization analysis to examine tissue-specific and temporal patterns of Hsp expression in zebrafish embryos under non-stress conditions. This approach serves as a first step in attempting to determine what role(s) different Hsps may be playing during embryogenesis. These experiments revealed that *hsp70* is expressed exclusively in lens fibre and lens epithelial cells during a period of zebrafish lens development characterized by the differentiation of lens fibre cells (Easter and Nichola, 1996). In support of this expression pattern, *hsp70* mRNA has also been detected during the period of lens fibre differentiation in both cave-dwelling and surface forms of the blind cavefish, *Astyanax mexicanus* (Hooven et al., 2004). Furthermore, 1.5 kb of the *hsp70* promoter was sufficient to drive GFP expression exclusively to the lens under non-stress conditions in transgenic fish, indicating that *hsp70* promoter sequences contain the regulatory elements necessary for lens specific *hsp70* expression in zebrafish.

Data acquired in this thesis also demonstrated that *hsp70* is expressed at equivalent stages in the embryonic chicken lens. Analysis of Hsp70 in chicken whole lens extracts suggests a prominent role in early lens fibre differentiation, with a continued requirement throughout the late stages of development when secondary lens fibres are continually emerging from the lens epithelium. A role for Hsp70 in fibre differentiation is supported by Dash et al. (1994), who reported constitutive expression of *hsp70* mRNA in chicken lens. Specifically, the authors report peak levels of *hsp70* transcript in the annular pad at ED6, with expression also detectable at ED 9 and ED 14. This study did not investigate the expression of Hsp70 protein in the chick lens, nor did it analyze *hsp70* gene expression at any other stages. However, *hsp70* mRNA expression correlates closely with the Hsp70 protein expression described for chicken lens extracts in this thesis. Importantly, peak levels of Hsp70 protein occurred at ED 6 and ED 8, correlating to a period of early lens

fibre differentiation, when the annular pad cells, the post-mitotic epithelial population committed to fibre formation, are first emerging (Ireland and Mrock, 2004). This suggests that increased levels of Hsp70 are required for early differentiation events in the lens fibres. However, Hsp70 was also detected at reduced levels from ED 10 to ED 14. By this stage in chick development all of the major inductive events in lens formation have occurred, and is characterized by the differentiation of secondary lens fibres, a process that continues throughout the life of the organism. Hsp70 expression during late stages of lens development was confirmed in chicken lens cell cultures, where Hsp70 expression was concentrated to differentiating lens fibre cells (lentoids) from ED8 to ED12. Thus, lower levels of Hsp70 may also be required for differentiation events among secondary fibres emerging in late lens development. Interestingly, we observe a marked increase of Hsp70 expression at ED16, an expression pattern that was reproducible in several repetitions. It is difficult to speculate as to the function of this increase in expression, especially since Hsp70 was no longer detectable by ED18. By this late stage of development (chicks will hatch at ED21), the chick lens is essentially mature and all major cells types within the lens have been formed. However, secondary lens fibre cells would still be differentiating. Thus, one possible explanation is that there may be a burst in the production of secondary lens fibre cells at ED16 requiring increased levels of Hsp70.

Although we do not have direct evidence for the involvement of *hsp70* in later zebrafish lens fibre differentiation, we cannot discount this possibility. For example, *hsp70* expression may be detectable at later stages in zebrafish if investigated using more sensitive protein assays such as Western blotting. eGFP protein expression driven by *hsp70* promoter sequences is detectable in the lens for up to 7 dpf. Prolonged eGFP expression could indicate that Hsp70 protein would persist in the zebrafish lens during these late developmental stages. However, eGFP is a very stable protein, and extended expression may also represent a property of the GFP protein itself.

In recent years, the zebrafish has emerged as a prominent model system in studies investigating vertebrate eye development, and most events occurring

throughout zebrafish eye morphogenesis remain conserved among vertebrates. The involvement of common genes in the eye development of zebrafish and other vertebrates is also well documented (Oliver and Gruss, 1997). Data generated in this thesis suggest that *hsp70* expression during lens fibre differentiation may be a conserved event. However, *hsp70* knockout mice did not exhibit any lens or eye related defects (Dix et al., 1998; Huang et al., 2001), suggesting that all vertebrates may not express *hsp70* constitutively during development, or that *hsp70* may not be required for proper lens formation in these organisms. Unfortunately, lens-specific expression of *hsp70* during embryogenesis has only been reported in chicken (Dash et al., 1994; Bagchi et al., 2001) and fish to date, and a conclusive answer as to the extent of *hsp70* expression in other phyla awaits further investigation.

Surprisingly, a number of other normally stress-inducible zebrafish Hsp encoding genes are expressed in very specific spatial and temporal patterns in early embryos under normal developmental conditions. For example, vertebrates express two *hsp90* genes, and studies in zebrafish indicate that these genes are differentially regulated (Krone and Sass, 1994). Whole-mount *in situ* hybridization analysis with gene specific probes revealed that constitutive *hsp90 $\alpha$*  mRNA is restricted primarily to a small subset of cells within the pre-somitic mesoderm, somites, and pectoral fin buds of developing embryos (Sass et al., 1996). Additional analysis revealed that this small subset of cells corresponds to muscle progenitors in both the slow and fast fibre lineages (Krone and Sass, 1994), whereas *hsp90 $\beta$*  mRNA was detectable within the CNS and anterior epidermis (Sass et al., 1999). *hsp90 $\alpha$*  is also expressed concurrently with transcription factors critical to normal muscle development, and was subsequently shown to be required for normal muscle formation (Lele et al., 1999). The zebrafish *hsp47* gene, which encodes an important collagen chaperone in vertebrate embryos, is also expressed in a highly tissue specific manner in embryos maintained at normal developmental temperatures. *hsp47* expression is restricted primarily to precartilagenous cells of the notochord that also express type II collagen, suggesting a conserved function for *hsp47* as a collagen chaperone in zebrafish (Lele and Krone, 1997).



## 4.2 Morpholino modified antisense oligonucleotide mediated knockdown of *hsp70* expression results in a reproducible small eye phenotype in the embryonic zebrafish

Correlations between *hsp70* expression and the developmental status of lenses imply a role predominantly in lens fibre development. A MO based strategy was used to investigate the potential role of *hsp70* in lens fibre development. MO function by inhibiting translational initiation (Summerton, 1999) and have been shown to bind to, and block translation of mRNA *in vitro* (Summerton, 1999; Summerton and Weller, 1997) and *in vivo* (Qin et al., 2000). This mechanism of inhibition has been successfully used and published in a variety of systems for gene-knockdown studies, including zebrafish, sea urchin, chicken, *Xenopus*, and *Drosophila*. For zebrafish, this is the first viable sequence-specific gene inactivation method (Ekker and Larson, 2001). In fact, Nascevicus and Ekker (2000) were able to produce phenocopies of well-characterized zebrafish mutations (such as *one eyed pinhead* and *chordin*) through introduction of MO via microinjection. Specifically, they showed that all nine genes studied were functionally depleted using the first MO designed against the leader sequence of each transcript (Nascevicus and Ekker, 2000).

In this thesis, fertilized eggs injected with two different MO targeting *hsp70* mRNA resulted in a consistent and reproducible small eye phenotype. 63% of 486 *hsp70*-MO injected embryos displayed a small eye phenotype discernable by 48 hpf, and a decrease in Hsp70 protein levels was confirmed through Western blots. Furthermore, 53% of 107 embryos injected with a second MO targeting *hsp70* (*hsp70*-MO2) exhibited an identical small eye phenotype (Table 3.1). This degree of penetrance is well within the range reported in previous studies. In some cases, extremely consistent results have been reported for MO effectiveness. For example, *bmp7* MO causes extreme dorsalization in 93% of embryos injected, while *chordin* and *no tail* mutations were phenocopied at 75% and 98%, respectively (Nascevicus and Ekker, 2000). However, in other cases, the results are much more variable. For example, MO targeted to *somitabun* and *one-eyed pinhead* displayed only 24% and

49% penetrance, respectively (Lele et al., 2001). Importantly, the penetrance of our positive control *chordin*-MO was also within this range, and embryos injected with this MO displayed the typical *chordin* phenotype in 75% of the embryos, identical to the number reported in a previous study using the same sequence of MO (Nascevicus and Ekker, 2000).

Previous studies employing MO to investigate the effect of genes on early zebrafish development have reported inconsistencies in the severity of the observed phenotypes (Heasman, 2002). Similarly, a proportion of *hsp70* and *hsf1*-MO injected embryos exhibited less severe phenotypes. However, it is important to realize that the observed phenotype might lie anywhere on the entire spectrum of phenotypes between complete depletion and only minimal depletion of the target protein. This factor will be influenced not only by MO concentration, but also by the function, amount, and stability of protein, the amount of diffusion, and the localization and time of expression of the targeted mRNA (Heasman, 2002). Therefore, the phenotypic range observed in small eye embryos is not unexpected for several reasons. Firstly, we have shown that the frequency of the small eye phenotype is dependent upon MO concentration, as embryos injected with *hsp70*-MO at 2.25  $\mu\text{g}/\mu\text{l}$  or 4.50  $\mu\text{g}/\mu\text{l}$  display dramatically lower penetrance, with only 13% and 16% displaying the small eye phenotype, respectively. Secondly, *hsp70* is not expressed until well into the second day of development and some MO degradation and dilution will have occurred by this point in development. Thirdly, since the MO is microinjected into the yolk, but the yolk is isolated from cell divisions, the segregation of MO to individual cells during development is random. Finally, because *hsp70* expression is isolated to a relatively small population of cells (i.e. the lens) within the entire embryo, it is unlikely that the same dose of MO is received by these cells in every injected embryo.

#### **4.2.1 Lens defects in the *hsp70*-MO induced small eye phenotype**

The prominent defect among *hsp70*-MO injected embryos is an extremely small and developmentally immature lens. In particular, lens fibre cells were fewer

in number, did not display the concentric organization characteristic of fibre cells at this age, and were not properly denucleated. These data suggest lens fibre differentiation is disrupted in the small eye phenotype. The recovery of *hsp70*-MO injected embryos at 5 dpf also supports the premise that the lens phenotype is caused by abnormally developing lens fibre cells. If the *hsp70*-MO were affecting inductive events occurring earlier in lens development, a complete recovery in lens structure would not be expected. In contrast, if the defect were within the lens fibres, it is likely that lens structure would recover as newly differentiating fibres emerged from the lens epithelium.

During zebrafish lens development, cell differentiation within the solid lens vesicle leads to the formation of a mature lens composed of two cell types: epithelial cells, and lens fibre cells. The initial population of primary lens fibre cells arises from differentiation of cells within the vesicle itself. Secondary lens fibres arise later, through the differentiation of the lens epithelial cells at the equatorial region, and will add to the primary fibres that form the core of the lens (Easter and Nichola, 1996). Consequently, the bulk of the lens consists of concentric layers of fibre cells that are formed throughout life by the differentiation of cells from the lens epithelium (Bassnett, 2002). Because the bulk of the lens is composed solely of lens fibre cells, an obstruction in fibre cell development would be expected to reduce the overall size of the lens. Other studies in which differentiation of lens fibre cells was disrupted also reported decreases in the size of the lens. For example, microinjection of MO targeted to *connexin 48.5*, the expression of which becomes restricted to differentiating lens fibres (Cheng et al., 2003), not only resulted in fibres that were abnormal and immature but decreased lens volume by 35.7% (Cheng et al., 2004). Suppressing lens fibre development by expressing diphtheria toxin A directed to these cells by the  $\alpha A$ -*crystallin* promoter in zebrafish similarly resulted in lenses that were markedly reduced in size (Kurita et al., 2003). Finally, the zebrafish *arrested lens* mutant is typified by the arrest of lens fibre cell differentiation at 48 hpf, resulting in an undersized lens by 3 dpf, and the total absence of a lens by 5 dpf (Vihtelic et al., 2001). Thus, there exists extensive evidence that disruption of lens fibre development in zebrafish is correlated with a considerable reduction in the

overall size of the lens and the reduction in lens diameter observed in *hsp70*-MO injected embryos is consistent with this model.

A small lens phenotype arising from a defect to the lens fibres may be caused by several factors: small lens fibre cells, decreased proliferation of lens fibre cells, or increased cell death among lens fibre cells. Histological analysis revealed that lens fibre cells are not undersized, but are fewer in number relative to control lens. However, cell proliferation in small eye lenses was likely unaffected as PCNA staining was similar to that of control embryos suggesting that new fibre cells are indeed emerging from the lens epithelium. Subsequent TUNEL analysis for apoptotic cells revealed that *hsp70*-MO injected embryos display an increase in TUNEL labeled nuclei in the lens fibre cells at 52 hpf, while TUNEL labeling was not detected in lenses of control embryos at this stage. These data suggest that the small lens phenotype is caused by increased cell death among lens fibre cells.

The *hsp70*-MO induced small eye phenotype was associated with a severely disrupted retinal structure, and concomitant reduction in retinal cell numbers. Even in more moderate small eye phenotypes, retinal morphology was still severely disorganized, and embryos completely lacked the normal laminated appearance characteristic of vertebrate retinas. Data presented in this thesis suggests that the observed retinal defect is a secondary effect caused by the impact of *hsp70*-MO in the lens. Expression analysis detected *hsp70* solely in the developing lens under non-stress conditions, and not in the retina. However, we cannot discount the possibility of low levels of retinal *hsp70* below assay detection limits. Furthermore, if the retinal defects were a direct effect of the MO on the developing retina, it would have to be a specific effect of the *hsp70*-MO, because retinal abnormalities were not observed in any of the control experiments. Unexpectedly, retinal cell structure appeared normal in optic cups receiving the Hsp70 depleted lens, and is similar to that observed on the unmanipulated side, and in uninjected controls. One possible explanation of this result is that signaling between the lens and retina occurs prior to 34 hpf, that is, prior to when the transplantations were performed. In lens transplantations conducted at 34 hpf, any signaling required for the initiation of

retinal neurogenesis would have already been completed by the normal lens, and as a result the retina develops normally.

A secondary retinal defect is not unexpected, given the number of studies citing the lens as playing a central role in the determination of several anterior eye structures, including the retina. The lens has long since been known to be an important source of inductive signals that can affect eye development. More recently, a study by Thut et al. (2001) has identified several candidate genes providing lens inductive signals, and the molecular mechanisms underlying the inductive properties of the lens are now being discovered. Specifically, Thut et al. (2001) demonstrated that the lens is a source of an evolutionarily conserved signal that instructs cells of the neural retina to express genes characteristic of the developing iris and ciliary body. The importance of the lens to direct the formation of subsequent eye structures was apparent in a study where suppression of lens growth by an  $\alpha$ A-crystallin promoter driving expression of diphtheria toxin to the embryonic lens, had a dramatic effect on retinal lamination in zebrafish (Kurita et al., 2003).

The most concrete evidence for the central role of the lens in eye development has emerged from studies of another teleost, the cavefish (*Astyanax mexicanus*). This species is unusually suited to investigating issues of eye development because of its two extant forms: an eyed surface dwelling and several blind cave-dwelling forms. Cavefish embryos initially form eye primordia, but the lens eventually dies through apoptosis, followed by the degeneration of the retina, and finally what remains of the eye sinks into the orbits (Jeffery, 2001). Using this unique system, lens transplant experiments have revealed that signals originating from the lens are required for the proper degeneration of the cavefish eye (Yamamoto and Jeffery, 2000). Specifically, lenses transplanted from surface-fish into cavefish are sufficient to promote proper eye development in these normally eyeless organisms. Reciprocal experiments demonstrate that lenses transplanted from cavefish into surface fish, are adequate to induce the degeneration of the surface fish eye. Thus, it seems likely that a signal from the lens controls tissue specification in the developing eyes of fish, and that disruption of lens formation

may also disrupt these signals, leading to abnormalities in their target tissues. Recently, Hedgehog proteins have been implicated as critical molecules in signaling cavefish eye degeneration (Yamamoto et al., 2004). Cave dwelling forms are characterized by expanded expression profiles of both the *sonic hedgehog* and *tiggy-winkle hedgehog* genes, leading to hyperactivation of downstream genes, lens apoptosis, and arrested eye growth and development. The processes occurring during cavefish eye degeneration can be mimicked in surface fish by the overexpression of either *sonic hedgehog* or *tiggy-winkle hedgehog*. The demonstration of the importance of the lens during cavefish eye development provides supporting evidence that eliminating Hsp70 from the embryonic zebrafish lens may not only disrupt lens development, but may also obstruct lens signaling to the retina, in turn affecting retinal development.

#### **4.2.2 Retinal defects in the *hsp70*-MO induced small eye phenotype**

Retinal cell layers are derived in a pre-determined, and evolutionarily conserved order from multipotent progenitor cells originating from neuroepithelial cells that line the optic cup (Link and Darland, 2001). Retinal ganglion cells are formed during the first wave of retinal neurogenesis, and are the first cells to become postmitotic and differentiate in vertebrates (Kay et al., 2001). Expression of the retinal ganglion cell markers *znp-6* and *zn-5* was undetectable in our assays, and suggests that the ganglion cell layer is completely unformed or undifferentiated in *hsp70*-MO induced small eye embryos (Figure 4B,C,F,G). However, we cannot eliminate the possibility that retinal ganglion cells are indeed present, but at a stage where neither of these markers are expressed. The target protein of *zn-5* has been identified as DM-GRASP, a cell adhesion molecule necessary for correct axon routing and fasciculation (Fashena and Westerfield, 1999). Retinal ganglion cells would likely express this marker late in their development, when differentiated cells were extending axons to meet the optic nerve. Unfortunately, the target protein of the *znp-6* antibody remains unknown, making it difficult to conclude with absolute certainty that the retinal ganglion cells are completely absent in small eye embryos.

However, retinal ganglion cells are certainly immature relative to uninjected embryos, suggesting the formation of these cells during the first wave of retinal neurogenesis is disrupted.

Retinal cell structure appeared normal when Hsp70 depleted lenses were transplanted into optic cups of uninjected embryos, and the retinal ganglion cell layer can be identified in these embryos. The presence of the ganglion cell layer in transplanted embryos supports the hypothesis that lens to retina signaling occurs prior to its differentiation between 29 and 36 hpf (Kay et al., 2001; Easter and Malicki, 2002). Accordingly, retinal dependence on the lens in our experiments would have to occur subsequent to 28 hpf, when *hsp70* expression is first detectable in the lens, but prior to 34 hpf, when the lens transplants were completed and the first wave of retina neurogenesis has signaled the formation of the retina ganglion cells. Therefore, these data suggest that important retinal differentiation events are signaled by the lens during a brief period from 28-34 hpf, and that the retinal defects observed in *hsp70*-MO injected embryos are a secondary effect resulting from an abnormally developed lens.

Although the formation of the retinal ganglion cells is disrupted, additional retinal layers, such as the inner plexiform layer appear to form independent of lens and/or retinal signaling in *hsp70*-MO injected embryos. Immunostaining with *zns-2*, a marker of the inner and outer plexiform layer, is abnormal in small eye embryos in that the two normally recognizable stripes present in wildtype retinas were absent in small eye embryos. Plexiform layers form subsequent to the retinal ganglion cells, and indicates that retinal neurogenesis is still disrupted at this later stage. However, we did observe some weak staining immediately adjacent to the lens. It is unlikely that this staining represents the outer plexiform layer, as this layer is formed much later in retinal neurogenesis. In support, immunohistochemical analysis demonstrated that the photoreceptors, cell types also differentiating late in retinal neurogenesis and immediately after the outer plexiform layer, were similarly absent in both small eye and uninjected embryos at 52 hpf (data not shown). An alternative explanation is that the inner plexiform layer, formed immediately after the ganglion cell layer, would come to occupy the region adjacent to the lens instead of the

retinal ganglion cells. The presence of the inner plexiform layer suggests that this retinal cell type develops independent of lens signaling and/or ganglion cells, or that signals arising from the immature lens or ganglion cells are sufficient for its formation. Studies have shown that subsequent retinal cell layers can develop normally, despite the absence of layers defined in earlier signaling events. For example, mutation of the zebrafish *lakritz* locus completely eliminates the retinal ganglion cells, but the inner nuclear layer cells formed during later retinal neurogenesis were unaffected (Kay et al., 2001).

#### **4.2.3 A model for Hsp70 function during apoptotic-like events associated with lens fibre differentiation**

Data presented in this thesis suggests that the small lens phenotype is caused by increased cell death among lens fibre cells. The increase in TUNEL labeled nuclei observed in the small lens phenotype may be related to a disruption in the apoptotic-like mechanism occurring during lens fibre cell differentiation. During lens development, cell differentiation within the lens vesicle leads to the formation of primary and secondary lens fibres. However, in order to ensure the optical clarity of the lens, lens fibre cells must degrade cellular organelles, but maintain cellular structure. Recent evidence suggests that the process of organelle degradation within lens fibre cells shares several common features with classical apoptotic events. For example, both events involve the degradation of chromatin leading to the presence of so-called “DNA ladders” (Appleby and Modak, 1977). In addition, the fragmented DNA is amenable to labeling via TUNEL analysis (Bassnett and Mataic, 1997). Ishizaki et al. (1998) also provided several pieces of evidence that lens fibre differentiation involves components of classical apoptosis, including the involvement of cysteine containing aspartate specific proteases, or caspases. Moreover, overexpression of *bcl-2*, a member of a key family of proteins that regulate apoptosis, has been shown to disrupt lens fibre cell denucleation, resulting in fibres that are disorganized and contain intact or fragmented nuclei (Fromm and Overbeek, 1997). Finally, Wride et al. (1999) confirmed these results,



demonstrating that several members of the *bcl-2* and caspase families are active during the course of lens fibre denucleation, in addition to their well-known roles in apoptosis.

There are two possible explanations for an increase in TUNEL labeled nuclei in *hsp70*-MO injected embryos. Firstly, the process of organelle degeneration occurring in lens fibre cells is prolonged in small eye embryos, or secondly, lens fibre cells are unable to attenuate the apoptotic-like events occurring during lens fibre development and fibre cells are undergoing complete apoptotic cell breakdown. If TUNEL labeling represented prolonged denucleation in lens fibre cells, but not in fibre cell death and elimination from the developing lens, such a dramatic reduction in the overall size of the lens would not be expected. *hsp70*-MO injected lenses also contained increased numbers of nuclei in the core of the lens, suggesting that denucleation was not properly occurring in the lens fibres of these embryos. Alternatively, lens fibre cells undergoing complete apoptotic cell breakdown would be eliminated from the lens, a process that would be expected to decrease the size of the lens. As discussed previously, there exists extensive evidence that disruptions of lens fibre cells can lead to significant reductions in the size of the lens in zebrafish, and in many cases these disruptions are associated with lens fibre cell death (Vihtelic et al., 2001; Kurita et al., 2003). Thus, the data presented here suggests that Hsp70 would function to maintain the ordered balance between nuclear/organelle degeneration and complete apoptotic cell breakdown in the differentiating lens fibres. Interestingly, the ability of Hsp70 to prevent apoptosis occurring through the mitochondrial-mediated or caspase independent pathways has been well established. Furthermore, molecules within these pathways, such as Apaf-1 (Beere et al., 2000) and AIF (Ravagnan et al., 2001) have been reported to directly interact with Hsp70. Since differentiating lens fibre cells have been shown to utilize components of these apoptotic pathways during differentiation, it is not unreasonable to suggest that Hsp70 could prevent cell death in lens fibres by direct interaction with and inhibition of components of the apoptotic pathway.

To summarize the proposed model, Hsp70 would function to maintain the ordered balance between nuclear/organelle degeneration and complete apoptotic cell breakdown in the differentiating lens fibres. In *hsp70*-MO injected embryos, lens fibre cells would be differentiating from the outer lens epithelium, but would be unable to regulate nuclear and organelle degeneration, and undergo complete cell death. The lack of lens fibre cells, which would normally constitute the bulk of the lens, would cause a dramatic decrease in lens size. As a secondary effect, signals originating from the lens fibres that would normally specify subsequent eye structures to form, such as the retinal layers, would also be disrupted, causing these structures to develop abnormally. Thus *hsp70*-MO injected embryos exhibit defects in both the lens and retina. Conversely, in the presence of functional Hsp70, denucleating lens fibre cells would successfully attenuate this apoptosis-like process, signals from the lens fibre cells would be unaffected, and eye development would proceed as normal.

#### **4.3 HSF1 is the major regulator of lens-specific *hsp70* expression in the embryonic zebrafish**

There are four known HSFs (HSF1-4). HSF1 is considered to be the universal HSF and mediates expression of heat shock genes upon reception of a stress signal such as high temperature. HSF2 has been associated with developmental events, while HSF3 is an avian specific HSF (Morimoto, 1998). Finally, HSF4, the most recent addition to the HSF family, is predominantly expressed in the embryonic and adult eye in mammals, where it plays a critical role in the prevention of cataracts. Like Hsps, HSFs are also expressed during non-stress conditions, and it is believed that their role under non-stress conditions may be an extension of their functions during stress. In zebrafish, very few studies have examined the function of HSFs under non-stress conditions, and none of these studies have yet identified a specific role for these molecules during normal embryonic development.

In this thesis, a developmental role for HSF1 in the regulation of constitutive lens specific *hsp70* expression has been established. This conclusion was based on several pieces of evidence. Firstly, morphological and histological analysis of *hsf1*-MO injected embryos revealed that these embryos displayed lens and retinal defects that closely parallel those of *hsp70*-MO injected embryos, including an under-developed lens and an immature retinal structure. Secondly, western blotting for Hsp70 in *hsf1*-MO injected embryo extracts demonstrated substantial decreases in Hsp70 under the normal growth temperature. Thirdly, the penetrance of the *hsf1*-MO induced small eye phenotype (53%) correlated closely to the penetrance of the small eye phenotype observed from *hsp70*-MO (63%) and *hsp70*-MO2 (53%) mediated knockdown. Fourthly, the small eye phenotype was not apparent until the second day of development in *hsf1*-MO injected embryos. Importantly, this correlated to both the appearance of *hsp70*-MO induced small eye phenotype, and to the expression of *hsp70* in the lens. Finally, expression analysis of *hsp70* demonstrated that promoter sequences were sufficient to drive eGFP expression specifically in the lens, suggesting that promoter elements, such as a HSE, regulate the lens-specific expression of *hsp70*. In support, gel mobility shift analyses demonstrated a marked reduction in heat inducible HSE binding activity in *hsf1*-MO injected embryos. Unfortunately, our assay conditions were not sensitive enough to reveal a similar decrease in the unstressed state. The lack of a HSF1 antibody with reliable reactivity in fish eliminated the possibility of performing other assays, such as Western blotting or supershifts, to investigate whether HSF1 protein or binding decreases in *hsf1*-MO injected embryos under non-stress conditions. However, a decrease in HSE binding activity under heat shock conditions still indicates that our *hsf1*-MO reduces HSF1 activity in injected embryos, and that our microinjection procedure was effective.

Histological analysis revealed that the cellular organization of both *hsf1*-MO and *hsp70*-MO induced small eye phenotypes are similar. Lenses were greatly reduced in size and exhibited an immature cell structure, including fewer total fibre cells, as well as a reduction in the number of fibre cells which have undergone complete differentiation and lie at the center of the lens. Furthermore, retinas of

both *hsf1*-MO and *hsp70*-MO injected embryos were characterized by the absence of any substantial retina patterning, and even more moderate small eye phenotypes showed limited evidence of retinal differentiation into specific cell types. However, measurements of overall eye diameter and pupil diameter in *hsf1*-MO injected embryos were on average larger than eye and pupil diameters observed in *hsp70*-MO injected embryos. This difference may be related to the activity of HSF1 as a transcription factor and the action of MO as a gene knockdown tool. If one molecule of *hsp70* mRNA were left uninhibited by *hsp70*-MO and translated into protein, the increase in Hsp70 would be minimal. However, if one molecule of *hsf1* mRNA were translated, the protein product has the ability to bind to the HSE of *hsp70*, and produce many copies of *hsp70* mRNA, which would substantially increase Hsp70 protein. Other studies using MO in zebrafish have noted that it is important to consider the function of the target protein (Heasman, 2002). This difference is illustrated in the western blots for Hsp70 in injected embryos. Western blotting of Hsp70 was not completely eliminated in *hsf1*-MO injected embryos under non-stress conditions, indicating that some protein is still produced. In contrast, the amount of Hsp70 protein in *hsp70*-MO injected embryos is undetectable under non-stress conditions.

The major effect of the *hsf1*-MO was on the developing eye, as measurements revealed no difference in total body length in *hsf1*-MO injected embryos. Similarly, measurements of *hsp70*-MO injected embryos revealed that the major effect was indeed to the developing eye, although a small, but significant decrease in body length was also apparent. This difference may be related to the higher effective MO concentration used in *hsp70*-MO injections. Higher concentrations of MO begin to have secondary effects on general growth and development. Such a phenomenon was certainly apparent in all MO injected at 4.50  $\mu\text{g}/\mu\text{l}$ , where dramatic but non-specific defects on growth and development were observed. Therefore, it is possible that the higher effective dose of *hsp70*-MO (3.46  $\mu\text{g}/\mu\text{l}$ ) relative to *hsf1*-MO (2.25  $\mu\text{g}/\mu\text{l}$ ) may be responsible for the minor differences in body length. Regardless, the major effect was clearly on the developing eye for both *hsf1*-MO and *hsp70*-MO.

The zebrafish genome contains genes encoding at least two other HSFs, namely HSF2 and HSFX. To address a possible role for these molecules in embryonic zebrafish development, MO targeted to HSF2 and HSFX were designed and microinjected. Neither *hsf2*-MO nor *hsfx*-MO were able to phenocopy the small eye phenotype at the same frequency observed by *hsf1* or *hsp70* MO injection. Multiple concentrations of each MO were used, indicating that the absence of a phenotype is not concentration based. At its greatest penetrance, *hsf2*-MO injection resulted in 5% of injected embryos displaying a small eye phenotype and subsequent statistical analysis revealed that this frequency did not differ significantly from control embryos. The cellular structure of eyes of *hsf2*-MO injected embryos also closely resembled the wildtype condition in histological sections. Considering that even the most moderate small eye phenotypes generated from either *hsp70*-MO or *hsf1*-MO injections exhibited completely abolished retinal layering, if *hsf2*-MO was affecting *hsp70* expression we would expect to see a defect in the retina. Therefore, HSF2 does not function during the first 48 hpf of zebrafish embryonic eye development, and is unlikely to be a major regulator of *hsp70* lens specific expression.

The conclusion that HSF2 is not involved in regulating the constitutive, lens specific *hsp70* expression in zebrafish is somewhat surprising, considering that several theories have suggested that this molecule functions as a regulator of constitutive Hsp expression and is not involved in the heat shock response. Initial supporting evidence for the role of HSF2 as a regulator of constitutive gene activity arose in studies showing HSF2 is unable to respond to classic stress stimuli, that HSF2 has different specificities for various HSE binding sites, and is under different regulation than HSF1 (Kroeger and Morimoto, 1994). HSF2-HSE binding activity has also been established in mouse embryonic stem cells found in early blastocysts under normal developmental conditions (Mezger et al., 1994). The expression of *hsp70* during erythroid maturation was shown to be mediated through a HSE, and it has been subsequently established that *hsp70* induced transcription in differentiating erythroid cells is mediated predominately by HSF2 (Morimoto, 1998). HSF2 expression and DNA binding activity is also detected in the developing mouse heart

(Eriksson et al., 2000), nervous system (Rallu et al., 1997), and testis (Sarge et al., 1994). HSF2 deficient mice do exhibit phenotypes related to this expression, including increased lethality associated with nervous system defects and reduced spermatogenesis due to aberrant meiosis (Kallio et al., 2002; Wang et al., 2003). Spermatogenic defects were subsequently linked to misregulation of the testis-specific *hsp70.2* gene found in mammals (Sarge et al., 1994). Furthermore, mouse embryonic fibroblasts lacking HSF2 exhibited proliferation defects, altered morphology, and remodeling of the fibronectin network, suggesting generalized functions in cells during development (Paslaru et al., 2003). These data led investigators to propose distinct functions for both HSF1 and HSF2 during development in mammals. However, recent studies on the function of HSF2 during development have been contradictory, and presently it remains unclear as to the precise function of HSF2 in vertebrate cells. This concept is best illustrated by the fact that two independently generated knock out mice deficient in HSF2 have yielded dramatically different results. The first study reported that HSF2 was not essential for embryonic development, fertility, or adult psychomotor function (McMillan et al., 2002). Conversely, a later study reported increased embryonic lethality, neuronal defects, and reduced spermatogenesis (Wang et al., 2003), confusing the issue of HSF2 function during development. Importantly, in both lines of HSF2 knockout mice, gene expression analysis did not reveal reduced Hsp expression levels, indicating the observed defects may not result from disruption of Hsp gene expression. Furthermore, the reduced fertility observed by Wang et al., (2003) could not be correlated to misregulation of the testis specific *hsp70.2* gene. These data suggest novel target genes under HSF2 regulation, and refute the previously proposed role for HSF2 as a regulator of constitutive Hsp expression. Importantly, such a conclusion is consistent with our data suggesting HSF2 is not a regulator of constitutive *hsp70* expression in the zebrafish lens, and the absence of any major embryological defects in *hsf2*-MO injected embryos.

Although HSF1 and HSF2 can be functionally distinct in unstressed cells, several studies have demonstrated that HSF1 and HSF2 can interact with each other under certain situations. For example, Wang et al. (2004) showed that knockout

mice deficient in both HSF1 and HSF2 possess a more severe fertility defect relative to the minor defects observed in HSF2 knockout mice. The finding suggests that additive or synergistic transcriptional activity of both HSF1 and HSF2 is required for normal mammalian spermatogenesis and male fertility. Additional evidence for the interaction of HSF1 and HSF2 is provided in a study showing that the transcription complex mediating the induction of the *clusterin* gene was an original association between HSF1 and HSF2 (Loison et al., 2005). Finally, He et al., (2003) demonstrated that HSF1 and HSF2 can be physically associated within the cell, and proposed a mechanism whereby active trimers are formed from HSF1/HSF2 heterocomplexes, rather than homotrimers. Thus, it may be possible that HSF1 and HSF2 are concomitantly active in regulating constitutive Hsp expression, and that such an event occurs during lens specific *hsp70* expression in zebrafish. However, if this were the case at least a minor phenotype would be expected when HSF2 levels were reduced. Although a very small percentage of *hsf2*-MO injected embryos displayed a small eye phenotype, statistical analysis deemed this result insignificant. Furthermore, histology performed on *hsf2*-MO injected embryos similarly did not reveal any significant abnormalities at the cellular level. Experimentally, simultaneous co-microinjection of both *hsf1*-MO/*hsf2*-MO into early zebrafish embryos would directly address the issue of HSF1 and HSF2 acting cooperatively. However, these experiments were not performed in this thesis. In conclusion, data presented here suggests that HSF1 is the primary regulator of lens specific *hsp70* expression in the zebrafish lens. Such a conclusion supports the increasing number of studies demonstrating that HSF2 is not exclusively responsible for constitutive Hsp expression during development.

Microinjection of *hsfx*-MO produced a small eye phenotype in 16% of injected embryos at the same MO concentration as *hsf1*-MO. Although statistically significant, *hsfx*-MO produces the small eye phenotype at a much lower frequency than both *hsf1*-MO and *hsp70*-MO. The majority of *hsfx*-MO screened as small eye embryos were only moderate relative to control embryos, and severe small eye phenotypes comparable to those observed in *hsp70*-MO or *hsf1*-MO injected embryos were not seen in *hsfx*-MO injections. Lens or retinal defects in histological

analyses of *hsfx*-MO injected embryos were not comparable to those observed in *hsf1*-MO injected embryos.

The reduced frequency of an eye related phenotype in *hsfx*-MO injected embryos supports the hypothesis that HSF1 is required to regulate *hsp70* expression in the embryonic lens. However, we cannot eliminate the possibility that HSF1 is playing a role in zebrafish eye development, especially since HSF1 is similar to mammalian HSF4. A surge of research in mammalian systems has shown HSF4 to be an important component of early lens development programs. For example, HSF4 is the predominant HSF present in the rat post natal lens, and HSF1 or HSF2 binding activities could not be detected. Furthermore, it is HSF4 and not HSF1 or HSF2 that interacts with the HSE of the sHsp  $\alpha\beta$ -crystallin, a major protein component of rat lenses (Somasundaram and Bhat, 2000; Somasundaram and Bhat, 2004). In mice, HSF4 is also required to maintain lens specific *y-crystallin* gene expression in lens fibre cells (Fujimoto et al., 2004), and to regulate *hsp25* expression in terminally differentiating lens fibres (Min et al., 2004). Mechanistically, it would appear that mammalian HSF4 regulates genes active in preventing the formation of protein aggregations, which lead to the development of lens cataracts. Several studies in which HSF4 was mutated (Smaoui et al., 2004; Min et al., 2004) have reported the formation of congenital cataracts. In addition, linkage analysis revealed human Marner cataracts are traced to a locus encoding a mutant DNA binding domain in HSF4 (Bu et al., 2002). The link between HSF4 and cataracts is consistent with a role for HSF4 in  $\alpha$ B-crystallin and  $\gamma$ -crystallin protein regulation. Crystallins compose approximately 50% of the total protein mass in lens fibres (De Jong, 1981), and  $\alpha$ A-crystallin deficient mice develop lens opacities leading to cataracts several weeks after birth (Brady et al., 1997). Interestingly, the expression of other Hsps, including Hsp70, was not affected in HSF4 knockout mice (Fujimoto et al., 2004), suggesting HSF4 may interact with novel target genes in the mammalian lens.

Precisely what role (if any) HSF1 is playing in zebrafish eye development can only be speculated upon. Although data presented here suggests that HSF1 does not play a prominent role in early eye development, it is possible that the effects of



HSFX dysfunction may not be manifested until larval stages beyond 48 hpf. Interestingly, mouse  $\alpha$ A-crystallin mutants exhibited slightly smaller eyes, but normal cellular structure during early mouse lens development. However, at late stages of development, lenses were characterized by the presence of cataracts (Brady et al., 1997). In zebrafish, a slight reduction in eye size in a proportion of *hsfx*-MO injected embryos at 48 hpf was observed, but the appearance of cellular defects occurring later in development was not investigated. However, *hsf1*-MO injected embryos develop lens occlusions resembling cataracts at 5 dpf; thus it is possible that HSFX may also affect late stage fibre differentiation. It is important to consider that lens fibre differentiation is occurring throughout life, and defects associated with differentiating fibre cells could become pronounced at any time during this period. Lens fibre defects observed in HSF4 knockout mice are indeed associated with later equivalent stages than our observed *hsp70*-MO defect in zebrafish (Fujimoto et al., 2004), and cataract formation associated with HSF4 mutant DNA binding domain showed an earliest onset of 15 months in humans (Bu et al., 2002). Unfortunately, MO have not been proven effective beyond 4 dpf in zebrafish, and new approaches to inhibiting HSFX must be used to address the possibility of late onset defects. Our lab is currently working toward characterizing the expression pattern of HSFX in the embryonic zebrafish. Obtaining expression data will provide valuable information on exactly when HSFX is expressed, and allow the design of new experiments that better address the functional aspects of HSFX during development.

In this thesis, several experimental lines of evidence demonstrated that the small eye phenotypes resulting from *hsf1*-MO and *hsp70*-MO injections parallel each other. However, one major difference existed in the extent of recovery observed in *hsf1*-MO induced small eye embryos. Histology performed at 5 dpf revealed the eye has not fully recovered its normal structure at this stage. Most notably, the lens core contained cellular aggregations resembling cataracts, and photoreceptors cannot be identified within the retina. The exact cause of this defect is unclear, but may be the result of abnormal expression of other genes that may be regulated by HSF1 in the lens. Speculating on possible target genes is difficult

because the role of HSF1 during eye development has not been investigated in any non-mammalian system. Since HSF1 knockout mice did not exhibit any eye defects, and *hsf1*-MO injected embryos show abnormalities exclusively in the eye, our data suggests that the developmental role of HSF1 was altered during vertebrate evolution. Combined with the finding that HSF4 is the predominant HSF in mammalian ocular lenses (Somasundaram and Bhat, 2004), it becomes difficult to attribute logical candidates, such as Hsps or crystallins, to HSF1 and not HSF4 regulation. To clarify, since all HSFs recognize the highly conserved HSE element, only *in vivo* studies analyzing HSF, Hsp, or other gene expression/function specifically in the lens provide suitable candidates, and studies of this nature have only been performed in mammals, where HSF4 appears to be the major HSF in the lens. Therefore, a justifiable explanation is that the evolutionary distance between fish and mammals have allowed mammals to utilize HSFs differently. Despite having genes encoding HSF2 and HSF4, fish may still rely on HSF1 to regulate Hsp expression during both development and stress conditions. In contrast, mammals have evolved the ability to utilize different HSFs for specific developmental events. Fujimoto et al. (2004) suggest that HSF1 might have originally played a role in the regulation of protein folding by up-regulating Hsps, but that the HSF4 gene evolved to adapt to the specific requirements of the lens, and molecules from within the stress pathway were recruited because of the dehydrated state of the lens fibre cells when differentiating. The same study was also able to show low levels of HSF1 are present in lens epithelia, and that HSF1 competes with HSF4 for HSE sites in fibroblast growth factor genes, which are important regulators of cell growth and differentiation. Thus, HSF1 may have played a more fundamental role in the past, but lost lens specific regulatory activity in mammals to the more specialized HSF4. This theory is consistent with early analyses of zebrafish HSF4. HSF4 shows similarity to mammalian HSF4 in that it lacks the inhibition of trimerization (HR-C) domain present in HSF1 and HSF2 in both zebrafish and mammals. This suggests that HSF4 may bind DNA constitutively, a feature exclusive to HSF4 in vertebrates. However, HSF4 is a much smaller protein and may represent a truncated version of mammalian HSF4, indicating important

differences between the two molecules. It is possible that during the evolution of mammals, HSFX may have acquired additional functional domains. As a result, mammalian HSF4 is a much larger protein that has evolved a specialized function during mammalian eye development. However, until additional studies are performed in lower vertebrates, the exact function of HSFX or its relation to mammalian HSF4 will remain unresolved.

#### **4.4 Analysis of thermoresistance in *hsp70*-MO and *hsf1*-MO injected embryos**

In this thesis the expression of two key components of the heat shock response, HSF1 and Hsp70, were markedly reduced. Hsp70 exhibits the highest fold increase upon heat shock, while HSF1 is considered the primary HSF involved in the heat shock response throughout eukaryotic phyla (Nollen and Morimoto, 2002). Inhibiting two molecules fundamental to the ability of a cell to cope with stress could have ramifications if these cells were exposed to an environmental challenge such as heat shock. To address whether cells injected with MO are susceptible to heat induced cytotoxicity, *hsp70*-MO and *hsf1*-MO injected embryos were exposed to heat shock conditions and monitored for effects. After 8 hours of continual heat shock, neither *hsp70*-MO nor *hsf1*-MO injected embryos exhibited any gross morphological defects. However, TUNEL analysis of *hsp70*-MO and *hsf1*-MO heat shocked for only 90 minutes, displayed significant increases in cell death that were specific to *hsp70*-MO and *hsf1*-MO. Standard sequence control MO injections or uninjected embryos did not exhibit elevated cell death in response to an identical 90 minute heat shock. These data indicated that injection of either *hsp70*-MO or *hsf1*-MO affects the heat shock response, and impairs cells ability to cope with stress. An experiment performed by Wang et al. (2001) yielded similar results when examining only HSF1. In this study, the authors utilized the same *hsf1*-MO sequence as used here, and similarly observed no gross morphological changes in embryos, but increases in cell death from a 90 minute heat shock.

Collectively, these studies indicated that HSF1 and Hsp70 function can be blocked through the introduction of MO. Furthermore, the function of these

molecules within the heat shock response is compromised, impairing the ability of a cell to cope with stress. Such results are consistent with other studies investigating the role of Hsp70 and HSF1 in the heat shock response. For example, in HSF1 deficient mouse embryonic cultured cells, thermoresistance was not acquired and cells underwent apoptosis when exposed to heat shock (McMillan et al., 1998). A similar finding was reported in HSF1 knockout mice (Zhang et al., 2002). HSF1 is also required to mediate the heat shock response in yeast (Sorger and Pelham, 1988), *Drosophila* (Jedlicka et al., 1997), and *C. elegans* (Walker et al., 2003). Importantly, these thermoresistance experiments indicate that although *hsp70* or *hsf1* function may be divergent among different organisms during developmental conditions, their role as critical players in the stress response remains conserved in fish as in many other phyla.

#### **4.5 Thesis summary and conclusions**

This thesis demonstrates that both *hsp70* and HSF1 are required for normal eye development in the embryonic zebrafish. Specifically, HSF1 appears responsible for activating *hsp70* expression in the developing lens fibre cells. Within the lens fibres, Hsp70 may function in regulating the apoptotic-like mechanism occurring during the final stages of lens fibre differentiation. However, this model is not considered conclusive. The role HSFs play in development is not well defined, and this thesis represented a first attempt to examine this question in fish. Wang et al. (2001) utilized the same MO sequence used in this study to investigate the overlapping functions of HSF1 during stress in fish and mammals. The authors observed a significant decrease in eGFP expression driven by *hsp70* promoter sequences and increases in cell death after heat shock in *hsf1*-MO injected zebrafish embryos. However, a role for HSF1 under non-stress conditions was not investigated, and the study makes no mention of any developmental defects in *hsf1*-MO injected embryos. Interestingly, embryos injected with *hsf1*-MO in Wang et al. (2001) appear to possess considerably smaller lenses, similar to those described in

this thesis. This observation strengthens the conclusion that HSF1 regulates lens specific *hsp70* expression in the zebrafish.

The *hsf1*-MO induced eye phenotype reported in this study is the first to describe a defect specifically to the developing eye. None of the mammalian knockout studies of HSF1 described an eye defect. However, lens specific *hsp70* expression has only been thoroughly documented in chick and teleost fish to date, and it is likely to have been reported if it were expressed similarly in mammals. Therefore, the absence of an eye-specific phenotype in HSF1 knockout mice may be a consequence of *hsp70* not being expressed in the mammalian lens. In support of this claim, *hsp70* knockout mice also lack any eye specific phenotypes (Dix et al., 1998; Dix et al., 1996; Huang et al., 2001). *hsp70* expression has also been thoroughly examined in *Xenopus*, and lens specific expression under non-stress conditions has not been observed (Ali and Heikkila, 2002). Consequently, lens specific *hsp70* expression during embryogenesis may be exclusive to fish and avian species. Unfortunately, the developmental role of *hsp70* during avian eye development has not been explored.

Although mammalian studies do not provide evidence that HSF1 is involved in eye development, they do indicate HSF1 is an important molecule in developmental processes. Mouse HSF1 is required for oogenesis, placental development, and normal growth (Xiao et al., 1999; Christians et al., 2000). In addition, HSF1 plays a critical role in spermatogenesis and male fertility (Wang et al., 2004). Recent studies have implicated HSF1 in the maintenance of olfactory epithelium in adult mice (Takaki et al., 2005) and in regulating genes related to the immune response and inflammation (Inouye et al., 2005). However, the molecular mechanisms controlling these processes are not understood. Several studies have shown a global disruption in the expression of Hsps or the heat shock response itself (Wang et al., 2004; Nakai et al., 2000; Takaki et al., 2005) but were unable to specifically link genes to a particular defect. Data obtained in this thesis, have correlated the small eye phenotype in *hsf1*-MO and *hsp70*-MO injected embryos to misregulation of *hsp70* expression in the lens fibres cells, and thus is the first to link an HSF1 related defect to a specific gene. The finding that HSF1, and not HSFX, is

the major regulator of *hsp70* expression in the embryonic zebrafish lens is unexpected in light of the established role for HSF4 in mammalian lens fibre development. It is possible that HSF4 established lens specific functions in higher vertebrates such as mammals, while in lower vertebrates such as fish, HSF1 acts as the major regulator of Hsp gene expression under both the stressed and unstressed state. However, the collective absence of data regarding zebrafish HSFs makes conclusions on their precise functions difficult. The present consensus in the literature is that different HSFs have evolved to meet specific developmental requirements in different organisms, that the recruitment of specific HSFs differs on a tissue-to-tissue basis, and that HSF activity may be dependent on both the timing of HSF expression and affinity to promoter elements.

#### **4.6 Future Directions**

Many issues surrounding the precise function of Hsp70 during embryonic zebrafish lens development remain unresolved. For example, this thesis has provided evidence that Hsp70 may function within the apoptotic like mechanism occurring during lens fibre differentiation. However, the direct interaction of Hsp70 with a molecule related to this process was not demonstrated. Several molecules playing key roles in apoptosis, such as Apaf-1 (Beere et al., 2000) or AIF (Ravagnan et al., 2001), have been shown to bind Hsp70, and are suitable candidates. Immunoprecipitation experiments on lens extracts during the period of Hsp70 expression would address this issue. However, performing such experiments in zebrafish is not feasible given the extremely small size of the developing lens. In contrast, chicken lenses are large, easily isolated from surrounding tissue, and express Hsp70 during lens fibre differentiation, making it an ideal system to investigate this issue. Furthermore, mouse and rabbit antibodies for most molecules within the apoptotic pathway have been developed, and usually exhibit more specific reactivity in chicken than zebrafish.

This thesis represented the first attempt to analyze the function of HSFs during development in zebrafish. As a consequence, several issues regarding their

function remain unresolved. Although HSF2 does not appear to play a specific role during embryonic eye development, it is possible that HSF2 is involved in the development of other cells. For example, a defect may be present in cells within the zebrafish embryo, but not manifested in an obvious phenotype. Since histology was only performed on eye tissue, other areas could exhibit more subtle defects not visible during the screening process. The issue would be resolved by expression analysis of HSF2 during zebrafish development. These experiments would identify target tissues that may be affected when injected with *hsf2*-MO. Similarly, insights into the function of HSF1 and HSFX during zebrafish development would benefit from expression analysis. Currently, zebrafish cDNAs are available for HSF1, HSF2, and HSFX, meaning *in situ* hybridization analyses are possible. Our laboratory has utilized this technique extensively, and is currently pursuing this line of experiments.

HSFX is a novel zebrafish HSF, and its relation to other HSFs in higher organisms can only be speculated. In addition, its role during development is unresolved. Importantly, HSFX was isolated from an embryonic library, indicating that it is expressed sometime during the first three days of zebrafish development. Data obtained in this thesis suggests it may play a role in embryonic eye development but additional experiments are required. For example, investigations into the effects on later stage zebrafish embryos, and expression analyses are required. In addition, the precise relationship of HSFX to HSF4 is unknown. DNA binding assays may provide valuable data concerning this relationship. Overall, a more in depth study of HSFX has the potential to generate important and novel data regarding the expression, function, and evolutionary origin of HSFs in fish.

## References

Ali, A., Heikkila, JJ. (2002) Enhanced accumulation of constitutive heat shock protein mRNA is an initial response of eye tissue to mild hyperthermia in vivo in adult *Xenopus laevis*. *Can. J. Physiol. Pharmacol.* 80: 1119-1123.

Andley, UP., Song, Z., Wawrousek, EF., Brady, JP., Bassnett, S., Fleming, TP. (2001) Lens epithelial cells derived from alphaB-crystallin knockout mice demonstrate hyperproliferation and genomic instability. *FASEB J.* 15: 221-229.

Appleby, DW., Modak, SP. (1977). DNA degradation in terminally differentiating lens fibre cells from embryos. *Proc. Nat. Acad. Sci.* 4: 5579-5583.

Arrigo, AP. (1987) Cellular localization of HSP23 during *Drosophila* development and following subsequent heat shock. *Dev Biol.* 122: 39-48.

Arrigo, AP. (1998) Small stress proteins: chaperones that act as regulators of intracellular redox state and programmed cell death. *J. Biol. Chem.* 379: 19-26.

Arrigo, AP., Landry, J. (1994) Expression and function of low molecular weight heat shock proteins. In: *The Biology of Heat Shock Proteins and Molecular Chaperones*. Cold Spring Harbour Laboratory Press. Plainview, NY.

Arrigo, AP., Ahmed-Zadeh, C. (1981) Immunofluorescence localization of small heat shock protein (hsp23) in salivary gland cells of *Drosophila melanogaster*. *Mol Gen Genet.* 185: 73-79.



- Arruti, C., Chaudun, E., De Maria, A., Courtois, Y., Counis, MF. (1995)  
Characterization of eye-lens DNases: long term activity in post-apoptotic lens fiber  
cells. *Cell Death Diff.* 2: 47-56.
- Askenazi, A., Dixit, VM. (1998) Death receptors: signaling and modulation.  
*Science.* 281: 1305-1308.
- Bagchi, M., Katar, M., Maisel, H. (2001). Heat shock proteins of chicken lens. *J. Cell Bioch.*  
82: 409-414.
- Bassnett, S. (2000) Lens organelle degradation. *Exp. Eye. Res.* 74: 1-6.
- Bassnett, S., Beebe, DC. (1992) Coincident loss of mitochondria and nuclei during lens cell  
fiber differentiation. *Dev. Dyn.* 194: 85-93.
- Bassnett, S., Mataic, DC. (1997). Chromatin degradation in differentiating fiber cells of the  
eye lens. *J Cell Bio.* 137: 37-49.
- Beere, HM., Green, GR. (2001) Stress management-heat shock protein-70 and the  
regulation of apoptosis. *Trends in Cell Biol.* 11: 6-10.
- Beere, H. M., Wolf, B. B., Cain, K., Mosser, D. D., Mahoubi, A., Kuwana, T., Taylor, P.,  
Morimoto, R. I., Cohen, G. M., Green, G. R. (2000). Heat shock protein 70 inhibits  
apoptosis by preventing recruitment of procaspase-9 to the Apaf-1 apoptosome. *Nat. Cell  
Biol.* 2: 469-475.
- Biggiogera M., Tanguay RM., Marin R., Wu Y., Martin TE., Fakan S. (1996)  
Localization of heat shock proteins in mouse germ cells: an immunoelectron  
microscopical study. *Exp. Cell Res.* 25: 77-85.

Billoud, B., Rodriguez-Martin, ML., Berard, L., Moreau, N., Angelier, N., Laine, CM. (1993) Constitutive expression of a somatic heat inducible hsp70 gene during amphibian oogenesis. *Development*. 119: 921-932.

Birnby, DA., Malone-Link, E., Vowels, JJ., Tian, H., Colacurcio, PL., Thomas, JH. (2000) A transmembrane guanylyl cyclase (DAF-11) and Hsp90 (DAF-21) regulate a common set of chemosensory behaviours in *Caenorhabditis elegans*. *Genetics*. 155: 85-104.

Borkovich, KA., Simon, MI. (1989) hsp82 is an essential protein that is required in higher concentrations for growth of cell at higher temperatures. *Mol. Cell Biol*. 9: 3919-3930.

Bosher, JM., Labousse, M. (2000) RNA interference: genetic wand and genetic watchdog. *Nat Cell Biol*. 2: E31-E36.

Braat, A. K., van De Walter, S., Korving, J., Zivkovic, D. (2001). A zebrafish vasa morphant abolishes vasa protein but does not effect the establishment of the germline. *Genesis*. 30: 183-185.

Brady, JP, Garland, DL, Greed, DE, Tamm, ER, Giblin, EJ, Wawrousek, EF. (2001) Alpha B-crystallin in lens development and muscle integrity: a gene knockout approach. *Invest Ophthalmol Vis Sci*. 42: 2924-2934.

Brady, JP., Garland, D., Duglas-Tabor, Y., Robinson, WG., Groome, A., Wawrousek, EF. (1997) Targeted disruption of the mouse  $\alpha$ A-crystallin gene induced cataract and cytoplasmic inclusion bodies containing the small heat shock protein  $\alpha$ B-crystallin. *Proc. Nat. Acad. Sci*. 94: 884-889.

Breitman, ML., Bryce, DM., Giddens, E., Clapoff, S., Goring, D., Tsui, LC., Klintworth, GK., Bernstein, A. (1989) Analysis of lens cell fate and eye morphogenesis in transgenic mice ablated for cells of the lens lineage. *Development*. 106: 457-463.

Bu, L., Jin, Y., Shi, Y., Chu, R., Ban, A., Eiberg, H., Andres, L., Jiang, H., Zheng, G., Qian M., Cui ,B., Xia, Y., Liu, J., Hu, L., Zhao, G., Hayden, MR., Kong, X. (2002) Mutant binding domain of HSF4 is associated with autosomal dominant lamellar and Marner cataract. *Nat. Genet.* 31: 276-278.

Cain, K., Brown, DG., Langlais, C., Cohen, GM. (1999) Caspase activation involves the formation of the apoptosome a large (~700 kDa) caspase activating complex. *J. Biol. Chem.* 274: 22686-22692.

Cande', C., Cohen, I., Daugas, E., Ravagnan, L., Larochette, N., Zamzami, N., Kroemer, G. (2002) Apoptosis inducing factor (AIF): a novel caspase-independent death effector released from mitochondria. *Biochimie.* 84: 215-222.

Candido, EP. (2002) The small heat shock proteins of the nematode *Caenorhabditis elegans*: structure, regulation and biology. *Prog. Mol. Subcell. Biol.* 28:61-78.

Chaudun, E., Arruti, C., Courtis, Y., Ferraf, F., Jeanny, JC., Patel, BN., Skidmore, A., Torriglia, A., Counis, MF. (1994) DNA strand breakage during physical apoptosis of the embryonic chick lens: free 3' OH end single strand breaks do not accumulate even in the presence of cation-independent deoxyribonuclease. *J. Cell Physiol.* 158: 354-364.

Cheng, S., Christie, T., Valdimarsson, G. (2003). Expression of connexin48.5, connexin44.1, and connexin43 during zebrafish (*Danio rerio*) lens development. *Dev. Dyn.* 228, 709-715.

Cheng, S., Shakespeare, T., Mui, R., White, TW., Vladimarsson, G. (2004) Connexin 48.5 is required for normal cardiovascular function and lens development in zebrafish embryos. *J. Biol. Chem.* 279: 36993-37003.

Cheney, CM., and Shearn, A. (1983) Developmental regulation of *Drosophila* imaginal disc proteins: synthesis of a heat shock protein under non-heat shock conditions. *Dev. Biol.* 95: 325-330.

Chow, RL, Lang, RA. (2001). Early eye development in vertebrates. *Annu. Rev. Cell Dev.* 17: 255-296.

Christians, ES., Zhou, Q., Renard, JP., Benjamin, IJ. (2003) Heat shock proteins and mammalian development. *Sem Cell Dev Biol.* 14: 283-290.

Christians, E., Davis, AA., Thomas, SD., Benjamin, IJ. (2000) Maternal effect of Hsf1 on reproductive success. *Nature.* 407: 693-694.

Cid, E., Velasco, A., Ciudad, J., Orfao, A., Aijon, J., Lara, JM. (2002). Quantitative evaluation of the distribution of proliferating cells in the adult retina in three cyprinid species. *Cell Tissue Res.* 308: 47-59.

Cole, L.K., Ross, L S. (2001). Apoptosis in the developing zebrafish embryo. *Dev Biol.* 240: 123-142.

Coucouvani, E., Martin, GR. (1995) Signals for cell death survival: a two step mechanism for cavitation in the vertebrate embryo. *Cell* 83: 279-287.

Creagh, EM., Carmody, RJ., Cotter, TG. (2000) Heat shock protein 70 inhibits caspase-dependent and independent apoptosis in Jurkat T cells. *Exp. Cell Res.* 257: 58-66.

Creagh, EM., Cotter, TG. (1999) Selective protection by hsp70 against cytotoxic drug-but not Fas induced T-cell apoptosis. *Immunology.* 97: 36-44.

Cutforth, T., Rubin, GM. (1994) Mutations in Hsp83 and cdc37 impair signaling by the sevenless receptor tyrosine kinase in *Drosophila*. *Cell*. 77: 1027-1036.

Dahm, R. (1999) Lens fiber cell differentiation-A link with apoptosis? *Ophthalmic Res*. 31: 163-183.

Dahm, R., Gribbon, C., Quinlan, RA., Prescott, AR. (1998) Changes in the nucleolar and coiled body compartments precede lamina and chromatin reorganization during fiber cell denucleation in the bovine lens. *Eur. J. Cell Biol*. 75: 237-246.

Dahm, R., Gribbon, C., Quinlan, RA., Prescott, AR. (1998b) Susceptibility of lens epithelial and fiber cells at different stages of differentiation of apoptosis. *Biochem. Soc. Trans*. 26: 349.

Dash, A., Chung, S., Zelenka, P. S. (1994). Expression of HSP70 mRNA in the embryonic chicken lens: Association with differentiation. *Exp. Eye Res*. 58: 381-387.

Davidson, SM., Morange M. (2000) Hsp25 and the p38 MAPK pathway are involved in differentiation of cardiomyocytes. *Dev Biol*. 218:146-160.

Day, RM., Gupta, JS., MacRae, TH. (2003) A small heat shock protein/ $\alpha$ -crystallin protein from encysted *Artemia* embryos suppresses tubulin denaturation. *Cell Stress Chaperones*. 8: 183-193.

Detrich, WH., Westerfield, M., Zon, L. (1999) eds. *The Zebrafish Biology. Methods in Cell Biology*. Vol 59. Academic Press, San Diego.

de Yong, WW. (1981) *Molecular and Cellular Biology of the Eye lens*. Wiley Press. New York. pp 221-278.

Ding, L., Candido, EP. (2000) HSP25, a small heat shock protein associated with dense bodies and M-lines of body wall muscle in *Caenorhabditis elegans*. *Biochem. J.* 349: 409-412.

Dix, D.J., Allen, JW., Collins, BW., Mori, C., Nakamura, N., Poorman-Allen, P., Goulding, E.H., Eddy, E.M. (1996). Targeted gene disruption of Hsp70-2 results in failed meiosis, germ cell apoptosis, and male infertility. *Proc. Nat. Acad. Sci.* 93: 3264-3268.

Dix, DJ., Allen, JW., Collins, BW., Poorman-Allen, P., Mori, C., Blizard, DR., Brown, PR., Goulding, EH., Strong, BD., Eddy, EM. (1997) HSP70-2 is required for desynapsis of synaptonemal complexes during meiotic prophase in juvenile and adult spermatocytes. *Development.* 124: 4595-4603.

Dix, DJ., Garges, BJ., Hong, RI. (1998) Inhibition of hsp70-1 and hsp70-3 expression disrupts preimplantation embryogenesis and heightens embryo sensitivity to arsenic. *Mol Reprod. Dev.* 51: 373-380.

Dodge, ME., Wang, J., Guy, C., Rankin, S., Rahimtula, M., Mearow, KM. (2005) Stress-induced heat shock protein 27 expression and its role in dorsal root ganglion neuronal survival. *Brain Res.* Dec 22. Epub ahead of print.

Driever, W., Solnica-Krezel, L., Schier, AF., Neuhass, SCF., Malicki, J., Stemple, DL., Stainier, DYR., Zwartkruis, F., Abdelilah, S., Rangini, Z., Belak, J., Boggs, C. (1998) A genetic screen for mutations affecting embryogenesis in zebrafish. *Development.* 123: 37-46.

Easter, SS. Jr., Malicki JJ. (2002). The zebrafish eye: developmental and genetic analysis. *Results Probl. Cell Differ.* 40: 346-370.

Easter, SS., Nichola, GN. (1996). The development of vision in the zebrafish (*Danio rerio*) *Dev. Biol.* 180: 646-663.

- Eddy, EM. (1999) Role of heat shock protein HSP70-2 in spermatogenesis. *Rev. Reprod.* 4: 23-30.
- Ekker, SC., Larson, JD. (2001). Morphant technology in model developmental systems. *Genesis.* 30: 89-93.
- Ellis, RE., Yuan, JY., Horvitz, HR. (1991) Mechanisms and function of cell death. *Annu. Rev. Cell Biol.* 7: 663-698.
- Eriksson, M., Jokinen, E., Sistonen, L., and Leppa, S. (2000) Heat shock factor 2 is activated during mouse embryogenesis. *Int. J. Dev. Biol.* 44: 471-477.
- Fadool, JM., Brockerhoff, SE., Hyatt, GA., Dowling, JE. (1997). Mutations affecting eye morphology in the developing zebrafish (*Danio rerio*). *Dev Gen.* 20: 288-295.
- Fashena, D., Westerfield, M. (1999) Secondary motorneuron axons localize DM-GRASP on their fasciculated segments. *J. Comp. Neurol.* 406: 415-424.
- Feder, ME., Hofmann, GE. (1999). Heat-shock proteins, molecular chaperones, and the stress response: evolutionary and ecological physiology. *Annu. Rev. Physiol.* 61: 243-282.
- Feder, JH., Ross, JM., Solomon, J., Solomon, N., Lindquist, S. (1992) The consequences of expressing hsp70 in *Drosophila* cells at normal growth temperatures. *Genes Dev.* 6: 1402-1413.
- Fishman, M. (2001) Zebrafish-the canonical vertebrate. *Science.* 294: 1290-2191.
- Fromm, L., Overbeek, PA. (1997). Inhibition of cell death by lens-specific overexpression of bcl-2 in transgenic mice. *Dev. Gen.* 20: 276-287.

Fujimoto, M., Izu, H., Seki, K., Fukuda, K., Nishida, T., Yamada, S., Kato, K., Yonemura, S., Inouye, S., Nakai, A. (2004) HSF4 is required for normal cell growth and differentiation during mouse lens development. *EMBO J.* 23: 4297-4306.

Galli-Taliadoros, LA., Sedgewick, JD., Wood, SA., Korner, H. (1995) Gene knockout technology: a methodological overview for the interested novice. *J. Immunol. Methods.* 181: 1-15.

Garrido, C., Gurbuxani, S., Ravagnan, L., Kroemer, G. (2001). Heat shock proteins: endogenous modulators of apoptotic cell death. *Biochem. Biophys. Res. Commun.* 286: 433-442.

Gilbert, SF. (2000) *Developmental Biology*. Sixth Ed. Sinauer Associates Inc. Sunderland, MA, USA.

Genis-Galvez, JM. (1966) Role of the lens in the morphogenesis of the iris and cornea. *Nature.* 210: 209-210.

Glaser, RL., Wolfner, MF., Lis, JT. (1986) Spatial and temporal pattern of hsp26 expression during normal development. *EMBO J.* 5: 747-754.

Glucksmann, A. (1951) Cell deaths in normal vertebrate ontogeny. *Biol Rev.* 26: 5986.

Gong, WJ., Golic, KG. (2004) Genomic deletions of the *Drosophila melanogaster* Hsp70 genes. *Genetics.* 168: 1467-1476.

Gotoh, T., Terada, K., Oyadomari, S., Mori, M. (2004) hsp70-DnaJ chaperone pair prevents nitric oxide and CHOP induced apoptosis by inhibiting translocation of Bax to mitochondria. *Cell Death Differ.* 4: 390-402.



Graham, A. (1998). Whole embryo assays for programmed cell death. In *Molecular embryology: methods and protocols*. Methods in Molecular Biology. Vol 97. Humana Press, Totowa, NJ.

Gross, A., McDonnell, JM., Korsmeyer, SJ. (1999) BCL-2 family members and the mitochondria in apoptosis. *Genes Dev.* 3: 1899-1911.

Gross, JM., Perkins, BD., Amsterdam, A., Egana, A., Darland, T., Matsui, JI., Sciascia, S., Hopkins, N., Dowling, JE. Identification of zebrafish insertional mutants with defects in visual system development and function. *Genetics.* 170: 245-261.

Haass, C., Klein, U., Kloetzel, PM. (1990) Developmental expression of *Drosophila melanogaster* small heat-shock proteins. *J Cell Sci.* 96: 413-418.

Haffter, P., Nusslein-Volhard, C. (1996) Large scale genetics in a small vertebrate, the zebrafish. *Int. J. Dev. Biol.* 40: 221-227.

Haffter, P., Granato, M., Brand, M., Mullins, MC., Hammerschmidt, M., Kane, DA., Odenthal, J., vanEeden, FJM., Jiang, JY, Heisenberg, CP., Kelsh, RN., Furutani-Seiki, M., Voglesang, E., Beuchle, D., Schach, U., Fabian, C., Nusslein-Volhard, C. (1996) The identification of genes with unique and essential functions in the development of the zebrafish, *Danio rerio*. *Development.* 123: 1-36.

Halloran, MC., Sato-Maeda, M., Warren, JT., Su, F., Lele, Z., Krone, PH., Kuwada, JY., Shoji, W. (2000). Laser-induced gene expression in specific cells of transgenic zebrafish. *Development* 127: 1953-1960.

Hamburger, V., Hamilton, HL. (1951) The developmental stages of the chick. *J. Morphol.* 88: 49-92.

Hammerschmidt, M., Pelegri, F., Mullins, M. C., Kane, D. A., van Eeden, F. J. M., Granato, M., Brand, M., Furutani-Seiki, M., Haffter, P., Heisenberg, C. P., Jiang, Y. J., Kelsh, R. N., Odenthal, J., Warga, R. M., Nusslein-Volhard, C. (1996). *dino* and *mercedes*, two genes regulating dorsal development in the zebrafish embryo. *Development*. 123: 95-102.

Hawkes, EL., Krueger,-Naug, AM., Nickerson, PE., Myers, TL., Currie, RW., Clarke, DB. (2004) Expression of *hsp27* in retinal ganglion cells of the rat during postnatal development. *J. Comp. Neurol.* 478:143-148.

He, H., Soncin, F., Grammatikakis, N., Siganou, A., Gong, J., Brown, SA., Kingston, RE., Calderwood, SK. (2003) Elevated expression of heat shock factor (HSF) 2A stimulates HSF1-induced transcription during stress. *J. Biol. Chem.* 278: 5789-5798.

Heasman, J. (2002) Morpholino oligos: making sense of anti-sense. *Dev. Biol.* 243: 209-214.

Heikkila, JJ. (2003) Expression and function of small heat shock protein genes during *Xenopus* development. *Sem Cell Dev Biol.* 14: 259-266.

Horwitz, J. (2000) Function of alpha-crystallin in vision. *Semin Cell Dev Biol.* 11: 53-60.

Horvitz, H., Ellis, H., Steinberg, P. (1982) Programmed cell death in nematode development. *Neurosci. Comment.* 1: 56-65.

Hooven, TA., Yamamoto, Y., Jeffery, WR.. (2004) Blind cavefish and heat shock protein chaperones: a novel role for *hsp90α* in lens apoptosis. *Int. J. Dev. Biol.* 48: 731-738.

Huang, L, Mivechi, NF., Moskophidis, D. (2001) Insights into regulation and function of the major stress –inducible *hsp70* molecular chaperone in vivo: Analysis of mice with targeted gene disruption of the *hsp70.1* or *hsp70.3* gene. *Mol Cell Biol.* 21: 8575-8591.

Humphrey, CD., Pittman, FE. (1974). A simple methylene blue-azure II- basic fuchsin stain for epoxy embedded tissue sections. *Stain Tech.* 49: 9-14.

Inoue, T., Takamura, K., Yamae, H., Ise, N., Kawakami, M., Tabuse, Y., Miwa, J., Yamaguchi, Y. (2003) *Caenorhabditis elegans* DAF-21 (Hsp90) is characteristically and predominantly expressed in germline cells: spatial and temporal analysis. *Develop. Growth Differ.* 45: 369-376.

Inouye, S., Izu, H., Takaki, E., Suzuki, H., Shirai, M., Yokota, Y., Ichikawa, H., Fujimoto M., Nakai, A. (2005). Impaired IgG production in mice deficient for heat shock transcription factor 1. *J Biol Chem.* 279: 38701-38709.

Ireland, ME., Mrock, LK. (2004) Expression and activation of epidermal growth factor in differentiating cells of developing and post-hatching chicken lens. *Exp. Eye Res.* 79: 305-312.

Ishizaki, Y., Jacobson, MD., Raff, MC. (1998). A role for caspases in lens fiber differentiation. *J. Cell Biol.* 140: 153-158.

Iwama, GK., Thomas, PT., Forsyth, RB., Vijayan, MM. (1998) Heat shock protein expression in fish. *Rev. Fish Biol.* 8: 35-56.

Jaatela, M., Wissing, D., Bauer, P. A., Li, G. C. (1992). Major heat shock protein hsp70 protects tumor cells from tumor necrosis factor cytotoxicity. *EMBO J.* 11: 3507-3512

Jaatela, M. (1995). Overexpression of hsp70 confers tumorigenicity to mouse fibrosarcoma cells. *Int. J. Cancer.* 60, 689-693.

Jacobson, MD, Weil, M., Raff MC (1997) Programmed cell death in animal development. *Cell.* 88: 347-354.

Jedlicka, P., Mortin, MA., Wu, C. (1997) Multiple functions of *Drosophila* heat shock transcription factor in vivo. EMBO J. 16: 2452-2462.

Jeffery, WR. (2001) Cavefish as a model system in evolutionary developmental biology. Dev. Biol. 231:1-12.

Jowett ,T. (1997) Tissue In Situ Hybridization: Methods in Animal Development. JohnWiley and Sons Inc., New York and Spektrum Akademisher Verlag, Heidelberg, Germany.

Kallio, M., Chang, Y., Manuel, M., Alastalo, TP., Rullu, M., Gitton, Y., Pirkkala, L., Loones, MT., Paslaru, L., Larney, S., Hiard, S., Morange, M., Sistonen, L., Mezger, V. (2002) Brain abnormalities, defective meiotic chromosome synapsis and female sub-fertility in HSF2 null mice. EMBO J. 21: 2591-2601.

Ka,y JN., Finger-Baier, KC., Roeser, T., Staub, W., Baier, H. (2001). Retinal ganglion cell genesis requires lakritz, a zebrafish atonal Homolog. Neuron. 30: 725-736.

Kawazoe, Y., Tanabe, M., Sasai, N., Nagata, K., Nakai, A. (1999) HSF3 is a major heat shock responsive factor during chicken embryonic development. Eur. J. Biochem. 265: 688-697.

Kimmel, CB., Ballard, WW., Kimmel, SR., Ullmann, B., Schilling, TF. (1995) Stages of embryonic development of the zebrafish. Dev. Dyn. 203: 253-310.

King, V., Tower, J. (1999) Aging specific expression of *Drosophila* Hsp22. Dev. Biol. 207: 107-118.

Kroeger, PE., Morimoto, RI. (1994) Selection of new Hsf1 and Hsf2 DNA binding sites reveals differences in trimer cooperativity. Mol. Cell. Biol. 14: 7592-7603.

Krone, PH., Lele, Z., Sass, JB. (1997). Heat shock genes and the heat shock response in zebrafish embryos. *Biochem. Cell Biol.* 75: 487-497.

Krone, PH., Evans, TG., Blechinger, SR. (2003). Heat shock gene expression and function during zebrafish embryogenesis. *Semin. Cell Dev. Biol.* 14: 267-274.

Krone, PH., Sass, JB. (1994) hsp90 $\alpha$  and hsp90 $\beta$  genes are present in the zebrafish and are differentially regulated in developing embryos. *Biochem Biophys. Res. Commun.* 204: 746-752.

Kuida, K., Haydar, TF., Kuan, CY., Gu, Y., Taya, C., Kaaarasuyama, H., Su, MS., Rakic, P., Flavell, RA. (1998) Reduced apoptosis and cytochrome c-mediated caspase activation in mice lacking caspase-9. *Cell.* 94: 325-337.

Kurita, R., Sagara, H., Aoki, Y., Link, BA., Arai, K., Wantanabe, S. (2003). Suppression of lens growth by  $\alpha$ A-crystallin promoter-driven expression of diphtheria toxin results in disruption of retinal cell organization in zebrafish. *Dev. Biol.* 255: 133-127.

Kurtz, S., Rossi, J., Petko, L., Lindquist, S. (1986) An ancient developmental induction: *Saccharomyces* sporulation and *Drosophila* oogenesis. *Science.* 231: 1154-1157.

Lele, Z., Bakkers, J., Hammerschmidt, M. (2001). Morpholino phenocopies of swirl, snailhouse, somitabun, minifin, silberback, and pipetail mutations. *Genesis.* 30: 190-194.

Lele, Z., Engel, S., Krone, PH. (1997). hsp47 and hsp70 gene expression is differentially regulated in a stress-and tissue-specific manner in zebrafish embryos. *Dev. Gen.* 21: 123-133.

Lele, Z., Hartson, SD., Martin, CC., Whiteshell, L., Matts, RL., Krone, PH. (1999). Disruption of zebrafish somite development by pharmacologic inhibition of Hsp90. *Dev. Biol.* 210: 56-70.

- Lele, Z., Krone, PH. (1997) Expression of genes encoding the collagen-binding heat shock protein (Hsp47) and type II collagen in developing zebrafish embryos. *Mech. Dev.* 61: 89-98.
- Li, CY., Lee, JS., Ko, YG., Kim, JI., Seo, JS. (2000) Heat shock protein 70 inhibits apoptosis downstream of cytochrome c release and upstream of caspase-3 activation. *J. Biol. Chem.* 275: 25665-25671.
- Li, P., Nilhawan, D., Budihardjo, I., Srinvasula, SM., Ahmad, M., Alnemri, ES, Wang, X. (1997) Cytochrome c and dATP dependent formation of apaf-1/caspase-9 complex initiates an apoptotic protease cascade. *Cell.* 91: 479-489.
- Li, Z., Joseph, NM., Easter, SS. Jr. (2000). The morphogenesis of the zebrafish eye, including a fate map of the optic vesicle. *Dev. Dyn.* 18: 175-188.
- Liang, P., McRae, TH. (1999) The synthesis of a small heat shock/ $\alpha$ -crystallin protein in *Artemia* and its relationship to stress tolerance during development. *Dev. Biol.* 207: 445-456.
- Link, BA., Darland, T. (2001) Genetic analysis of initial and ongoing retinogenesis in the zebrafish: comparing the central neuroepithelium and marginal zone. *Prog. Brain Res.* 131: 565-577.
- Liossis, SN. (1997) Overexpression of the heat shock protein 70 enhances the TCR/CD3-and Fas/Apo-1/CD95-mediated apoptotic cell death in Jurkat T cells. *J. Immunol.* 158: 5668-5675.
- Liu, L., Stamler, JS. (1999) NO: inhibitor of cell death. *Cell Death Differ.* 6: 937-942.

- Lockshin, RA., Williams, CM. (1964) Programmed cell death II. Endocrine potentiation of the breakdown of the intersegmental muscles of silkworm. *J. Insect Physiol.* (5: 1505-1516.
- Lockshin, RA., Williams, CM. (1969) Programmed cell death. Activation of lysis by a mechanism involving the synthesis of protein. *J Insect Physiol.* 15: 1510-1516.
- Loison, F., Debure, L., nizard, P., LeGoff, P., Michel, D., LeDrean, Y. (2005) Up-regulation of the clusterin gene after proteotoxic stress. Implication of HSF1/HSF2 heterocomplexes. *Biochem J.* Epub ahead of print.
- Loones, MT., Morange, M. (1998) Hsp and chaperone distribution during endochondral bone development in mouse embryo. *Cell Stress Chaperones.* 3: 237-244.
- Mailhos, C., Howard, MK., Latchman, DS. (1993). Heat shock protects neuronal cells from programmed cell death by apoptosis. *Neuroscience.* 55: 621-627.
- Malicki, J. (2000) Genetic analysis of eye development in zebrafish. *Results and Problems in Cell Differentiation.* 31: 257-282.
- Masuda, H., Hosokawa, N., Nagata, K (1998) Expression and localization of collagen-binding stress protein Hsp47 in mouse embryo development: comparison with types I and II collagen. *Cell Stress Chaperones.* 3: 256-264.
- Mayer, MP., Bakau, B. (1998) Hsp70 chaperone systems: diversity of cellular functions and mechanisms of action. *Biol Chem.* 379: 261-268.
- McDowell, AL., Dixon, LJ., Houchins, JD., Bilotta, J. (2004) Visual processing of the zebrafish optic tectum before and after optic nerve damage. *Vis. Nerosci.* 21: 97-106.

McRae, T.H. (2003) Molecular chaperones, stress resistance and development in *Artemia franciscana*. *Semin. Cell. Dev. Biol.* 14: 251-258.

McMillan, DR., Christians, E., Forster, M., Xiao, XH., Connell, P., Plumier, JC., Zuo, XX., Richardson, J., Morgan, S., Benjamin, IJ. (2002) Heat shock transcription factor 2 is not essential for embryonic development, fertility, or adult cognitive and psychomotor function in mice. *Mol. Cell Biol.* 22: 8005-8014.

Meacham, GC., Browne, BL., Zhang, Z., Kellermeier, R., Bedwell, DM., Cyr, DM. (1999) Mutations in the yeast Hsp40 chaperone protein Ydj1 cause defects in Axl1 biogenesis and profactor a processing. *J Biol Chem.* 274: 34396-34402.

Mezger, V., Rallu, M., Morimoto, RI., Morange, M., Renard, JP. (1994) Heat shock factor-2 like activity in mouse blastocysts. *Dev. Biol.* 166: 819-822.

Michuad, S., Marin, R., Tanguay, RM. (1997) Regulation of heat shock gene induction and expression during *Drosophila* development. *Cell Mol Life Sci.* 53: 104-113.

Min, JN., Zhang, Y., Moskopidid, D., Mivechi, NF. (2004) Unique contribution of heat shock transcription factor 4 in ocular lens development and fibre cell differentiation. *Genesis.* 40: 205-217.

Miyaishi, O., Sakata, K., Matsuyama, M., Saga, S. (1992) Distribution of collagen binding heat shock protein in chicken tissues. *J. Histochem. Cytochem.* 40: 1021-1029.

Montagutelli, X. (2000) Effect of the genetic background on the phenotype of mouse mutations. *J Am. Soc. Nephrol.* 16(Supp) 101-105.



Morely, JF., Morimoto, RI. (2004) Regulation of longevity in *Caenorhabditis elegans* by heat shock factor and molecular chaperones. *Mol. Biol. Cell.* 15: 657-664.

Morimoto, RI. 1998. Regulation of the heat shock transcriptional response: cross talk between a family of heat shock factors, molecular chaperones, and negative regulators. *Genes Dev.* 12: 3788-3796.

Morimoto, RI., Tissieres, A., Georgepoulos, C. (1994) *The Biology of Heat Shock Proteins and Molecular Chaperones.* Cold Spring Harbour Laboratory Press. Plainview, NY.

Morrow, G., Tanguay, RM. (2003) Heat shock proteins and aging in *Drosophila melanogaster*. *Sem. Cell Dev. Biol.* 14: 291-299.

Morrow, G., Battistini, S., Zhang, P., Tanguay, RM. (2004) Decreased lifespan in the absence of expression of the mitochondrial small heat shock protein Hsp22 in *Drosophila*. *J. Biol. Chem.* 279: 43382-43385.

Moses, MJ. (1968) Synaptonemal complexes. *Ann. Rev. Genetics.* 2: 363-412.

Mosser, DD., Martin, LH. (1992). Induced thermotolerance to apoptosis in a human T lymphocyte cell line. *J. Cell Physiol.* 151: 561-570.

Mosser, DD., Caron, AW., Bourget, L., Larose-Denis, C., Maise, B. (1997) Role of the human heat shock protein hsp70 in protection against stress induced apoptosis. *Mol. Cell Biol.* 17: 5317-5327.

Mosser, DD., Caron, AW., Bourget, L., Meriin, AB., Sherman, MY., Morimoto, RI., Massie, B. (2000) The chaperone function of hsp70 is required for protection against stress-induced apoptosis. *Mol. Cell Biol.* 20: 7146-7159.

- Nagai, A., Morimoto, R.I. (1993) Characterization of a novel heat shock transcription factor, heat shock factor 3, suggests new regulatory pathway. *Mol. Cell. Biol.* 13: 1983-1997.
- Nagai, N., Hosokawa, M., Itohara, S., Adachi, E., Matsushita, T., Hosokawa, N., Nagata, K. (2000). Embryonic lethality of molecular chaperone hsp47 knockout mice is associated with defects in collagen biosynthesis. *J. Cell Biol.* 150: 1499-1506.
- Nagata, K. (2003) HSP47 as a collagen-specific molecular chaperone: function and expression in normal mouse development. *Sem Cell Dev Biol.* 14: 275-282.
- Nagata, K. (1996) Hsp47: a collagen specific molecular chaperone. *Trends Biochem. Sci.* 21: 22-26.
- Nagata, K., Saga, S., Yamada, K.M. (1986) A major collagen-binding protein of chick embryo fibroblasts is a novel heat shock protein. *J. Cell Biol.* 103: 223-229.
- Nakai, A., Suzuki, M., Tanabe, M. (2000). Arrest of spermatogenesis in mice expressing an active heat shock transcription factor 1. *EMBO J.* 19: 1545-1554.
- Nasevicius, A., Ekker, S.C. 2000. Effective targeted gene 'knockdown' in zebrafish. *Nat. Gen.* 26: 216-220.
- Neckers, L. (2002) Hsp90 inhibitors as novel cancer chemotherapeutic agents. *Trends Mol. Med.* 8: 55-61.
- Neuhauss, S.C.F., Biehlmaier, O., Seeliger, M.W., Das, T., Kohler, K., Harris, W.A., Baier, H. (1999). Genetic disorders of vision revealed by a behavioural screen of 400 essential loci in zebrafish. *J. Neurosci.* 19: 8603-8615.

- Nollen, EAA., Morimoto, RI. (2002) Chaperoning signaling pathways: molecular chaperones as stress sensing heat shock proteins. *J Cell Sci.* 115: 2809-2816.
- Oka, M., Nakai, M., Endo, T., Lim, CR., Kimata, Y., Kohno, K. (1998) Loss of hsp70-hsp40 chaperone activity causes abnormal nuclear distribution and aberrant microtubule formation in M-phase of *Saccharomyces cerevisiae*. *J Biol Chem.* 273: 29727-29737.
- Oliver, G., Gruss, P. (1997) Current views in eye development. *Trends Neurosci.* 20: 415-421.
- Pan, H., Griep, AE. (1994) Altered cell cycle regulation in the lens of HPV-16 E6 or E7 transgenic mice: implications for tumor suppressor gene function in development. *Genes Dev.* 9: 2157-2169.
- Parsell, DA., Lindquist, S. (1994) Heat Shock Proteins and Stress Tolerance. In: *The Biology of Heat Shock Proteins and Molecular Chaperones*. Cold Spring Harbour Laboratory Press. Plainview, NY.
- Paslaru, L., Morange, M., Mezger, M. (2003) Phenotypic characterization of mouse embryonic fibroblasts lacking heat shock factor 2. *J. Cell. Mol. Med.* 7: 425-435.
- Pauli, D., Tonka, CH., Tissieres, A., Arrigo, AP. (1990) Tissue specific expression of heat shock protein HSP27 during *Drosophila melanogaster* development. *J Cell Biol.* 111: 817-828.
- Petko, L., Lindquist, S. (1986) Hsp26 is not required for growth at high temperatures, nor for thermotolerance, spore development, or germination. *Cell.* 45: 885-894.
- Piatigorsky, J. (1981). Lens differentiation in vertebrates. *Differentiation.* 19: 134-153.

Pirkkala, L., Nykanen, P., Sistonen, L. (2001) Roles of the heat shock transcription factors in regulation of the heat shock response and beyond. *FASEB J.* 15: 1118-1131.

Qin, G., Taylor, M., Ning, Y. Y., Iverson, P., Kobzik, L. (2000). In vivo evaluation of a morpholino antisense oligomer directed against tumor necrosis factor- $\alpha$ . *Antisense Nuc. Acid Drug Dev.* 10: 11-16.

Queitsch, C., Sangster, TA., Lindquist, S. (2002) Hsp90 as a capacitor of phenotypic variation. *Nature.* 417: 618-624.

Raha, S., Robinson, BH. (2001) Mitochondria, free radicals, and apoptosis. *Am. J. Med. Genet.* 106: 62-70.

Raha, S., Robinson, BH. (2000) Mitochondria, oxygen free radicals and protein oxidation in the aging process. *Trends in Biochem. Sci.* 25: 502-508.

Rallu, M., Loones, MT., Lallemand, Y., Morimoto RI., Morange, M., Mezger, V. (1997) Function and regulation of heat shock factor 2 during mouse embryogenesis. *Proc. Nat. Acad. Sci.* 94: 2392-2397.

Ravagnan, L., Gurbuxani, S., Susin, SA., Maise, C., Daugas, E., Zamzami, N., Mak, T., Jaattela, M., Penninger, JM., Garrido, C, Kroemer, G. (2001). Heat-shock protein 70 antagonizes apoptosis-inducing factor. *Nat Cell Biol.* 9: 839-843.

Ritossa, F. (1962) A new puffing pattern induced by temperature and DNP in *Drosophila*. *Experimentia.* 18: 571-573.

Ruden, DM., Garfinkel, MD., Sollars, VE., Lu, X. (2003) Waddington's widget: Hsp90 and the inheritance of acquired characters. *Sem. Cell Dev. Biol.* 14: 301-310.

- Rutherford, SL., Lindquist, S. (1998) Hsp90 as a capacitor for morphological evolution. *Nature*. 396: 336-342.
- Ryan, JA., Hightower, LE. (1999) Heat shock proteins: molecular biomarkers of effect. In: A. Puga, KB. Wallace, eds., *Molecular Biology of the Toxic Response*. Taylor and Francis, Philadelphia. pp 449-466.
- Sanders, EJ., Parker, E. (2002) The role of mitochondria, cytochrome c, and caspase-9 in embryonic lens fibre cell denucleation. *J. Anat.* 210: 121-135.
- Samali, A., Cotter, T. G. (1996). Heat shock proteins increase resistance to apoptosis. *Exp. Cell Res.* 223: 163-170.
- SantaCruz, H., Vriza, S., Angelier, N. 1997. Molecular characterization of a heat shock cognate cDNA of zebrafish, hsc70, and developmental expression of the corresponding transcripts. *Dev. Genet.* 21: 223-233.
- Santoro, GM. (2000) Heat shock factors and the control of the heat shock response. *Biochem. Pharmacol.* 59: 55-63.
- Sarge, KD., Park-Sarge, OK., Kirby, JD., Mayo, KE., Morimoto, RI. (1994) Expression of heat shock factor 2 in mouse testis: potential role as regulator of heat shock protein gene expression during spermatogenesis. *Biol. Reprod.* 50: 1334-1343.
- Sass, JB., Martin, CC., Krone, PH. (1999) Restricted expression of zebrafish hsp90alpha gene in fast and slow muscle fibre lineages. *Int. J. Dev. Biol.* 43: 835-838.
- Sass, JB., Krone, PH. (1997) Hsp90 $\alpha$  gene expression may be a conserved feature of vertebrate somitogenesis. *Exp. Cell. Res.* 233: 391-394.

Sass, JB., Weinberg, ES., Krone, PH. (1996) Specific localization of zebrafish hsp90 $\alpha$  mRNA to myo-D expressing cells suggests a role for Hsp90 $\alpha$  during normal muscle development. *Mech. Dev.* 54: 195-204.

Schmitt, A., Dowling, JE. (1994). Early eye morphogenesis in the zebrafish, *Brachydanio rerio*. *J. Comp. Neurol.* 344: 532-542.

Simon, MM., Krone, C., Schwarz, A., Luger, TA., Jaatela, M., Schwarz, T. (1995). Heat shock protein 70 overexpression affects the response to ultraviolet light in murine fibroblasts. Evidence for increased cell viability and suppression of cytokine release. *J. Clin Invest.* 95: 926-933.

Sistonen, L., Sarge, KD., Phillips, B., Abravaya, K., Morimoto, RI. (1992) Activation of heat shock factor 2 during hemin induced differentiation of human erythrocytes. *Mol. Cell. Biol.* 12: 4104-4111.

Sollars, V., Lu, X., Xia, L., Wang, X., Garfinkel, MD., Ruden, DM. (2003) Evidence for an epigenetic mechanism by which hsp90 acts as a capacitor for morphological evolution. *Nat. Genet.* 33: 70-74.

Somasundaram, T., Bhat, SP. (2004) Developmentally dictated expression of heat shock factors: exclusive expression of HSF4 in the postnatal lens and its specific interaction with  $\alpha$ B-crystallin heat shock promoter. *J. Biol. Chem.* 279: 44497-44503.

Somasundaram, T., Bhat, SP. (2000) Canonical heat shock element in the  $\alpha$  $\beta$ -crystallin gene shows tissue specific and developmentally controlled interactions with heat shock factor. *J. Biol. Chem.* (275): 17154-17159.

Sorger, PK. (1991) Heat shock factor and the heat shock response. *Cell*. 65: 363-366.

Sorger, PK., Pelham, HR. (1988) Yeast heat shock factor is an essential DNA-binding protein that exhibits temperature-dependent phosphorylation. *Cell*. 6: 855-864.

Soulez, KA., Link, BA. (2005) Morphogenesis of the anterior segment of the zebrafish eye. *BMC Dev Biol*. 5: 12.

Stankiewicz, AR., LeChapelle, G., Foo, CPZ., Radicioni, SM., Mosser, DD. (2005) Hsp70 inhibits heat induced apoptosis upstream of mitochondria by preventing Bax translocation. *J. Biol. Chem*. 280: 38729-38739.

Stroeva, OG. (1963) The role of the lenticular epithelium in the induction of the tissue of the iris and the ciliary body. *Dokl. Acad. Nauk. SSSR*. 151: 464-467.

Summerton, J. (1999). Morpholino antisense oligomers: the case for an RNase-H independent structural type. *Biochem. Biophys. Acta*. 1489: 141-158.

Summerton, J., Weller, D. (1997). Morpholino antisense oligomers: design, preparation, and properties. *Antisense Nuc. Acid Drug Dev*. 7: 187-195.

Takaki, E., Fujimoto, M., Sugahara, K., Nakahari, T., Yonemura, S., Tanaka, Y., Hayashida, N., Inouye, S., Takemoto, T., Yamashita, H., Nakai, A. (2005) Maintenance of olfactory neurogenesis requires HSF1, a major heat shock transcription factor in mice. *J Biol Chem*. 2005 Nov 23 (Pub ahead of print).

Tanabe, M., Nakai, A., Kawazoe, Y, Nagata, K. (1997) Different thresholds in the responses of two heat shock transcription factors, HSF1 and HSF3. *J. Biol. Chem*. 272: 15389-15395.

Tanabe M, Kawazoe TM, Takeda S, Morimoto RI, Nagai K, Nakai A. (1998) Disruption of HSF3 gene results in the severe reduction of heat shock gene expression and loss of thermotolerance. *EMBO J.* 17: 1750-1758.

Tata, JR. (1966) Requirement for RNA and protein synthesis for induced regression of the tadpole tail in organ culture. *Dev. Biol.* 13: 79-94.

Thut, CJ., Rountree, R. B., Hwa, M., Kingsley, D. M. (2001). A large in situ screen provides molecular evidence for the induction of eye anterior segment structures by the developing lens. *Dev. Biol.* 231: 63-76.

Torriglia, AE., Chaudun, E., Chany-Fornier, F., Jeanny, JC., Courtus, Y., Counis, MF. (1995) Involvement of DNase II in nuclear degradation during lens cell differentiation. *J. Biol. Chem.* 270: 28579-28585.

van der Straten A, Rommel C, Dickson B, Hafen E. (1997) The heat shock protein 83 (Hsp83) is required for raf-mediated signaling in *Drosophila*. *EMBO J.* 16: 1961-1969.

Vihtelic, TS., Yamamoto, Y., Sweeny, WT., Jeffery, WR., Hyde, DR. (2001). Arrested differentiation and epithelial cell degeneration in zebrafish lens mutants. *Dev. Dyn.* 222: 625-636.

Vihtelic, TS., Hyde, DR. (2002). Zebrafish mutagenesis yields eye morphological mutants with retinal and lens defects. *Vis. Res.* 42: 535-540.

Verhagen, AM., Vaux, DL. (2002) Cell death regulation by mammalian IAP antagonist Smac/Diablo. *Apoptosis.* 2: 163-166.

Voellmy, R. (2004) On mechanisms that control heat shock transcription factor activity in metazoan cells. *Cell Stress Chaperones.* 9: 122-133.



Vogt, C. (1842) Untersuchungen über die entwicklungsgeschichte der geburtshelferkoete (*Alytes obstetricans*).

Voss, AK., Thomas, T., Gruss, P. (2000) Mice lacking hsp90 $\beta$  fail to develop a placental labyrinth. *Development*. 127: 1-11.

Vowels, JJ., Thomas, JH. (1994) Multiple chemosensory defects in daf-11 and daf-21 mutants of *Caenorhabditis elegans*. *Genetics*. 138: 303-319.

Walker, GA., Lithgow, GJ. (2003) Lifespan extension in *C. elegans* by a molecular chaperone dependent upon insulin like signals. *Aging Cell*. 2: 131-139.

Walker, GA., Thompson, FJ., Brawley, A., Scalon, T., Devaney, E. (2003) Heat shock factor functions at the convergence of the stress response and developmental pathways in *C. elegans*. *FASEB J*. 17: 1960-1962.

Walker, GA., White, TM., McColl, G., Jenkins, NL., Babich, S., Candido, EP., Jonhson, TE., Lithgow, GJ. (2001) Heat shock protein accumulation is upregulated in a long-lived mutant of *Caenorhabditis elegans*. *J. Gerontol. A Biol. Sci. Med. Sci*. 56: B281-B287.

Wang, G., Huang, H., Dai, R., Lee, KY., Lin, S., Mivechi, NF. (2001) Suppression of heat shock transcription factor HSF1 in zebrafish causes heat induced apoptosis. *Genesis*. 30: 195-197.

Wang, G., Ying, Z., Jin, X., Tu, N., Zhang, Y., Phillips, M., Moskophidis, D., Mivechi, NF. (2004) Essential requirement for both hsf1 and hsf2 transcriptional activity in spermatogenesis and male fertility. *Genesis*. 38: 66-80.

- Wang, G., Zhang, J., Moskophidis, D., Mivechi, NF. (2003) Targeted disruption of heat shock transcription factor (hsf)-2 gene results in increased embryonic lethality, neuronal defects, and reduced spermatogenesis. *Genesis*. 36: 48-61.
- Welsh, MJ., Wu, W., Parvinen, M., Gilmont, RR. (1996) Variation in expression of hsp27 messenger ribonucleic acid during the cycle of seminiferous epithelium and co-localization of hsp27 and microfilaments in Sertoli cells of the rat. *Biol Reprod*. 55: 141-151.
- Werner-Washburne, M., Stone, DE., Craig, EA. (1987) Complex interactions among members of an essential subfamily of hsp70 genes in *Saccharomyces cerevisiae*. *Cell Mol Biol*. 7: 2568-2577.
- Wheeler, JC., Bieschke, ET., Tower, J. (1995) Muscle-specific expression of *Drosophila* Hsp70 in response to aging and oxidative stress. *Proc. Nat. Acad. Sci*. 92: 10408-10412.
- Westerfield, M. (1995). *The Zebrafish Book: A guide for the laboratory use of zebrafish (Danio rerio)*. University of Oregon Press, Eugene.
- Wolf, B., Green, DR. (1999) Suicidal tendencies: apoptotic cell death by caspase family proteases. *J. Biol. Chem*. 274: 20049-20052.
- Wride, MA., Parker, E., Sanders, EJ. (1999). Members of the bcl-2 and caspase families regulate nuclear degeneration during chick lens fibre differentiation. *Dev. Biol*. 213: 142-156.
- Wride, WA. (2000). Apoptosis as seen through a lens. *Apoptosis*. 5: 203-209.
- Xiao, XZ., Zuo, XX., Davis, AA., McMillan, DR., Curry, BB., Richardson, JA., Benjamin, IJ. (1999) HSF1 is required for extraembryonic development, post natal growth and protection during inflammatory responses in mice. *EMBO J*. 18: 5943-5952.

Yamamoto, Y., Jeffery, WR. (2000). Central role for the lens in cave fish eye degeneration. *Science*. 289: 631-632.

Yamamoto, Y., Jeffery, WR. (2002). Probing teleost eye development by lens transplantation. *Methods*. 28: 420-426.

Yamamoto, Y., Stock, DW., Jeffery, WR. (2004) Hedgehog signaling controls eye degeneration in blind cavefish. *Nature*. 431: 847-847.

Yue, L., Karr, TL., Nathan, DF., Swift, H., Srinivasan, S., Lindquist, S. (1999) Genetic analysis of viable *hsp90* alleles reveals a critical role in *Drosophila* spermatogenesis. *Genetics*. 151: 1065-1079.

Zatsepina, OG., Velikodvorskaia, VV., Molodstov, VB., Garbuz, D., Lerman, DN., Bettencourt, BR., Feder, ME., Evgenev, MB. (2001) A *Drosophila melanogaster* strain from sub-equatorial Africa has exceptional thermotolerance but decreased Hsp70 expression. *J. Exp. Biol.* 204: 1869-1881.

Zimmerman, LE., Font, RL. (1966). Congenital malformations of the eye: some recent advances in knowledge of the pathogenesis and histopathological characteristics. *J. Am. Med. Assoc.* 196: 684-692.

Zhang, Y., Huang, L., Zhang, J., Moskophidis, D., Mivechi, NF. (2002) Targeted disruption of *hsf1* leads to lack of thermotolerance and defines tissue-specific regulation for stress-inducible Hsp molecular chaperones. *J. Cell Biochem.* 86: 376-393.

Zhivotovsky, B., Burgess, DH., Orrenius, S. (1996) Proteases in apoptosis. *Experientia*. 52: 968-978.

Zhu, D., Dix, DJ., Eddy, EM. (1997) HSP70-2 is required for CDC2 kinase activity in meiosis I of mouse spermatocytes. *Development*. 124: 3007-3014.

Zou, H., Li, Y., Liu, X., Wang, X (1999) An APAF-1 cytochrome c multimeric complex is a functional apoptosome that activates procaspase-9. *J. Biol. Chem.* 274: 11559-11556.

Zylicz, M., Wawrzynow, A. (2001) Insights into the functions of Hsp70 chaperones. *IUBMB Life*. 5: 283-287.

Zhu, D., Dix, DJ., Eddy, EM. (1997) HSP70-2 is required for CDC2 kinase activity in meiosis I of mouse spermatocytes. *Development*. 124: 3007-3014.

Zou, H., Li, Y., Liu, X., Wang, X (1999) An APAF-1 cytochrome c multimeric complex is a functional apoptosome that activates procaspase-9. *J. Biol. Chem.* 274: 11559-11556.

Zylicz, M., Wawrzynow, A. (2001) Insights into the functions of Hsp70 chaperones. *IUBMB Life*. 5: 283-287.